# GALACTIC RADIO NOISE ATTENUATION IN THE IONOSPHERE

PRESENTED

BY

M.A.ABDU

for

The Degree of

DOCTOR OF PHILOSOPHY

OF

THE GUJARAT UNIVERSITY

October 1966

043

B2717

PHYSICAL RESEARCH LABORATORY,

AHMEDABAD-9,

INDIA.

# P R E F A C E

Studies of cosmic radio noise and its absorption in the atmosphere were started at Ahmedabad in 1956 using a receiving and recording equipment for 25 MHz constructed by Bhonsle (1958). The present author has maintained this equipment since 1961 with the help of Mr.A.K.Sud. He has also set up three riometers, one at 21.3 MHz at Ahmedabad in January 1963 and the other two at 21.3 and 16.5 MHz at Thumba Equatorial Rocket Launching Station in 1964-65. The present thesis contains mainly the studies made at Ahmedabad using 25 MHz and 21.3 MHz data.

At the latitude of Ahmedabad, where the critical frequency of the $F_2$ layer generally reaches its peak value, the major contribution to the total CR noise attenuation arises in the F region. The observed absorption has been separated into two components, a component which is mainly due to absorption in the D region and the other component which depends on $f_0F_2$. The diurnal, seasonal and solar activity changes in each of these components have been analysed. The total absorption at 25 MHz decreased considerably from 1958 to 1964 with the decrease in solar activity.

The absorption in the F region due to electron-ion collision was calculated using N(h) profiles deduced from ionograms. This is found to be a major contributor to the

total absorption of cosmic radio noise. The residual absorption arising in the topside of the ionosphere has also been obtained and its variations studied. It is found that in order to explain the results, the electron temperature $T_e$ has to be much larger than the neutral gas temperature $T_g$, particularly during morning hours, and also when the ionosphere is disturbed.

The effect of a disturbed ionosphere on cosmic radio noise absorption is studied in the last chapter. Observations of SCNA's at both Ahmedabad and Thumba at 25, 21.3 and 16.5 MHz have been used to find the dependence of enhanced ionization in the D region on the solar zenith angle and the exploring frequency.

The changes in attenuation which occur during magnetic storms have also been examined.

M A Abdu

(author)

## ACKNOWLEDGEMENTS

I express my sincere thanks to Prof.K.R.Ramanathan under whose guidance the above work was done. I am grateful to Dr.S.S.Degaonker for help in preparing this thesis and critical suggestions for improving it. Dr.J.S.Shirke helped me greatly in setting up the riometers. I express my gratitude to him. Thanks are also due to Dr.R.G.Rastogi for help and advice.

I thank Messrs A.K.Sud and K.J.John for their cooperation in maintaining the riometers at Ahmedabad and Thumba. Thanks are also due to my colleagues, Mr.S.Ramakrishnan for providing electron content data from S66 satellite, and Mr.S.Sanatani for providing the computer program for the reduction of N(h) profiles from ionograms.

My thanks are also due to the Department of Atomic Energy, Government of India for financial assistance.

M A Abdu

(M. A. Abdu)

# C O N T E N T S

# LIST OF TABLES

## FIGURE CAPTIONS

# CHAPTER I

## GALACTIC RADIO NOISE AND ITS ATTENUATION IN THE IONOSPHERE

### 1.1 Galactic radio noise

The first observation of galactic radio noise was made in 1932 by Karl G. Jansky (1932). In the course of his observations on atmospheric radio noise, he noticed a steady static at 20 Mhz coming from certain definite directions in the sky. The time of maximum of this was found to change gradually during a year following the revolution of the earth round the sun. The source of this noise was therefore recognised to be of stellar origin. The intensity maximum of this radio noise was found to occur when the galactic equator was in the antenna beam.

Further work on cosmic radio noise was carried out by Reber (1940) at 160 Mhz. He found several subsidiary maxima in directions other than the galactic equator. He also noticed that the intensity at 160 Mhz was much less than what Jansky had observed at 20 Mhz. The work of Hey, Parsons and Phillips (1946) at 64 Mhz provided the first clue to the existence of discrete radio sources. This was later confirmed by Bolton and Stanley (1948) who determined the angular sizes of the radio source in the constellation of Cygnus. The signals from such individual sources were found to have short period fluctuations. A detailed study of these intensity fluctuations were made by Stanley and Slee (1950) who proved that the cause of fluctuations was not

in the source but was the earth's atmosphere. The study of these fluctuations has now become an important tool for investigating the structure of irregular electron concentrations in the ionosphere.

The cosmic radio noise continuum extends over the entire frequency range accessible to observation within the limits imposed by the earth's atmosphere. The lower limit of the observable range under favourable conditions is about 1.0 MHz and the upper limit is determined by the strength of the signal and its absorption in the micro-wave region beyond 3000 MHz.

The flux density of cosmic radio noise in any direction of the sky decreases with increase of frequency. In general the spectral distribution is of the form $T_b \propto f^{-\alpha}$, where $T_b$ is the brightness temperature of the sky and $f$ is the frequency. The value of the index $\alpha$ would depend on the particular mechanism of production of this noise. Early investigators believed (Reber, 1940) that this noise was of thermal origin, produced by the movement of interstellar ionized gas. Such a source would require the value of $\alpha = 2$. Later investigations at different frequencies and in different parts of the sky showed that $\alpha$ was generally about 2.5, indicating that the source of the noise was not wholly thermal. The present understanding of the origin of cosmic radio noise is based on three distinct types of emission processes : (1) A line emission from interstellar atomic neutral hydrogen at $\lambda = 21$ cm, (2) A thermal component due to the movement of fully ionized interstellar gas in the HII region

and (3) A nonthermal component due to spiralling of relativistic electrons round magnetic field lines in interstellar space (synchrotron emission). The emission spectrum of HII source is of the form $T_b \propto f^{-2}$ as mentioned earlier and that for a nonthermal source is $T_b \propto f^{-2.7}$ (Pawsey and Hill, 1961). Thus HII region should become relatively more intense at high frequencies and this is found to be so in the direction of the galactic plane. At low frequencies (say 20 MHz) HII region generally appears in absorption against the background.

## 1.2 Sources of absorption of cosmic radio noise

The clouds of ionized interstellar gas which are known to be common in the galactic disc absorbs the radio waves passing through them. Since the absorption coefficient of a fully ionized gas varies as $f^{-2}$, this process is important for the absorption of low frequency cosmic radio noise observed in the direction of the galactic equator. An evidence for this was first obtained by Shain (1951) who observed the radio noise intensity over a zone of sky at declination $-34^{\circ}$ and showed that the ratio of maximum to minimum intensity at 18.3 MHz was much less than would be obtained at 100 MHz with identical antennas. Assuming that the ionized hydrogen is distributed uniformly in a parallel layer and substantially all the radiation originate outside it, he was able to calculate the absorption coefficient of the medium in the plane of the galaxy.

Another source of cosmic radio noise absorption is in

the earth's ionosphere. The lower frequency end of the CR noise spectrum as observed at the ground is limited due to its absorption in the earth's atmosphere. This part of the spectrum therefore could be used to measure its attenuation.

## 1.3 Survey of ionospheric absorption studies using cosmic radio noise at different frequencies at various stations in middle latitudes

The early investigations carried out at 20 MHz by Jansky (1937) showed that the cosmic radio noise intensity was generally more during night then during day. This was rightly thought to be due to less ionospheric absorption during night. The first quantitative estimate of this absorption was made by Shain (1951) working at 18.3 MHz at Hornsby in Australia. From systematic observation carried out over a period of one year, he concluded that the effect of ionospheric absorption at 18.3 MHz cosmic radio noise was negligible when the critical frequency of the $F_2$ layer was less than 9.0 MHz.

A further study by Mitra and Shain (1953) revealed that the total absorption suffered by the cosmic radio noise in the whole of ionosphere can be divided into two parts, one due to absorption in the D region and the other in the F region. The latter was found to depend on the critical frequency of the F layer and not on its height. They also obtained evidence of increased absorption at night which was attributed to irregularities in the upper part of F region. Maximum total absorption

of CR noise observed by these authors was about 1.3 db in November and December and 0.75 in July and September. The $F_2$ component of absorption was not more than 0.3 db in any season.

Blum and others (1954) working on 29.5 MHz at Manchester reported a linear relationship between the observed attenuation and $f_0F_2$. The total absorption observed by them was not more than 0.5 db with a maximum of about 0.2 db due to absorption in the D-region. Warwick and Zirin (1957) working at 18 MHz in Colorado obtained maximum absorption less than 0.4 db. They assumed that the observed attenuation took place entirely in the D-region and calculated the electron density variation with height and time from the observed attenuation.

From the analysis of 27.5 MHz CR noise measurement made at Stanford and Pullman, Lusignan (1962) pointed out that the total attenuation could be represented by (i) a component attributable to D region, (ii) a component which depends on $f_0F_2$ and (iii) a residual part which did not show correlation with any ionospheric parameters. This residual absorption was found to be often larger than the sum of the other two and did not show any clear diurnal variation.

Ellis (1963) calculated the absorption of CR noise in the F region using F region electron density profiles from the backscatter measurements of Pineo and Hyneck (1962) and Bowles (1962). He showed that the measured cosmic noise absorption could be accounted for by the F region. He noted that the higher

absorption in the night reported by earlier workers could be partly due to decrease of temperature in the night.

## 1.4 High latitude CR noise absorption

Riometer (relative ionospheric opacity meter) studies in high latitudes have revealed several interesting and important features of the high latitude ionosphere. The problems encountered are somewhat different from those at middle latitudes. That is because in high latitudes the additional ionization produced by the impact of charged particles coming from the sun contributes substantially to the absorption of radio noise whereas at middle and low latitudes this phenomenon is almost absent.

Little and Leinbach (1958) studied the CR noise absorption in the Arctic ionosphere and showed that all the absorption took place below the E region. Regions of anomalous absorption having lateral dimensions in excess of 100 km were first observed. Marked difference in absorption was found to occur during disturbed periods at stations separated by 800 km. Correlation was found between the anomalous absorption and the $K_p$ index, and it was suggested that corpuscular streams from the sun which produce the aurorae are apparently responsible for this. There is a sudden cosmic noise absorption (SCNA) associated with solar flares. In addition to this, two types of abnormal absorption occur in high latitudes. One of these, known as type II absorption, is associated with visible aurorae and is very frequent after midnight. This is attributed by Chapman and Little (1957)

to the increase of ionization in the lower ionosphere due to bombardment of electrons of solar origin and their associated bremsstrahlung radiation. The other is known as the polar black-out or type III absorption, and is more frequent during day than during night. It sometimes covers the whole polar cap. It is also correlated with the magnetic activity and its diurnal variation of frequency of occurrence is twelve hours out of phase with that of magnetic activity. Long duration black-outs have been identified with polar cap absorption (PCA) (Agy and Davies, 1962) events which are caused by the arrival of low energy cosmic ray particles from the sun following some solar flares.

## 1.5 Observations at tropical latitudes

Bhonsle, Ramanathan and Degaonkar (1958-61) studied the cosmic radio noise absorption at 25 Mhz over Ahmedabad during the IGY period. From the analysis of the data for the period 1957-59, they showed several interesting features of the ionosphere over Ahmedabad during years of high sunspot activity. The total absorption obtained by them at 25 Mhz was much more than at 18.3 Mhz obtained by Mitra and Shain. This was unexpected since the absorption is known to vary inversely as the square of frequency (Ratcliffe, 1962). Further the total absorption was shown to have strong correlation with the critical frequency, $f_0F_2$, when it exceeded 8.0 Mhz. An empirical relationship between the total absorption A and $f_0F_2$ was established; viz. $A = \frac{1}{2}\left(\frac{f_0F_2}{8}\right)^{3.4}$.

Maximum attenuation occurred in equinoxes (exceeding 6.0 db) and minimum absorption (around 2.0 db) during summer. A secondary peak in absorption, sometimes exceeding daytime peak, was found to occur at night at about 20 hr IMT in equinox and winter. They separated the total absorption into (i) a symmetrical component which varied as $\cos^n \chi$ , which was mainly due to D region and (ii) a component which closely followed the changes of $f_0F_2$.

The F region absorption observed at Ahmedabad was found to be much more than at any other latitude. The nighttime attenuation was found to be more than the daytime F region component of absorption and it appeared to be so even for the same $f_0F_2$. Ramanathan and Bhonsle (1959) suggested that scattering by ionospheric irregularities at night might be a possible source of such attenuation. This feature was similar to that reported by Mitra and Shain (1953).

Bhonsle and Ramanathan (1960) studied the geomagnetic effect on the ionosphere over Ahmedabad following a magnetic storm, using the 25 Mhz absorption data. A decrease in attenuation in the first two days of the storm and an increase on the third day was observed. Ramanathan, Bhonsle and Degaonkar (1961) calculated the absorption due to electron-positive ion collisions upto the $F_2$ peak using N(h) profiles and showed that a considerable part of the total measured attenuation can occur in the F region. An application of this method to the study of absorption during magnetic storms showed that large changes in electron density took place in the topside of the ionosphere above $F_2$ peak following a storm (Degaonkar and Bhonsle, 1962).

Mitra and Sarada (1962) using their cosmic radio noise absorption data at 22.4 MHz at New Delhi computed approximate values of total electron content in the topside ionosphere and the total absorption upto the $F_2$ peak using N(h) profiles. The difference between the total observed attenuation and that calculated upto the $F_2$ peak was then accounted for by an exponential distribution of electron density above the $F_2$ peak.

## 1.6 Theory of radio wave absorption in the ionosphere

Free electrons in the ionosphere oscillate in unison with the electric field of a radio wave passing through the medium with the same frequency as that of the wave. While doing so they reradiate most of the energy they absorb from the wave, and a fraction of this absorbed energy is scattered in direction other than the original direction of the wave. On the whole there is no net loss of energy of radio waves passing through the ionized medium. If, however, the electrons collide with heavier particles their ordered energy of oscillatory motion is partly converted into random kinetic energy. The rate of conversion depends upon the number of collision per unit time and the number density of electrons and neutral particles. Thus the original signal undergoes attenuation. The electric field intensity E of a radiowave traversing a medium through a distance ds is given by

$$E = E_0 \exp(-\int k ds)$$

where $E_o$ is the original intensity before attenuation and K the absorption coefficient of the medium per unit path length.

From the magneto-ionic theory of Appleton-Hartree, K can be derived as (see Ratcliffe, 1962)

$$K = \frac{2\pi e^2}{mc} \frac{1}{\mu} \frac{N\nu}{(\omega \pm \omega_L)^2 + \nu^2} \qquad (1)$$

in the quasi longitudinal (QL) approximation.

Where $c$ = velocity of electromagnetic wave in free space,

$\omega$ = angular frequency of the wave,

$\omega_L$ = longitudinal component of the gyro frequency,

$\mu$ = refractive index of the medium given by

$\mu^2 = 1 - \frac{4\pi Ne^2}{m\omega^2}$

$\nu$ = the effective collision frequency of electrons,

and $N$ = electron density per cc.

If N and $\nu$ vary along the path of radio waves, the total attenuation is given by

$$\log\left(\frac{E_o}{E}\right) = \int K ds$$

$$= \frac{2\pi e^2}{mc} \int \frac{N\nu \, ds}{\mu((\omega + \omega_L)^2 + \nu^2)} \qquad (2)$$

Two cases of absorption arise

(a) <u>Nondeviative absorption</u>

When the refractive index $\mu$ is of the order unity the attenuation is purely collisional and is known as nondeviative

absorption. In the recording of CR noise, the exploring frequency is usually fixed at a frequency higher then the maximum $f_0F_2$ at that particular station. So we generally get $\nu^2 << \omega^2$ and $\omega_L < \omega$. The total nondeviative absorption is then from equation 2,

$$\int k\,ds = \frac{2\pi e^2}{mc\omega^2} \int N\nu\,ds \qquad (3)$$

We thus see that the nondeviative absorption is inversely proportional to the square of the exploring frequency.

(b) Deviative absorption

When $\mu$ departs considerably from unity, the wave undergoes retardation and the effective path traversed increases, resulting in more attenuation of the wave. The additional attenuation is known as the deviative absorption. The absorption coefficient for this case is given by

$$k = \frac{\nu}{2c}\left(\frac{1}{\mu} - \mu\right) \qquad (4)$$

1.7 Collision frequency of electrons with neutral particles and ions

If the average velocity $v_e$ of the electrons is known, the average $\nu_{em}$ of their collision with neutral particles is given by the relation $\nu_{em} = \frac{v_e}{l_e}$

where $l_e = (\pi r_a^2 n_a)^{-1}$

where $r_a$ = radius of a molecule,

$n_a$ = number density of atoms or molecules.

From gas kinetic theory

$$\frac{1}{2}mv_e^2 = \left(\frac{3}{2}\right)kT$$

or $$v_e = \left(\frac{3kT}{m}\right)^{\frac{1}{2}}$$

Thus $$\nu_{em} = \pi r_a^2 n_a \left(\frac{3kT}{m}\right)^{\frac{1}{2}}$$

For levels where the dissociation of air molecules are not appreciable, Nicolet (1959) has given the formula

$$\nu_{em} = 5.4 \times 10^{-10} N_m T^{1/2} \qquad (5)$$

where $N_m$ = the number density of the neutral molecules per cc and $T$ = the atmospheric temperature in $^oK$.

At higher levels, $r_a$ will get smaller owing to the dissociation of oxygen and nitrogen. Since electrons have got higher collision cross section with positive ions than with neutral particles due to the Coulomb forces between them, this type of collisions becomes important at the attitudes above 150 km and the effective collision frequency is given by

$$\nu_{eff} = \nu_{em} + \nu_{ei} \qquad (6)$$

where $\nu_{eff}$ is the collision frequency of electrons with ions

If an electron approaches a distance $r_{eff}$ from the ions such that its potential energy is equal to the original kinetic energy (when $\frac{3}{2}kT = \frac{e^2}{r_{eff}}$), then the deflection of an

electron can be sufficiently great so that the event can be called a collision (Ratcliffe, 1962). The effective cross section for collision, $\pi r_{eff}^2$ , thus depends on the velocity of the electron and is proportional to $T^{-2}$. The collision frequency is proportional to the product of the velocity and the collision cross section and therefore, proportional to $T^{-3/2}$. A full investigation undertaken by Cowling (1945) leads to the expression

$$\nu_{ei} = 6.1 \times 10^{-3} \left(\frac{Te}{300}\right)^{-\frac{3}{2}} n_i \qquad (7)$$

where $T_e$ = the temperature of electron,

and $n_i$ = number density of ions.

For temperatures of 1200-1500 $^0$K which is the normal F region temperature, each ion contributes as much to the collision frequency as about $10^4$ neutral particles.

Cowling's expression as revised by Nicolet (1959) is given by

$$\nu_{ei} = \left[34 + 4.18 \log\left(\frac{Te^3}{Ne}\right)\right](1+\lambda) N_i T_e^{-3/2} \qquad (8)$$

where $\lambda$ is the ratio of the negative ions to electrons which can be neglected in most part of the ionosphere and $N_i$ is the ion density which can be assumed to be equal to $N_e$ (electron density), when ions are singly charged. Thus

$$\nu_{ei} = \left[34 + 4.18 \log\left(\frac{Te^3}{Ne}\right)\right] N_e T_e^{-3/2} \qquad (9)$$

The total nondeviative absorption due to electron-neutral

particle collision is proportionnal to $n_e N_m T^{\frac{1}{2}}$. That due to electron-positive ion collision is proportional to $N_e^2 T^{-3/2}$.

It will be shown later(in Chapter IV) that the total nondeviative absorption of a radio wave penetrating the $F_2$-region vertically is given by

$$\int k ds = \frac{C(f_0 F_2)^4 H T_e^{-3/2}}{f^2} \qquad (10)$$

where $C$ = a constant

$H$ = the effective scale height at the $F_2$ peak

and $f$ = the exploring frequency

## 1.8 Other causes of radio wave absorption

There can be other causes of radio wave absorption such as :-

(i) Incoherent scattering of radio waves by electrons in the ionosphere can result in the attenuation of the signal passing through the medium. This is analogous to Rayleigh scattering of light by air molecules. The scattered energy will be doppler shifted from the incident wave frequency due to the thermal motion of the electrons. This phenomenon is used to study the electron density and temperature distributions in the ionosphere using very high frequency (of the order of 50 MHz) radio waves. The attenuation of the signal however is very small.

(ii) Scattering by irregularities of varying sizes (irregular horizontal gradients of ionization) can cause attenuation. The scattered power depends on the size of the irregularity relative to the wavelength of the incident wave.

(iii) When the wave frequency is comparable to the longitudinal component of gyrofrequency, the amplitude fading due to polarisation is important. This problem is encountered mainly in the case of waves reflected from the E region, when absorption measurements are made using the vertical incidence pulse reflection method. Since the cosmic noise is unpolarised and the exploring frequency is in the VHF range, the polarisation effect is negligible.

## 1.9 Method of measuring ionospheric absorption

The most widely used techniques to measure ionospheric absorption can be classified broadly into two groups :-

### (1) Ground based transmitter and receiver

This is the earliest method of studying the ionospheric absorption in which the amplitude of a radio wave reflected from the ionosphere, after it is transmitted from a ground transmitter is measured. The absorption measured is that due to the regions below the reflecting layer. As the exploring frequency approaches the critical frequency of the layer, deviative absorption sets in. Hence a study of the frequency dependence of absorption becomes more difficult as it is necessary to know the absorption due to deviative causes. Polarization phenomena, ionospheric scattering and partial reflection also contribute to the uncertainty in the measurement of absorption.

(11) Extraterrestrial radio sources and/or signals from satellites

Here the waves traverse the path only once. The intensity of the radio wave transmitted from a source situated either in the ionosphere or outside is measured at the ground. Radio signals transmitted from an artificial earth satellite can be monitored on the ground to measure the absorption of the signal. However the present work is mainly concerned with the study of absorption of galactic radio noise in the atmosphere.

## 1.10 Advantage of cosmic radio noise method of measuring ionospheric absorption over other methods

The use of extra-terrestrial radio waves enables one to study the total absorption in the ionosphere. It is possible to use a frequency sufficiently high so that the effects due to devistive absorption and polarization can be removed although the effects due to scattering remain. Since no transmitter is involved, the equipment needed is relatively simple and continuous measurement is possible on a routine basis. The fact that the data can be obtained even during severe sudden ionospheric disturbances at a sufficiently high exploring frequency is of particular advantage at high latitudes where anomalous absorption events are very frequent.

## 1.11 A brief discussion on the experimental results of absorption measurements in the lower ionosphere

Earliest investigations on the absorption of radio

waves in the lower ionosphere were carried out using vertical pulse reflection method. From a detailed analysis of the data collected over an extended period Appleton and Piggott (1954) showed that the absorption varied according to

$$\log \ell = \frac{A \cos^{n} \chi}{(f \pm f_L)^{m}} \qquad (11)$$

where $\log \ell$ = absorption expressed in decibels,

$A$ = a constant,

$\chi$ = solar zenith angle,

$f$ = wave frequency

and $f_L$ = longitudinal component of gyrofrequency.

(a) Solar control of absorption of radio waves reflected from the ionosphere

At a given frequency the absorption varies as $\cos^{n}\chi$. In the case of nondeviative absorption for the Chapman type layer, Appleton (1937) showed that $\int k\,ds \propto (\cos\chi)^{3/2}$. The values of the index n obtained from experiments were generally less then the theoretical value 3/2. Appleton and Piggott (1954) obtained a value of 0.75 for Slough. Skinner and Wright (1956) showed for equatorial station that $\log \ell \propto (\cos\chi)^{0.7}$. The value of n determined from cosmic noise methods is higher than that obtained by the pulse method. Mitra and Shain (1953) obtained 1.1, 0.9 and 0.8 for summer, equinoxes and winter respectively at Hornsby using 18.3 MHz CR noise. Those obtained by Bhonsle during IGY period at Ahmedabad were comparable with Mitra and Shain's values.

(b) Frequency variation of absorption

According to the quasilongitudinal approximation of magneto-ionic theory, when the collision frequency is small compared with the wave frequency, the value of the index m is obtained as 2.0. Results of multifrequency absorption measurements made at middle and high latitude stations are found to agree with the theory. At equatorial and low latitude stations the value of the index m is found to be less than 2.0. In this connection the results of Skinner and Wright (1956) obtained for Ibadan are interesting. These authors obtained a value m = 1.0. The discrepancy between theory and observation was explained by them as due to the neglect of the collision frequency in the original derivation. They showed that when becomes comparable with the exploring frequency, the value of m can fall rapidly from 2.0, and the low value obtained by them was attributed to the lower height of the absorbing region. Ramamurthy and Ramachandra Rao (1964) working at Waltair, a low latitude station, obtained m = 1.5 and noted that there is a systematic increase in the value of m as we go from the equator towards higher latitudes.

The occurrence of a strong solar flare provides an excellent opportunity for determining the dependence of ionospheric absorption on the zenith angle and on frequency. This is possible if the flare is recorded on a number of riometers situated at different stations, corresponding to different zenith angles at a given frequency and at different frequencies for a given zenith angle. Since the solar flare effect is mainly in the D region

the value of n and m for this region can be accurately determined from such a study. Horowitch and Goldman (1963), using a flare event recorded at Accra, Addis Ababa, Athens, Hermanus, New Delhi and Bedford, obtained n = 1.5 and m = 2.0 (frequencies used were 28, 30, 27.6 and 58 MHz). Analysis of a recent flare observation by the present author, simultaneously at Thumba (near magnetic equator) and at Ahmedabad at frequencies 25, 21.3 and 16.5 MHz yielded n = 3/2 (at Ahmedabad and Thumba) and m = 2 (for Ahmedabad) and m = 1.6 (for Thumba).

1.12 Use of multifrequency observation of cosmic noise absorption to derive electron density profiles in the lower ionosphere

The value of the index n, which shows the frequency variation of absorption between any two frequencies, varies with height due to the height variation of collision frequency . A new method of deriving electron density profiles in the lower ionosphere from simultaneous measurement of ionospheric absorption at a number of frequencies which satisfy the above condition has been developed by Parthasarathy et al (1963). For higher height and frequency ranges, m approaches the value 2.0 and for lower ranges it decreases rapidly.

They applied the method to derive electron density profiles during a polar cap absorption event in July 1961. The profiles showed that electron density greater than $10^2$ occured at a height as low as 35 km during that disturbance. A determination of the height of the absorbing layer is of considerable importance

to understand various modes of propagation during quiet as well as disturbed periods.

## 1.13 Latitudinal variation of cosmic noise absorption

It is clear that both D and F regions contribute to the absorption of cosmic radio noise. The D region absorption depends on the product of the densities of electrons and neutral particles while the F region absorption is very sensitive to the critical frequency of the layer ($f_0F_2$). It is wellknown that the latitudinal variation of $f_0F_2$ shows a maximum at about $15^0$ geomagnetic latitude with a trough at the magnetic equator. $f_0F_2$ decreases by a factor of approximately one half from geomagnetic latitude $15^0$ to $60^0$. The corresponding decrease in the F region absorption, assuming that the absorption is proportional to $f_0F_2^4$, should be by a factor 1/16. Such a latitudinal variation does not occur in D region absorption. Thus the relative contribution from the F region to the total attenuation of cosmic radio noise is maximum at geomagnetic latitude near $15^0$ and decreases rapidly as we go towards higher latitudes. The total absorption measured at higher latitudes is essentially D region absorption.

# CHAPTER II

## EXPERIMENTAL SET UP FOR RECORDING COSMIC RADIO NOISE AT 21.3 MHz AND 16.5 MHz AT AHMEDABAD AND THUMBA

### 2.1 Introduction

A simple equipment to record the cosmic radio noise intensity was set up by Bhonsle et Ahmedabad in 1956. It consists of a directive antenna connected to the input side of a sensitive receiver through a transmission line. The detected output of the receiver which is a measure of the input power is further amplified using a dc amplifier and is fed to a recording milliammeter. Calibration of the record is done using a noise generator which can replace the antenna whenever required. The basic disadvantage in this system is that the record is susceptible to variations in the gain of the receiver. The gain of the receiver has to be assumed to remain constant between two calibrations. The detected output being usually nonlinear is another disadvantage. Little and Leinbeck (1958) devised a new instrument called riometer (relative ionospheric opacity meter) at College Alaska to overcome the main disadvantages of the total noise power recording meter. The riometer has now become a valuable tool for the study of ionospheric propagation and absorption.

### 2.2 Principle of operation of a riometer

The riometer is a self balancing system in which the

noise power generated in a local noise source (a noise diode) is compared to that received from the antenna and adjusted till it becomes equal to the antenna power. The receiver input is switched at a rate of about 340 cps using an rf switching unit. Any inequality between the power from the antenna and the noise diode will result in a square wave output at the switching frequency at the receiver detector. The amplitude of the square wave depends on the degree of inequality between the two signals. This is further amplified in an audio amplifier and detected in a phase sensitive detector the output of which is proportional to the square wave amplitude. The polarity of the phase detected output is determined by the stronger signal (either antenna or noise diode signal). This dc signal is further amplified and is used to vary the filament temperature which changes the power output of the noise diode in such a way as to make the difference between the two signals equal to zero. Thus the local noise power is always made equal to the noise power from the antenna. As the noise power from the diode is proportional to the dc current flowing through it, the antenna noise, in effect, can be measured on a linear scale by recording this dc current.

## 2.3 Circuit details

Fig.2.1(a) shows the block diagram of the riometer at 21.3 MHz and 16.5 MHz constructed by the author on the basis of the original design given by Little and Leinbeck. The 21.3 MHz riometer is in operation at Ahmedabad since 1963 and the 21.3 and 16.5 MHz riometers have been working at Thumba since 1964-65.

# BLOCK DIAGRAM OF RIOMETER

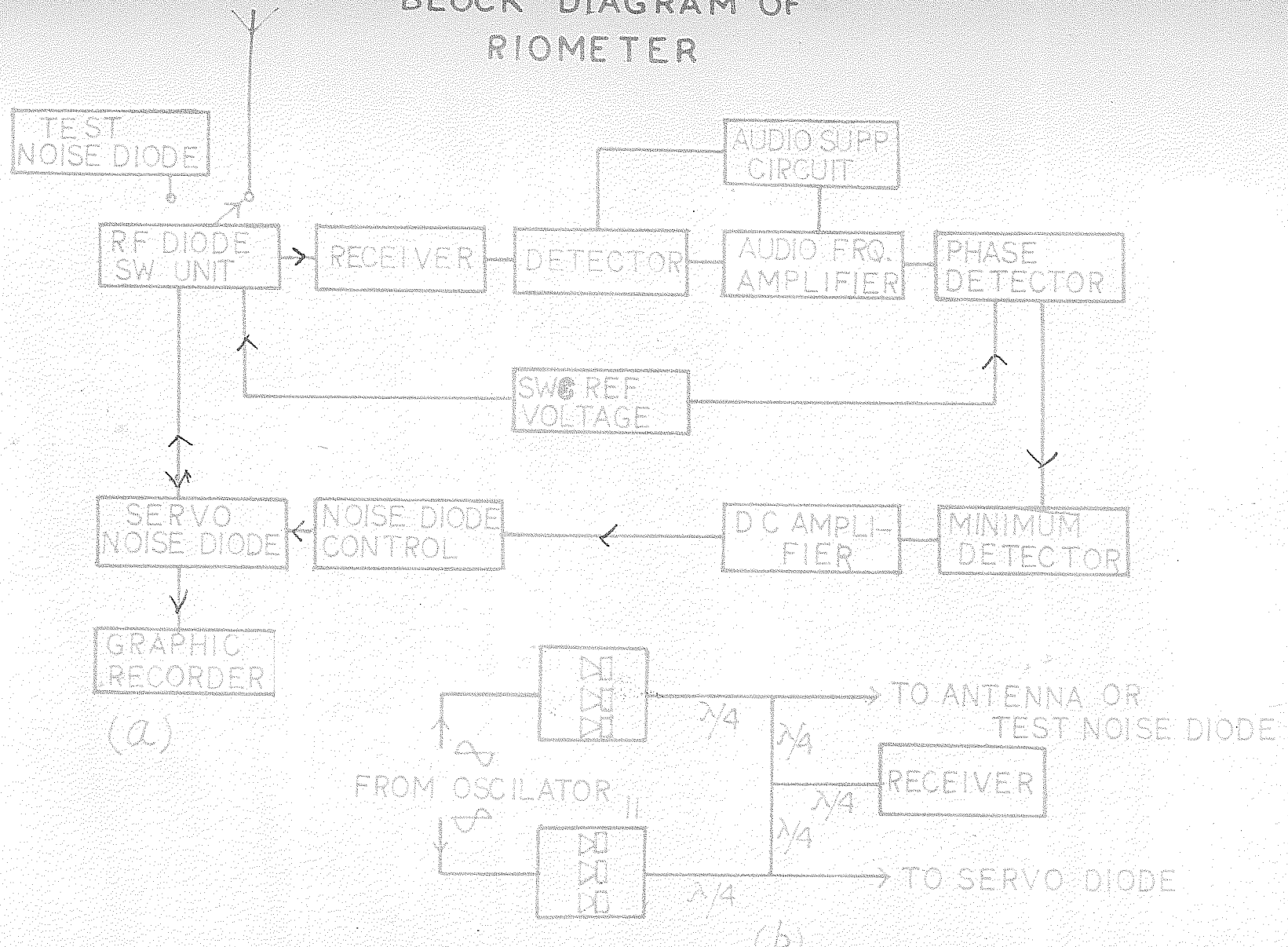


FIG. 2.1

Certain modifications were made in the original circuit to suit our requirements and local conditions. A brief description of the circuits is given below.

(1) Diode switching unit

Schematic diagram of the diode switching unit for switching the receiver input to antenna and noise diode is shown in Fig.2.1(b). A sine wave of 340 cps generated by a phase shift oscillator is fed to the diode switches (See Fig.2.2(a)). The output of the phase shift oscillator is also used as a reference voltage for the phase sensitive detector. The switching unit is designed with a view to obtain (1) a large switching ratio between the on and off conditions, (2) a small feed-through loss in the on condition, (3) negligible noise generation in the unit itself and (4) long term stability. It consists of three 1N270 crystal diodes connected in parallel and a net work of quarter wavelength transmission lines connected as shown in Fig.2.1(b). The voltage from the phase shift oscillator is fed to the two sections of the switch out of phase. When one section of the diode switch conducts, the end of the transmission line connected to it becomes shorted, reflecting an open circuit at the other end of the quarter wave line to which the antenna is connected. The end of the quarter wave line corresponding to the other section and to which the noise diode is connected then becomes shorted. Thus the receiver accepts power from either the antenna or the noise diode during each half cycle of the oscillator output.

(ii) Audio suppression circuit

In the presence of an interfering signal, the riometer is subject to overloading, due to the high gain of the system. The audio suppression circuit is incorporated to prevent overloading. The circuit diagram of this is shown in Fig.2.2(a). The detected output of the receiver is dc coupled to the grid of the suppression tube (6AH6 sharp cutoff pentode) and ac coupled to the plate of the same tube and the grid of 12AU7 AF amplifier. The 6AH6 tube is kept in cutoff position for normal cosmic noise intensities using the bias control potentiometer. In the presence of an interfering signal more powerful than the cosmic noise, this tube starts conducting, lowering the plate voltage, from about 80 V to 30 V and the grid potential of 12AU7. This will cutoff the audio amplifier, and the servo-loop will be broken, preventing the servo noise diode from following the interfering signal. During the time the servo-loop is interrupted, the noise diode current rises to a level determined by the bias setting of the 6Y6 control tube.

(iii) Interference discrimination

The sweep frequency and minimum detecting technique is incorporated in the riometer to discriminate against unwanted signals. This ensures that the riometer records the minimum signal strength received, as a 6-8 kc/s exploring band is swept through a 100 kc/s search band once every minute. The mode of operation is as follows,

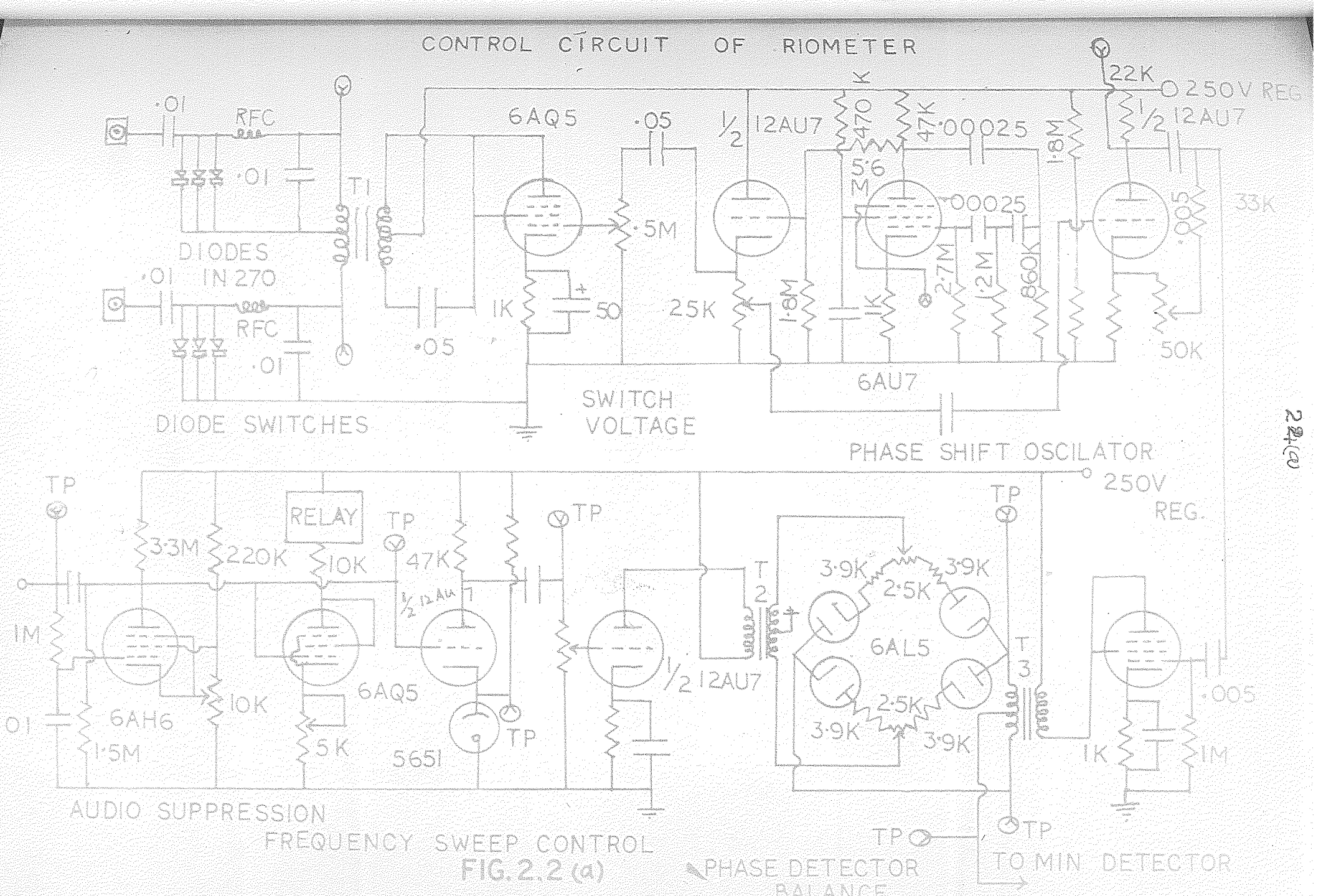
CONTROL CIRCUIT OF RIOMETER
.01
RFC
.01
T1
DIODES IN 270
.01
RFC
.01
DIODE SWITCHES
6AQ5
.05
1/2 12AU7
.5M
1K
50
.05
SWITCH VOLTAGE
25K
5.6 M
.00025
2.7M
2.2M
860K
6AU7
22K
250V REG
1/2 12AU7
33K
50K
PHASE SHIFT OSCILATOR
TP
3.3M
220K
RELAY
10K
TP
47K
1/2 12AU7
TP
1M
6AH6
1.5M
10K
5K
6AQ5
5651
TP
1/2 12AU7
T2
3.9K
2.5K
3.9K
6AL5
2.5K
3.9K
3.9K
T3
TP
250V REG.
.005
1K
1M
AUDIO SUPPRESSION
FREQUENCY SWEEP CONTROL
TP
PHASE DETECTOR BALANCE
TP
TO MIN DETECTOR

FIG. 2.2 (a)

2.21(a)

# CONTROL CIRCUIT OF RIOMETER

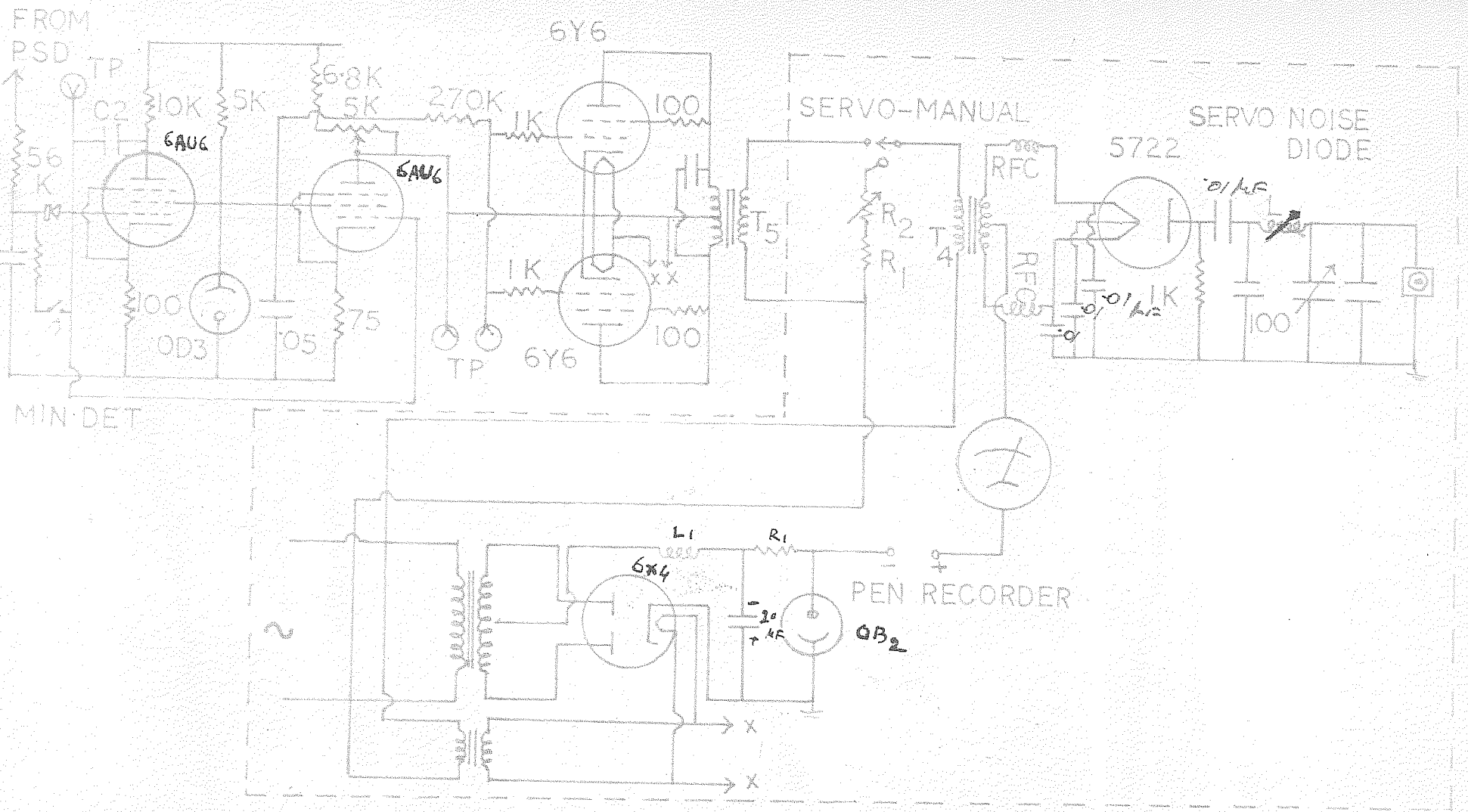


FIG. 2.2(b)

During the frequency sweep, when the receiver tunes to any signal stronger than the cosmic noise level, a positivegoing pulse appears at the output of the phase sensitive detector. This reverse biases the IN270 minimum detector diode (See Fig.2.2(b) and makes it nonconducting. The resulting large impedance in combination with the large capacitance of 6AU6 amplifier presents a large time constant (of the order of 30-40 second) for the stronger signal. The negative going pulse will have a very short time constant. Thus if there is a clear channel for the cosmic noise in the search band, that level will be recorded. The minimum signal level thus recorded will be the cosmic noise level.

(iv) Modifications made in the sweep system of 16.5 MHz riometer

The usual type of interference signals encountered are those from broadcasting stations. The above method of discrimination against the unwanted signal is found to work well, when there are not more than two or three interference sources in the search band. This is found to be so in the case of 21.3 MHz riometer; but greater interference is found to be present in the band at 16.5 MHz and the record obtained is found to be unsatisfactory for most of the time. This was overcome by modifying the system as follows. The sweeping of the frequency is not done continuously, but the frequency is kept constant in the absence of any interfering signal, and is made to drift only when any interfering signal is received. The frequency continues to drift till the interfering signal is detuned, and then remains at that position till the next interfering signal is detected. The operation of this system is as follows.

The plate side of the audio suppression tube which is connected to the grid of 12AU7 audio amplifier is also coupled to the grid of a power amplifier tube 6AQ5 (see Fig.2.2(a)). The plate circuit of 6AQ5 contains a relay as shown in the figure. The voltage variations (of the order of 30 to 40 V) produced in the plate of 6AL6 tube due to an interfering signal, can cause current variations in the plate of 6AQ5 sufficient to trigger the relay on or off. The optimum condition can be set using the bias control. The relay used in the equipment can be operated with a current of about 8-10 mA. The relay switches on or off the mechanical sweeping system which consists of an electric motor and a sweeping condenser.

(v) Receiver

A single conversion super heterodyne communication receiver (Eddystone 680X) is used for the 21.3 MHz riometer. The two rf sections and three if sections of the receiver provide sufficient gain of the order of $10^6$. A Hammerlund communication receiver (SP600) of double conversion type is used for the 16.5 MHz riometer set up at Thumba. These are operated at bandwidths of 8 and 10 kc/s.

The frequency sweep is done mechanically as follows. Small butterfly condensers are mounted on a spindle with appropriate spacing in between, so that each condenser can be connected to each section of the main tuning gang condenser of the receiver. The spindle is then rotated by an electric motor at a rate of one rpm. In the case of 21.3 MHz the sweeping is

done continuously while for 16.5 MHz. sweeping is done only when interfering signals are present as explained above.

(vi) Noise diode control circuits

This consists basically of two variable reactance transformers, $T_4$ and $T_5$ whose primaries are connected in series. The secondary of $T_5$ is the plate load of 6Y6 servo-control tube (see Fig.2.2(b)). The currents through these tubes are controlled by the amplified dc signals from the phase sensitive detector. A positive signal from the phase sensitive detector corresponds to a higher antenna power than the noise diode signal and it decreases the grid bias of 6AU6 dc amplifier and hence its plate potential. The bias of 6Y6 is thus reduced since the cathode of this tube is coupled to the plate of the 6AU6. Due to the resulting increase in the plate current the reactance of the primary of $T_5$ is reduced, causing more voltage to develop across the primary of $T_4$. This increases the filament temperature of the noise diode till the noise power from the noise diode becomes equal to that from the antenna and the dc signal in the phase detected output becomes zero. A negative signal acts in a reverse way.

(vii) Noise diode plate circuit and its matching to the receiver input

The plate circuit of the servo noise diode is shown in Fig.2.2(b). It is necessary that the noise diode should operate within a certain optimum range of the dc current flowing

through the tube. Therefore it is required that the plate load across which the noise power of the diode is generated has to be adjusted, depending on the cosmic radio noise frequency. For the lower ranges of the exploring frequency, the load resistance has to be increased, as otherwise a large current will flow through the diode to match with the large cosmic noise power available at that frequency. This reduces the life of the diode. A load resistance of 1-1.5 K is found suitable for the frequency range 15-20 MHz when the noise diode current is between 5-10 ma.

The total noise power developed across the load is to be fed to the receiver without any loss in the feeding system. The receiver input impedence is usually 70-100 ohms. The matching of the two impedances is done by means of a $\pi$ network which makes the noise diode load look like the receiver impedance. Accurate matching was done using a GR admittance meter. The difference between the equivalent noise input power of the receiver, when connected to the cold impedances of antenna and noise diode, can itself generate a square wave at the detector of the receiver and affect the reading. Considerable attention was given to the impedance matching since this difference can be made zero only if the antenna and noise diode present equal impedance to the receiver input when connected via the switch.

## 2.4 Calibration of the records

For calibrating the records, the antenna is replaced by a standard noise source i.e. the test noise diode, the circuit diagram of which is the same as that of the servo noise diode

(shown in the dotted lines in Fig.2.2(b)). Due to the fact that the riometer records are insensitive to relative changes in the receiver gain, the system has got long-term stability and unlike in the case of total power equipment, frequent calibration is not necessary. However calibration was done every day to ensure the reliability of the records.

## 2.5 Directional aerial used for cosmic radio noise measurement at 21.3, 16.5 and 25 MHz

The antenna used is a broadside collinear array consisting of 16 halfwave dipoles spread in E-W direction in 4 rows and 4 columns. The schematic diagram of the aerial is shown in Fig.2.3. The aerial is backed by a parallel wire reflecting screen stretched along the ground at a distance of $0.2\lambda$ below the dipole elements. This arrangement increases the gain of the antenna by a factor of 2 and maintains constant reflectivity under changing meteorological conditions. The aerial is directed vertically upward. For a broadside collinear array of this type a spacing of $0.5\lambda$ between adjacent rows is particularly convenient since right phase relationship is easily obtained by the feeder lines. The total impedance of the antenna is easy to estimate since the elements are all in parallel. The beamwidth of the aerial array to half-power points is approximately given by $60\ \lambda/a$ in degrees, where a is length of the array in terms of wavelength and $\lambda$ the wavelength. In the case of our antenna, the length in E-W direction is $2\lambda$ and the width is $3/2\ \lambda$. This means that the beamwidth of our aerial

BROADSIDE COLLINEAR ARRAY FOR RECEIVING COSMIC RADIO NOISE

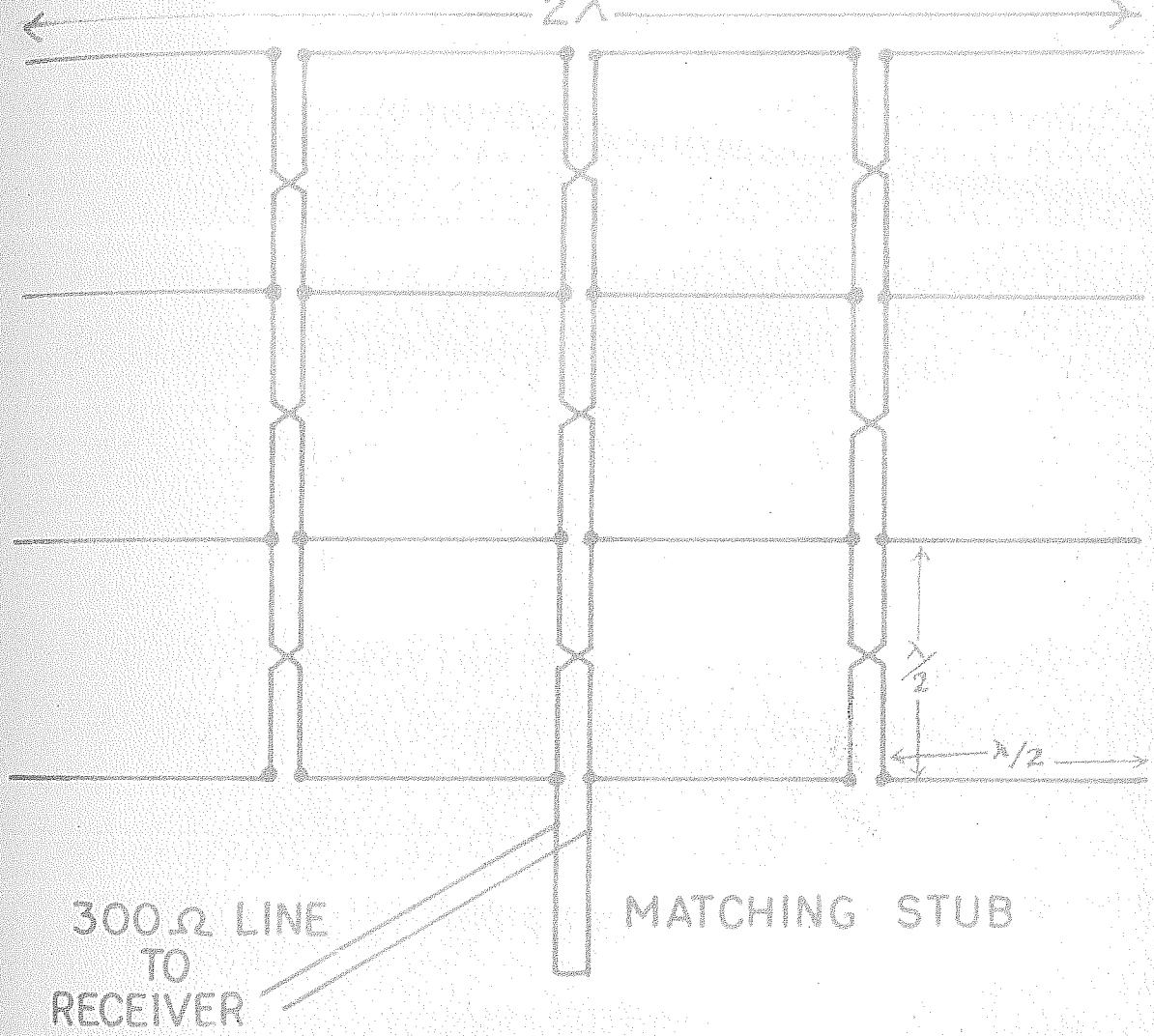


NUMBER OF DIPOLES, 16
CALCULATED GAIN, 17.2 DBS
BEAMWIDTH TO HALF POWER POINTS, 30° N.S PLANE
40° E.W "

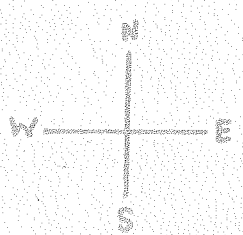


FIG. 2.3

to half-power points is about $30^{\circ}$ in E-W and $40^{\circ}$ in N-S plane. The power gain of an array over a single dipole is equal to the product n (number of half wave dipoles) and the absolute gain G, and is equal to 1.64 x n. As there is a conducting screen behind the aerial, the whole energy is concentrated in one direction and the gain is increased by a factor of 2. Thus the absolute gain of our array is equal to 3.28 x 16 = 52.48, i.e. equivalent to 17.2 db over an isotropic radiator.

(i) Matching of the antenna to the receiver

It is known that the impedance of a thin full wave dipole fed at the centre is about 2000 ohms and hence four full wave dipoles in parallel give an impedance of about 500 ohms (balanced) in our case. It should be noted that the antenna may be considered to be in parallel since they are spaced at interval of $\lambda/2$ along the feeder and the feeder is twisted round between each full wave dipole so as to obtain correct phase relation for broadside radiation. Matching of the antenna impedance of 500 ohms to the switching unit through a 75 ohm coaxial cable is done as follows.

A balanced parallel wire transmission line of 300 ohms impedance is connected to the antenna impedance of 500 ohms. A transmission line having a length less than $\lambda/4$ when terminated with an impedance greater than the characteristic impedance of the line, will have a reactive component of input impedance which is capacitive. If this can be tuned out by connecting another line of equal impedance but of opposite sign (inductive),

then the input impedance becomes purely resistive and is the same as the characteristic impedance of the line. This principle is used and the matching is done by means of a shorted stub of appropriate length. The transmission line of 300 ohms impedance is then connected to a balun transformer which converts it into an impedance of 75 ohms unbalanced. The output from the balun is then connected to the switching cable network through RG 11A/U coaxial cable. Final matching was done by adjusting the position of the stub slightly to obtain the same impedance as that of the noise diode when seen from the receiver input end. This was done with the help of a CR admittance meter.

We shall describe in the next section some sample records of CR noise intensity recorded at 45, 25, 21.3 and 16.5 MHz at Ahmedabad and at Thumba.

## 2.6 CR noise records

Some sample records of cosmic radio noise on 16.5, 21.3 and 45 MHz taken at Ahmedabad and Thumba with a riometer are shown in Fig.2.4 and Fig.2.5. A 25 MHz CR noise record made at Ahmedabad by the total power type radiometer is also shown in Fig.2.4. The normal chart speed of the records is one inch per hour and the time is adjusted to $75^{\circ}$ EMT at Ahmedabad and to the Indian Standard Time at Thumba. IST is ahead of EMT by half an hour. The intensity of CR noise at a given time depends upon the portion of the sky which the aerial is looking at and the ionospheric attenuation.

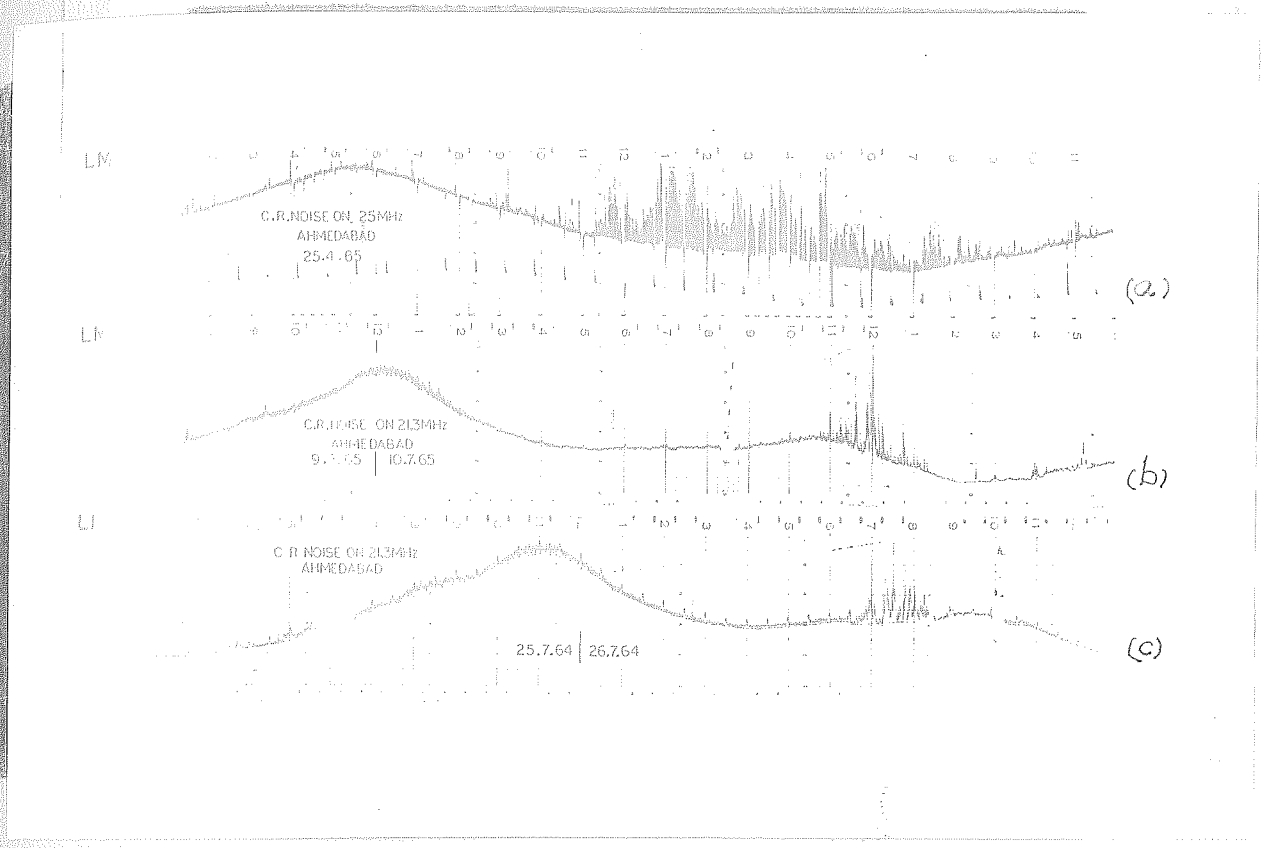


Fig.2.4 Sample records of cosmic radio noise at Ahmedabad

(a) at 25 MHz on 25th April 1965; the spikes between 11 hr and 20 hr LMT are due to atmospherics,

(b) at 21.3 MHz on 9 and 10 July 1965; solar radio bursts can be seen between 11 hr and 13 hr LMT and

(c) at 21.3 MHz on 25 and 26 July 1964; radio bursts from Jupiter can be seen between 6-30 hr and 6-30 hr LMT.

Fig.2.4(a) illustrates the CR noise record at 25 MHz on 25 April 1965. The receiver noise level is recorded automatically once every 45 minutes by replacing the aerial with an equivalent cold impedance at the receiver input, by means of a relay. The zero noise level marks can be seen on the records. The recording instrument is automatically paralysed to avoid

pick up of strong rf radiation from the nearby ionosonde. In this record the galactic peak corresponding to the passage of the galactic equator over the antenna beam occurs between 5 and 6 hr LMT. This corresponds to 19 hr sidereal time. We see a broad maximum because of the galaxy being a diffuse source. After about 10 hrs we see another small peak when the galactic equator once again crosses the antenna beam. Calibration of the record is done every day. Between 11 and 20 hrs we can see the record being disturbed due to atmospherics.

Fig.2.4(b) illustrates the riometer record at 21.3 MHz made at Ahmedabad on 9th and 10th July 1965. Since recording is possible on a linear scale using riometer technique, the galactic peak can be seen more prominently than in Fig.2.4(a). The zero levels at frequent intervals is not necessary here since the receiver noise is eliminated in the riometer. The short duration disturbances seen at intervals of 30 minutes or more in this otherwise smooth record is due to the pick up from the nearby pulse transmitter of the ionosonde. The galactic peak on 10th July 1965 occured at about 00 hr LMT. A powerful solar radio burst accompanied by noise storm is recorded between 11 and 13 hrs on 10 July 1965. Calibration of the records is done between 8 and 9 hr LMT every day by replacing the antenna by a test noise diode and marking on the chart the levels of servo noise diode currents corresponding to a number of equal steps of test noise diode currents. Another record on 28 July 1965 is shown in Fig.2.4(c). A noise storm which can be seen in this record

between 0630 and 0830 LMT corresponds to the passage of planet Jupiter over the antenna beam. Several such powerful Jupiter radio noise bursts have been recorded at Ahmedabad at 25 and 16.5 MHz also.

Fig.2.5(a) and (b) illustrate the records of CR noise intensity made at Thumba (situated at the magnetic equator) using 16.5 and 21.3 MHz riometers. It should be noted that the time is adjusted to IST which is half an hour ahead of LMT.

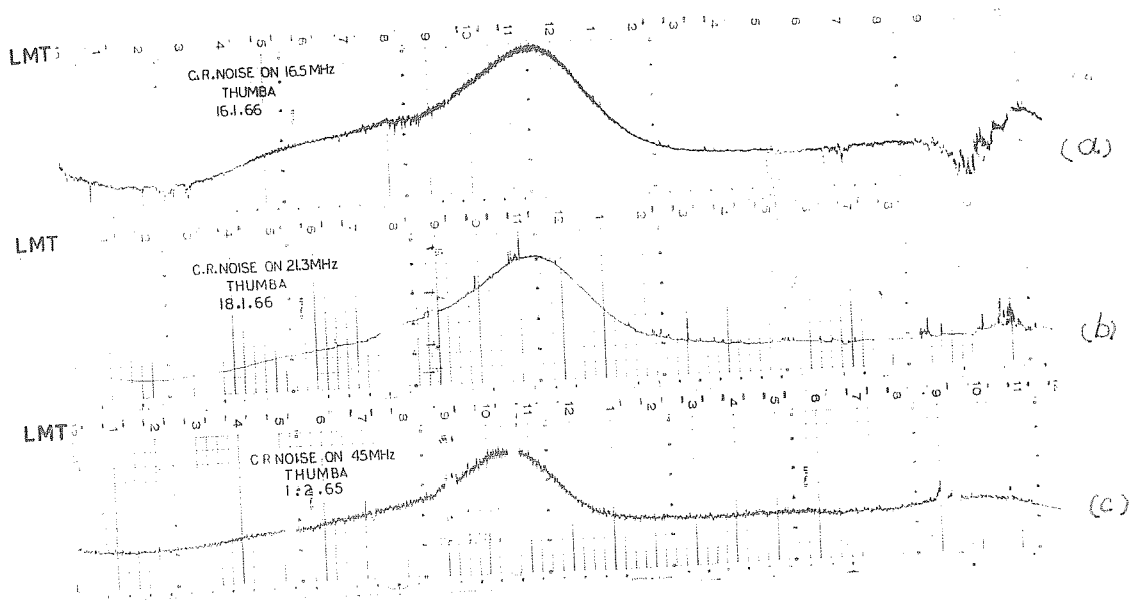


Fig.2.5 Sample records of cosmic radio noise at Thumba

(a) at 16.5 MHz on 16 January 1966,

(b) at 21.3 MHz on 18 January 1966; Jupiter radio bursts can be seen between 22 hr and 23 hr IST and

(c) at 45 MHz on 1 February 1965.

The record at 16.5 MHz is broader as compared to 21.3 MHz record. This is because the receiver bandwidth in the former case is only 8 KHz as against 70 KHz for the latter which can suppress short period fluctuations effectively. The galactic peak appears to be much sharper in Thumba than at Ahmedabad even though identical antennas are used. This is due to the latitude difference of the two places with respect to the galactic nucleus.

A moderate radio burst from Jupiter can be seen on 21.3 MHz record in Fig.2.5(b) at about 23 hr IST. There are some records when the Jupiter radio bursts have exceeded the galactic radio noise peak intensity.

## 2.7 A comparison of CR noise record of 45 and 21.3 MHz

Observation of CR noise was carried out at 45 MHz and 21.3 MHz both at Ahmedabad and Thumba with a view to compare the shape of the curves at these frequencies under minimum ionospheric attenuation condition. As can be seen in Fig.2.6(a) and (b), the galactic peak at 45 MHz is more prominent than at 21.3 MHz. This is also illustrated in Fig.2.7, where the cosmic radio noise intensity normalised to minimum intensity is compared between 21.3 and 45 MHz at Ahmedabad. It can be seen that the normalised intensity in the direction of the galactic equator is more at the higher frequency than at lower frequency. This is in agreement with the multifrequency observations using narrow beam antenna (Ellis and Hamilton, 1964) and is believed to be due to the larger

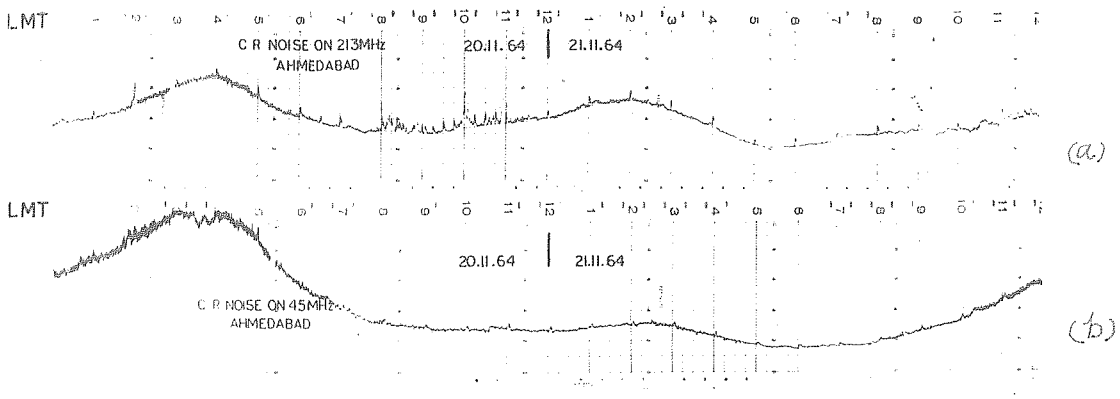


Fig.2.6 Sample records of cosmic radio noise at Ahmedabad

(a) at 21.3 MHz on 20 and 21 November 1964,

(b) at 45 MHz on the same day. It may be noted that the radio bursts from Jupitor at 21.3 MHz seen between 8 and 1130 hr LMT is absent at 45 MHz.

absorption of low frequency cosmic radio waves by the interstellar ionized gas in the galactic disc. The first evidence of this kind was obtained by Shain (1951) who observed that the ratio of maximum to minimum galactic radio noise intensity was more at 100 MHz than at 18 MHz in the strip of the sky centered around $-34^{\circ}$ declination. It is possible to calculate the density of the absorbing matter in the direction of galactic equator if observations are made at a wide range of frequencies

# AHMEDABAD

Cosmic radio noise recorded at Ahmedabad on 45 and 21.3 MHz normalized to the minimum intensity

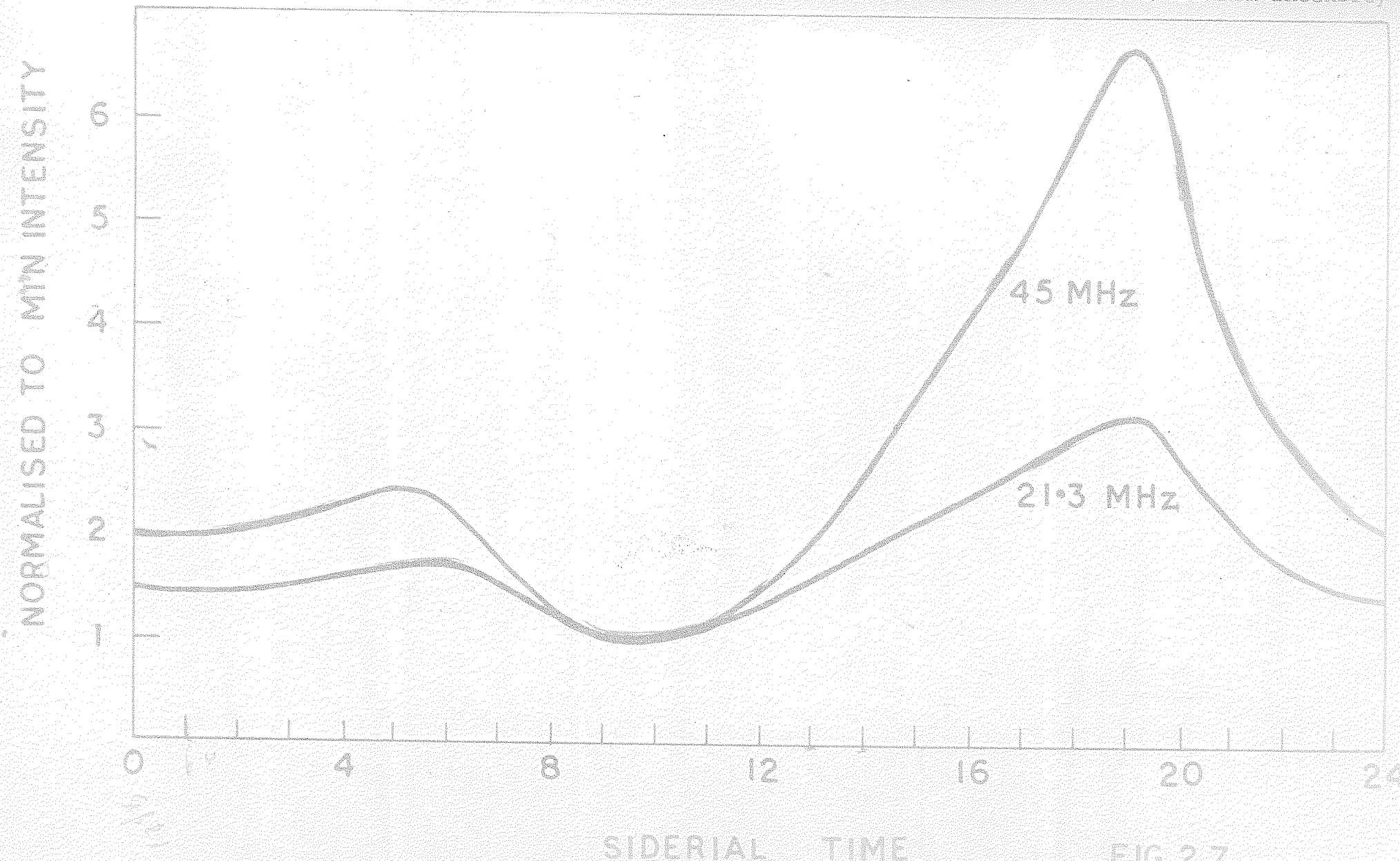


FIG.2.7

using very narrow beam antennas. An interesting point which may be noted with reference to Fig.2.6(a) and (b) is that the Jupitor radio bursts recorded between 20-23 hr on 21.3 MHz are completely free at 45 MHz.

## 2.8 Standard CR noise curve used for calculating the ionospheric absorption

To calculate the amount of ionospheric absorption of cosmic radio noise received at the ground, it is first necessary to know its intensity outside the earth's atmosphere. As the directional antenna fixed on the ground scans the same portion of the sky once in a day due to earth's rotation, the intensity of cosmic radio noise received on the ground depends on the sidereal time and the transparency of the earth's atmosphere. A curve showing the intensity variation for a complete sidereal day is first prepared. This can be done with good accuracy if one has got reliable data for one year. From this data, the value of CR noise intensity for each sidereal hour with minimum ionospheric attenuation is determined. The time of minimum attenuation usually occurs between 03 and 06 hrs IST, when the critical frequency of $F_2$ layer is minimum. Good data obtained at these hours are plotted against sidereal time for one complete year to correspond to one sidereal day. The envelope of all the points showing maximum intensity is taken to represent the unattenuated standard curve. Fig.2.8 shows the standard curve, thus obtained for 25 and 21.3 MHz. It is a smooth double humped curve. The smaller hump occurs at 06 hr and the larger one at

19 hr sidereal time with a sharp minimum at about 09 hr sidereal time. It may be noted that the curves for both frequencies are similar in shape. Their intensities shown in terms of the calibrating noise diode current in milli-amperes are however different for the two cases, since they depend on the value of the plate load of the noise diode.

Now if one compares the observed intensity at any hour with that given by the standard curve for the same sidereal time, then one can calculate the ionospheric attenuation by the following formula.

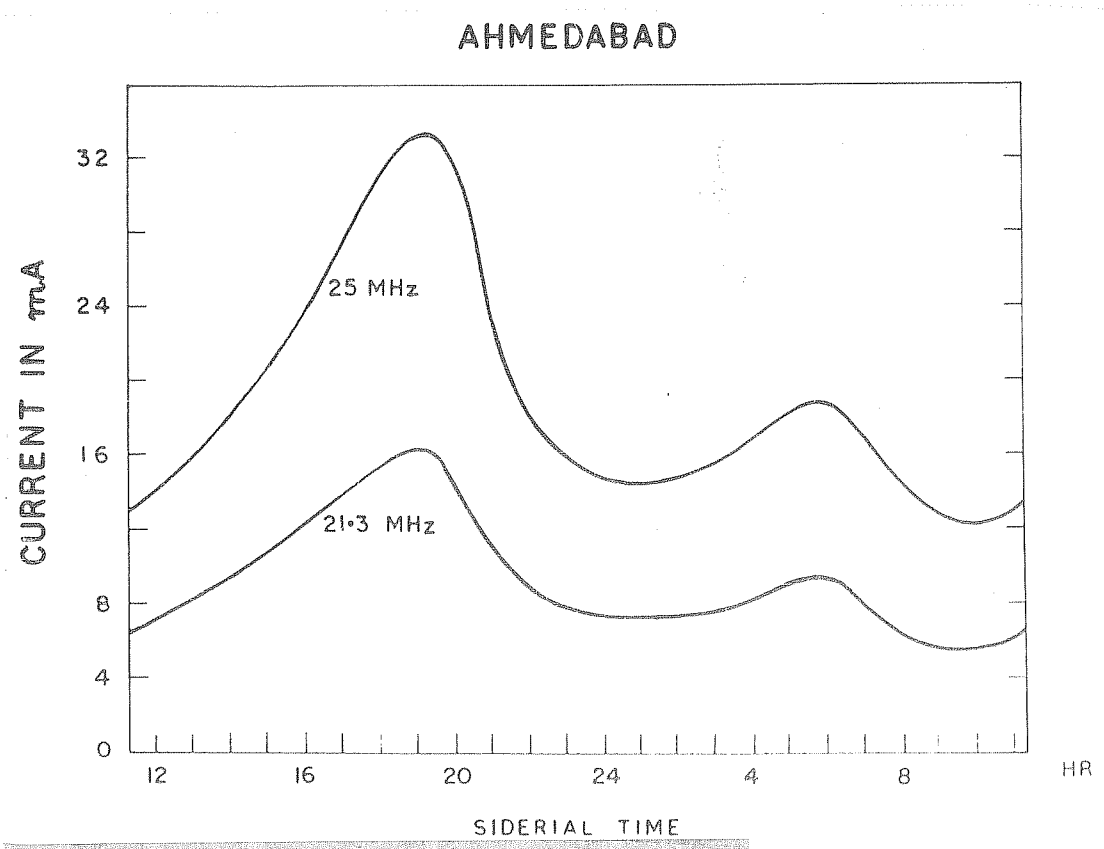


Fig.2.8 Standard curves at 25 MHz and 21.3 MHz for Ahmedabad.

$$\text{Attenuation in decibels} = 10 \log_{10} (P_s/P_o) \qquad (1)$$

where $P_s$ and $P_o$ are the unattenuated and the observed noise power respectively at the same sidereal time. The noise power however is calibrated in terms of the local noise diode current and hence the above expression may be written as

$$\text{Attenuation in decibels} = 10 \log_{10} (I_s/I_o) \qquad (2)$$

where $I_s$ is the calibration current corresponding to the CR noise intensity on the standard curve at any sidereal hour and $I_o$ the observed value at the same sidereal times.

## 2.9 Standard curve at 25 MHz from 1958-65

The standard curves obtained as explained above for each year from 1958-65 were examined to find out the long term variation of the intensity, if any, which can arise due to reasons such as (1) a solar cycle variation in absorption under minimum $f_oF_2$ condition of the ionosphere and (2) any additional noise source in the direction of the antenna beam such as from Van Allen radiation belts, whose intensity can vary in the course of observation. A study of the shape of the standard curve after normalising the intensity at each sidereal hour to that corresponding to the minimum of the curve did not show any noticeable long term change from 1958-65.

## 2.10 Changes observed in CR noise intensity following high altitude nuclear explosion of 9 July 1962

Certain short term changed which were detected in the 25 MHz standard curve had interesting origin. For example, there was a sudden increase in the noise intensity in July 1962 associated with the high altitude nuclear bomb explosion on 9-7-62 over Johnston Island. The synchrotron radiation emitted by the relativistic electrons, generated in the explosion and trapped in the earths magnetic field was observed at several riometer stations (Oches et al, 1963). Dyce and Horowitch (1963) reported maximum signal strength at equatorial stations. The synchrotron radiation decreased as the observing point moved away from the equator. No signal could be detected by the riometers situated at latitudes more than about $20^{\circ}$ geomagnetic latitude. In Fig.2.9 we have plotted the cosmic radio noise intensity each day at 06 hr LMT from June to October 1962 at Ahmedabad and a continuous line is drawn through them. The date of the explosion was 9 July 1962 and is indicated by an arrow. We can see a sudden increase in the noise intensity following the explosion, which continued to increase for a week after the explosion and remained nearly steady for about 3 weeks before decaying. The broken line drawn through these points shows the part of the standard curve during this period corresponding to 1961. It can be seen that the enhanced intensity continued for about two months after the event. At equatorial stations such as Huancayo (Dyce and Horowitch, 1963) the increased intensity persisted for a much longer time.

CHANGES IN 25 MHz CR NOISE INTENSITY FOLLOWING THE HIGH ALTITUDE NUCLEAR EXPLOSION ON 9 JULY 1962 FIG. 29

# CHAPTER III

## RESULTS OF COSMIC RADIO NOISE ABSORPTION MEASUREMENTS AT 21.3 AND 25 MHz MADE AT AHMEDABAD DURING THE LOW SUNSPOT YEARS 1963-65

### 3.1 Introduction

A summary of the results of absorption measurements made at various places using cosmic radio noise technique is given in Chapter I including the work done at Ahmedabad on 25 MHz during 1957-59. In this chapter the results at 21.3 and 25 MHz for the low sunspot years 1963, 1964 and 1965 are presented. As mentioned before, a riometer has been installed at Ahmedabad at 21.3 MHz since 1963 in addition to the 25 MHz CR noise equipment. The 21.3 MHz riometer data are considered to be very satisfactory and hence more weight is given to it in discussing the results.

Absorption of the cosmic radio noise was calculated for those hours at which reliable observations were available in 1963-65 using the standard curve as described in the earlier chapter. On an average, good data are available for over 25 days in a month. Monthly mean diurnal variation of absorption was worked out.

### 3.2 Total absorption of cosmic radio noise in the ionosphere

Fig.3.1(a) and (b) shows the monthly mean diurnal variation of absorption for 21.3 MHz radio noise for the years 1963, 1964 and 1965. The corresponding absorption values at 25 MHz are shown in Fig.3.2(a) and (b) for 1964 and 1965. These

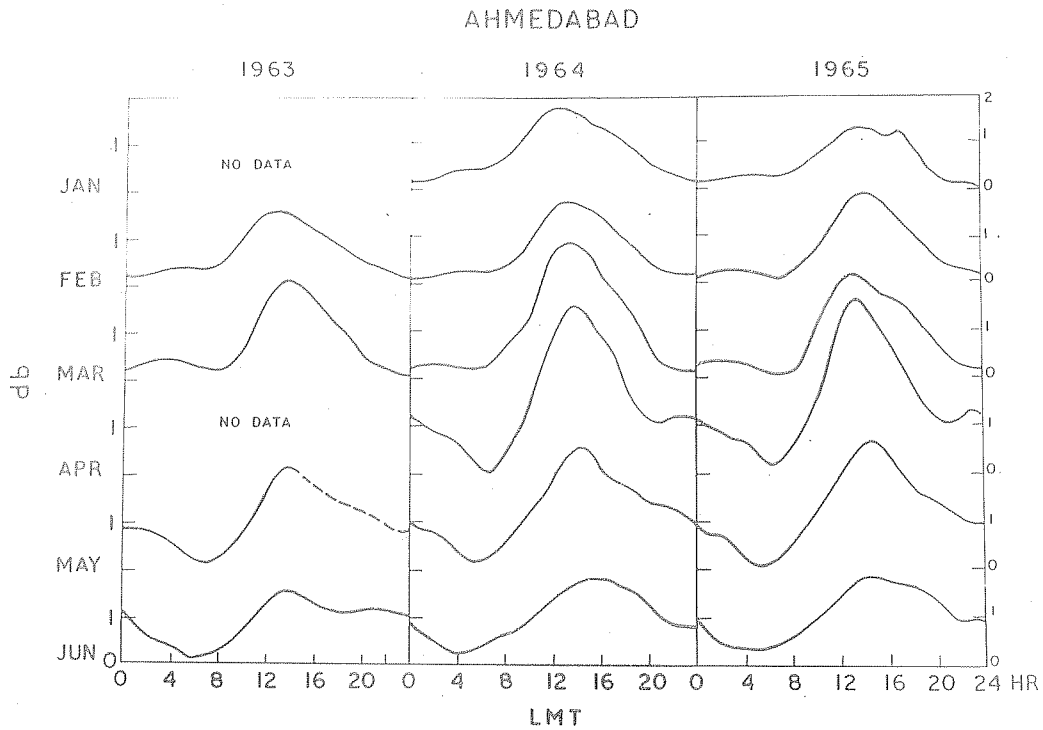


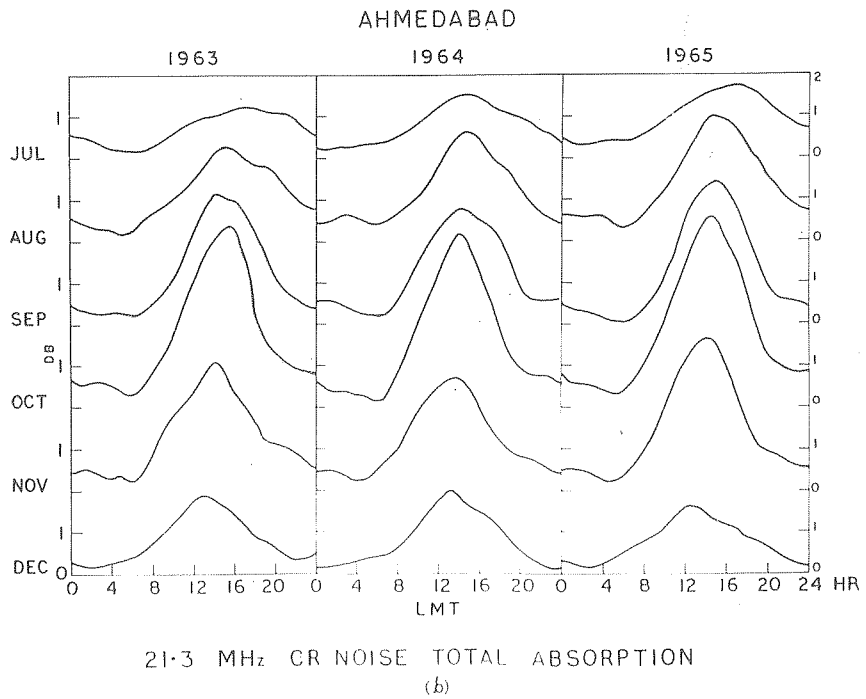


Fig.3.1 Monthly mean diurnal variation of total absorption of 21.3 MHz CR noise, during 1963, 1964 and 1965.
(a) From January to June and (b) from July to December.

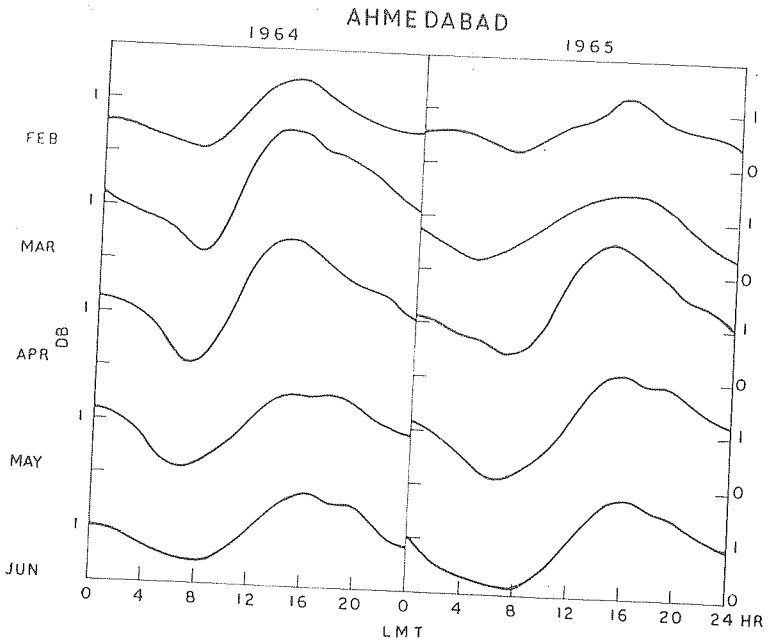


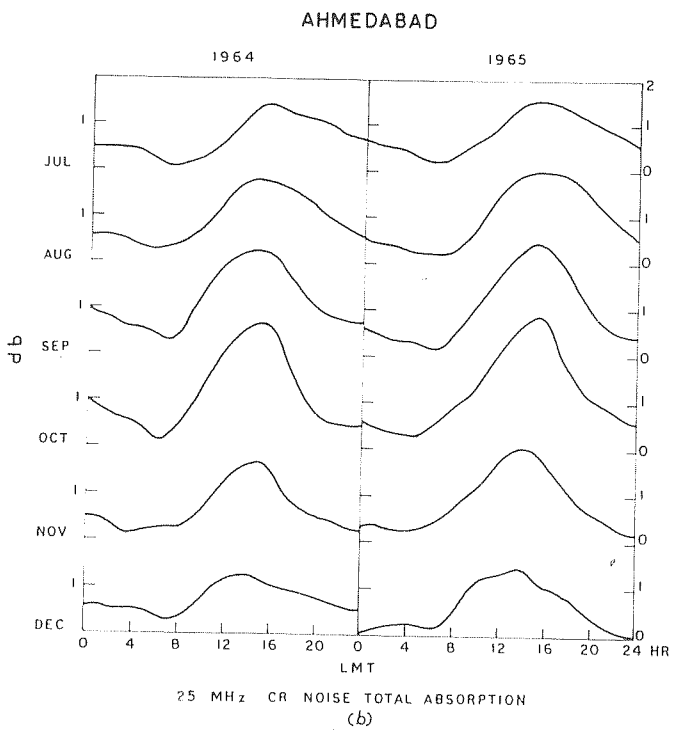


Fig.3.2 Monthly mean diurnal variation of total CR noise absorption at 25 MHz during 1964 and 1965.
(a) From January to June and (b) from July to December.

curves show a minimum before sunrise in all seasons and epochs of solar activity. Diurnal maximum occurs generally between 13 and 14 hrs. The time of maximum appears to shift to later hours as summer approaches. It can be seen that there is no premidnight peak in total absorption observed so prominently in equinoctial and winter months in high sunspot years.

The seasonal variation of monthly mean diurnal maximum of total absorption is characterised by a peak in equinoctial months and a minimum in summer and winter months. This is shown in Fig.3.3(a) where the monthly mean diurnal maximum and the

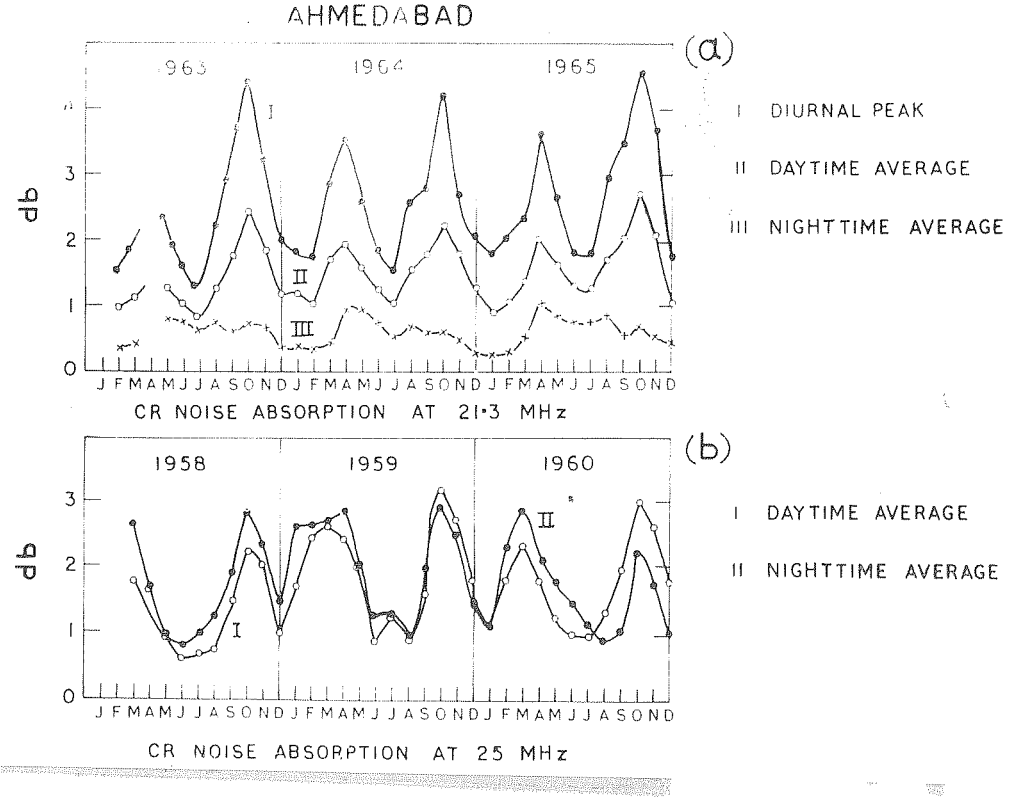


Fig.3.3(a) Variation of diurnal maximum and daytime and nighttime separate averages of monthly mean absorption at 21.3 MHz from 1963-65, and

(b) Variation of daytime and nighttime separate averages of monthly mean absorption at 25 MHz from 1957-59.

daytime and nighttime averages of absorption at 21.3 MHz are plotted for each month from 1963 to 1965. The minima which occur in summer and winter months are of the same order whereas the October peak is larger than that in April. These characteristics are nearly similar to those found by Bhonsle (1960) for high sunspot years. If we consider the average values of absorption for daytime and nighttime separately, we find that the daytime average followed the same general trend of maximum in equinoxes and minimum in summer and winter, but the nighttime average showed a minimum only in winter. This is in contrast with its seasonal variation during high sunspot years when both daytime and nighttime averages showed the same behaviour as can be seen in Fig.3.3(b). Of the three years analysed, 1964 seems to show the lowest values of total absorption both as regards its diurnal peak and the average values.

## 3.3 Dependence of total absorption on $f_0F_2$

Mitra and Shain (1953), from their 18.3 MHz CR noise absorption data at Hornsby, found correlation between the total absorption and the critical frequency of the $F_2$ layer, when the latter exceeded 5.0 MHz. The absorption increased rapidly with $f_0F_2$ for $f_0F_2$ 5 MHz. Rammathan at al (1961) obtained a linear relationship between $f_0F_2$ and the total absorption when plotted on a log-log graph, thus indicating that the absorption varied with some power of $f_0F_2$. From a plot of a large amount of data covering 1957-59, the following empirical relation was shown to hold good beyond 8.0 MHz,

PRL
AHMEDABAD

Total absorption $A = k\left(\frac{f_0F_2}{\theta}\right)^{3.4}$

Steiger and Warwick (1961), working at 18 MHz at Hawaii also found that the total absorption increased rapidly when $f_0F_2$ 10 MHz. They observed high absorptions of the order of 10-15 db, part of which could be interpreted in terms of ionospheric window effect since their antenna consisted of a single dipole which had a wide beamwidth.

Fig.3.4(a) shows the mass plot of the monthly mean values of total absorption at 10, 11, 12, 13 and 14 hrs for 25 MHz against the corresponding $f_0F_2$ values during the high

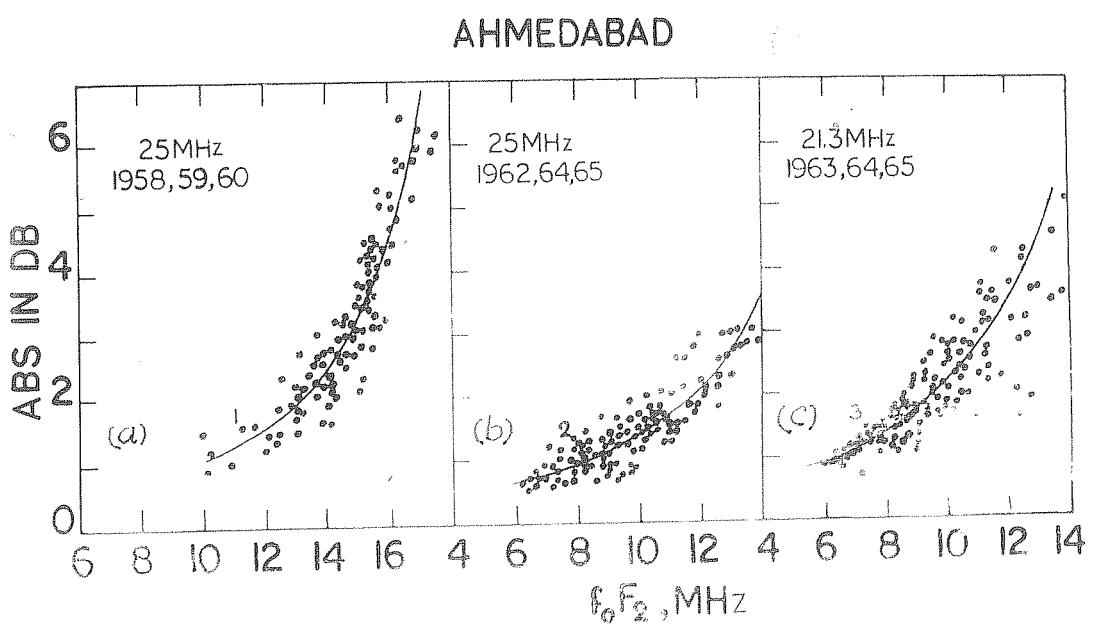


Fig.3.4(a) Mass plot of the monthly mean total attenuation at 25 MHz against the corresponding $f_0F_2$ values during 1959-60,

(b) Similar to (a) during 1962-65 and

(c) Similar plot as in (a) and (b) for 21.3 MHz during 1963-65.

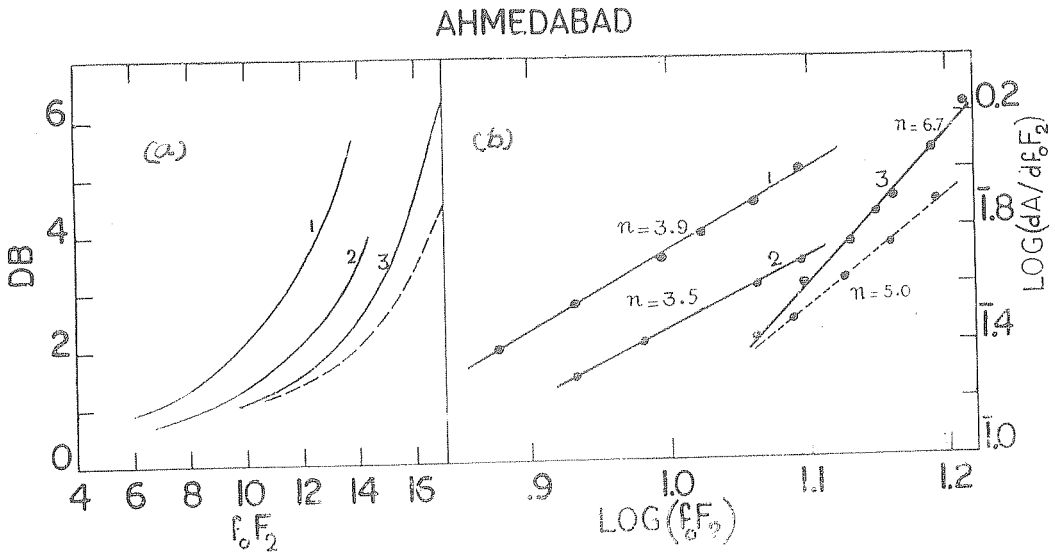


Fig.3.5(a) The mean curves corresponding to Fig.3.4(a), (b) and (c), and

(b) Log ( $dA/df_o$ ) plotted against Log($f_oF_2$) corresponding to Fig.3.5(a).

sunspot years 1959-60. In Fig.3.4(b) and (c) the corresponding values during the low sunspot years 1962-65 are plotted for 25 MHz and 21.3 MHz respectively. The mean curves which can be drawn through the mossplot are shown in Fig.3.5(a) for the three cases. It is clear from these curves that the total absorption depends on some power of $f_oF_2$, viz. $A \propto f_oF_2^n$. It can also be seen that the curves if extrepolated to zero value of $f_oF_2$, would intercept the absorption axis at a point which corresponds to the average absorption $A_D'$ which is independent of $f_oF_2$, between 10-14 hrs. Thus in general one can write the equation of these curves as

$$A - A_D' = K(f_0F_2)^n \qquad (1)$$

where $A$ = the total absorption,

$A_D'$ = the absorption independent of $f_0F_2$, and

$K$ = a constant which depends on the temperature and scale height H of the layer.

An important feature which can be noticed in these curves is that the absorption at 25 MHz for a given $f_0F_2$ is more during low sunspot years than during high sunspot years. Since $A_D'$ decreases with decrease of sunspot number, the observed increase of total absorption appears to be due to an increase in K from high to low sunspot years. It is shown in Appendix 4.1 (Chapter IV) that $K \propto H/(T_e)^{3/2}$ where $T_e$ is the electron temperature and H is the scale height at the $F_2$ peak. The observed phenomenon therefore can be interpreted as due to a decrease of $T_e$ from high to low sunspot years. If $A_D'$ and K are constant for a given portion of the curve, the value of index n can be evaluated as follows.

Differentiating equation (1) and taking logarithms, one can write

$$\log(dA/df_0) = \log(Kn) + (n-1)\log(f_0) \qquad (2)$$

where $f_0$ stands for $f_0F_2$. In Fig.3.5(b), $\log(dA/df_0)$ is plotted against $\log(f_0F_2)$ for the three curves separately. From the slope of these straight lines, n was evaluated which ranged from 3.5-6.7; the higher value 6.7 corresponds to the higher range of $f_0F_2$. Such a high value of n can be due to an additional

absorption by deviative mechanism as the $f_0F_2$ approaches the exploring frequency f. The deviative absorption was calculated as explained in Appendix 4.2 (Chapter IV) and was subtracted from the curve 1. The index for the resulting curve (shown by broken line) came down from 6.7 to 5.0. This was encouraging since it was nearer to 4.0 which is the expected value for nondeviative absorption in the F region as will be shown in the next chapter.

The differentiation of equation (1) would not be strictly valid if $A_D'$ and K changed during the long period involved in each graph. So the value of n derived would also be inaccurate. However if we consider absorption values confined to shorter time intervals (say one month) and the curve is plotted for each hour, then $A_D'$ and K could be assumed to remain reasonably constant. This method is utilised in the next section to evaluate a more correct value of n.

## 3.4 Separation of total absorption into two components

Separation of the total absorption into (1) a component which depends on $f_0F_2$ and (2) that which does not depend on $f_0F_2$ can be effected by plotting the total absorption against $f_0F_2$. Assuming that the functional shape of such a curve is independent of the time of the day, Mitra and Shain (1953) separated out the $f_0F_2$ independent component from the total absorption by extrapolating the resulting curve to the zero value of $f_0F_2$. The residual component of absorption was

proportional to $\cos^{m}\chi$, indicating that it arises mainly in the lower ionosphere which is under direct solar control.

This method was successfully applied by Bhonsle and Ramanathan (1958) for 25 Mlz cosmic noise data at Ahmedabad during 1957-59. They found it convenient to separate the total absorption into a component which is symmetrical about noon and an asymmetrical component which followed closely the variation of $f_0F_2$. The method of separating the D region component by extrapolating the $f_0F_2$ absorption curve to zero $f_0F_2$ is not difficult during morning hours. However it becomes inaccurate when the range of $f_0F_2$ values for the period considered is not large enough to derive the shape of the curve in the lower ranges of $f_0F_2$. This situation arises mainly during afternoon hours when the $f_0F_2$ values are generally high. In such cases it is possible to extrapolate if the actual dependence of absorption on $f_0F_2$ is known. In other words if the values of n and K in equation (1) are known, $A_D'$ can be determined more accurately than can be obtained by visual extrapolation.

Fig.3.6(a) shows the individual values of total absorption plotted against $f_0F_2$ at 12 hr. IST in May 1965 for 21.3 Mlz. It is clear that the points lie reasonably well on a smooth curve drawn through them. Assuming that $A_D'$ and K do not change in the course of a month for a given hour, equation (1) can be differentiated, and n and hence $A_D'$ can be determined as explained in the previous section.

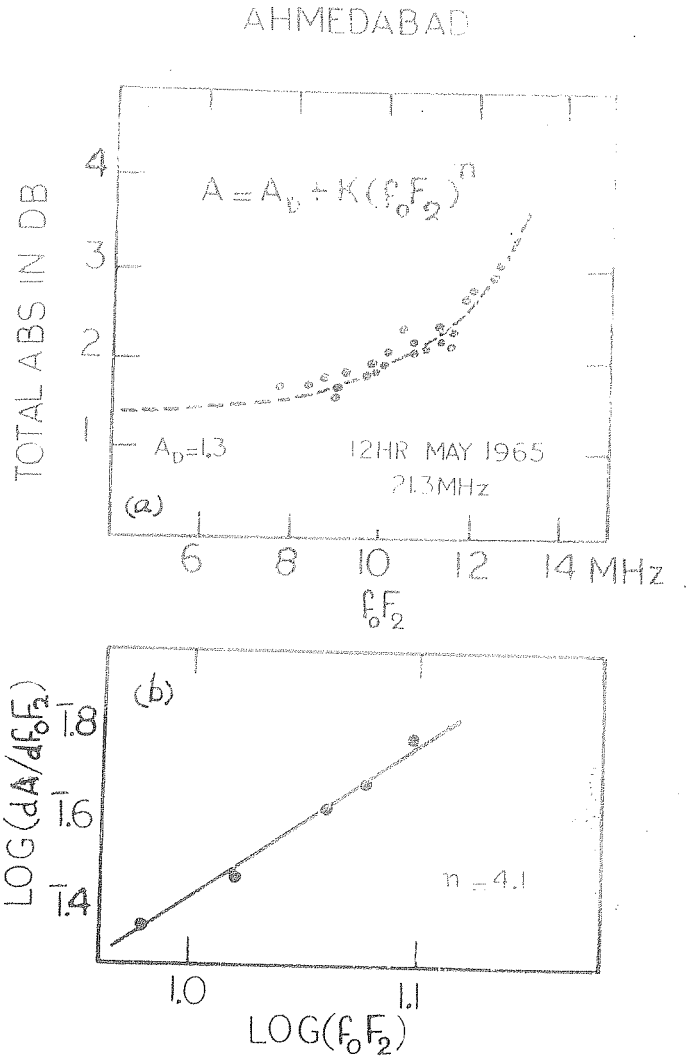


Fig.3.6(a) Individual values of the total attenuation at 21.3 MHz plotted against $f_0F_2$ for 12 hr May 1965,
(b) $\log(dA/df_0)$ plotted against $\log(f_0F_2)$ corresponding to Fig.3.6(a).

Fig.3.6(b) shows log $(dA/df_o)$ plotted against log$(f_oF_2)$. From the slope of the line drawn through the points n is found to be 4.1 which is satisfactory. Now by taking two sets of absorption values $A_1$ and $A_2$ corresponding to $(f_o)_1$ and $(f_o)_2$ along the curve, $A_D'$ can be calculated from

$$\frac{A_1 - A_D'}{(f_o)_1^n} = \frac{A_2 - A_D'}{(f_o)_2^n} \qquad (3)$$

This direct evaluation gives reasonably accurate values of $A_D'$ when there is less scatter of points. This method is very useful during afternoon hours when $f_oF_2$ does not extend to lower ranges. Thus reliable absorption values available from 1958 to 1965 were plotted against $f_oF_2$ for each individual month. From several such plots, n was determined for a wide range of the ratio, $f_oF_2/f$, where f is the exploring frequency, 25 MHz or 21.3 MHz. Fig.3.7 shows the scatter plot of n vs $f_o/f$. Average value of n is about 4.2 for $f_o/f$ less than 0.6 and n increases rapidly afterwards. This can be understood on the basis of deviative absorption. For the antenna beamwidth used at Ahmedabad, the ionospheric window effect becomes significant only when $f_oF_2$ is more than 0.9f (see appendix 3.1).

## 3.5 Monthly mean absorption independent of $f_oF_2$, $A_D'$

The $f_oF_2$ independent component $A_D'$ of total absorption was found for all months of 1964-65 for 21.3 MHz as described above and is shown in Fig.3.8. A $\cos^m\chi$ dependence, where $\chi$

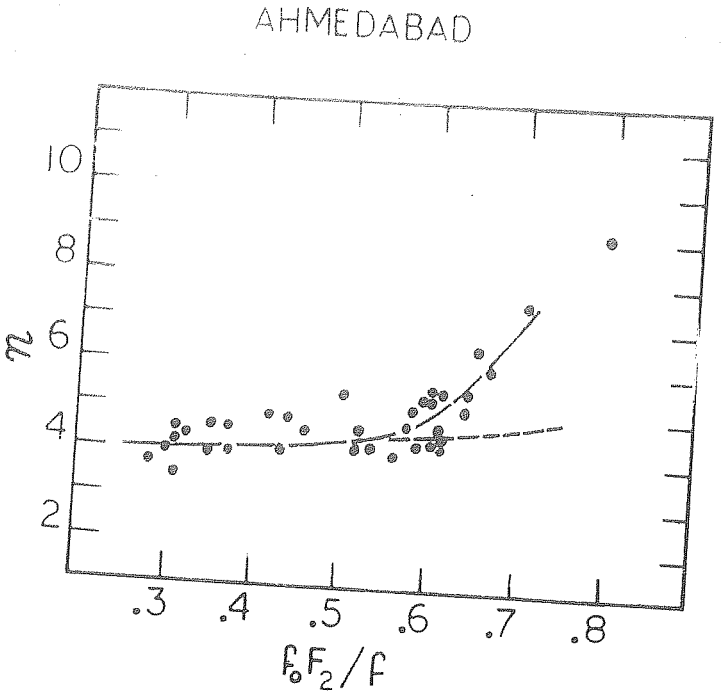


Fig.3.7 Plot of n vs $f_0F_2/f$

is the solar zenith angle, is clearly seen in these curves which are nearly symmetrical about noon. The annual variation of noontime $A_D'$ shows a minimum in winter and maximum in equinox. In summer $A_D'$ is considerably higher, though not maximum according to $\cos^m \chi$ variation. The peak in October is higher than in April in both 1964 and 1965. Similar results were obtained by Rammathan and Bhonsle (1959) during 1957-59. More D region absorption in equinoxes than in summer was also reported at Ahmedabad by Shirke (1959) using method A of pulse reflection at 2.5 and 2.6 MHz during 1957-58.

For the years 1964-65, the value of m using 21.3 MHz data is found to be 1.35, 1.15 and 0.75 for summer, equinox and

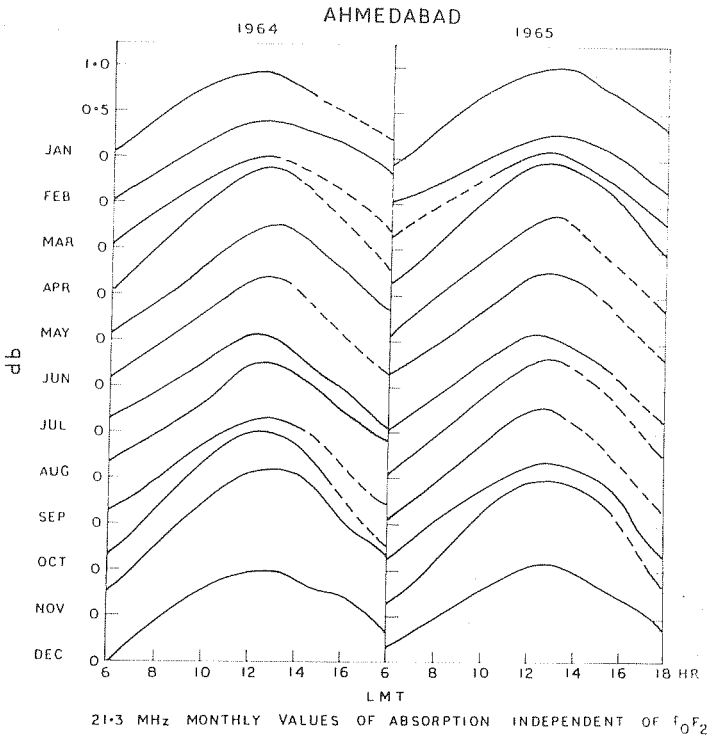


Fig.3.8 Diurnal variation of the monthly mean values of the component of CR noise absorption independent of $f_0F_2$, $A_p'$, at 21.3 MHz during 1964-65.

winter respectively. Those obtained by Bhonsle for high sunspot years were 1.1, 1.0 and 0.8 respectively. The corresponding values given by Mitra and Shain for Hornsby were 1.1, 0.9 and

0.5 in 1950. The values of n derived from vertical pulse reflection method at other places were consistently lower than these values. Appleton and Piggott from a series of observations extending over two solar cycles obtained a mean value of n = 0.75. For Ahmedabad the value obtained by Shirke (1959) for the IGY period were 0.86, 0.74 and 0.69 for summer, equinox and winter respectively.

Appleton (1937) has shown theoretically that for the D layer, the nondeviative absorption varies as $\cos^{n}\chi$ with n = 1.5. Thus the theoretically expected value of n is greater than experimentally derived results. This discrepancy has been explained by some authors by modifying the assumptions made in the original derivation of the formula. For example, Skinner and Wright (1956) have shown that when absorption takes place in height regions where the collision frequency $\nu$ is comparable with the exploring frequency the index n can decrease rapidly. Even if the collision frequency is comparable with the exploring wave frequency in the pulse reflection method, it can still be negligible when compared with the much higher cosmic radio noise exploring frequency. Therefore the higher value of n obtained by cosmic radio noise method is not impossible. The average value of n obtained from the present analysis is slightly higher than that obtained for high sunspot years and on this basis it may be argued that the effective region of absorption is higher in low sunspot years than in high sunspot year.

## 3.6 Variation of noon absorption between 21.3 and 25 MHz

Fig.3.9(a) shows the noon value of the symmetrical component of absorption $A_D'$ for 21.3 and 25 MHz plotted for all months in 1964 and 1965. The logarithm of the averages of these curves are plotted against logarithm of exploring frequency in Fig.3.9(b). The slope of the line is around -2.1 which indicates the dependence of absorption on inverse square frequency when the absorption takes place in the region where $\nu$ is very small compared to the exploring frequency.

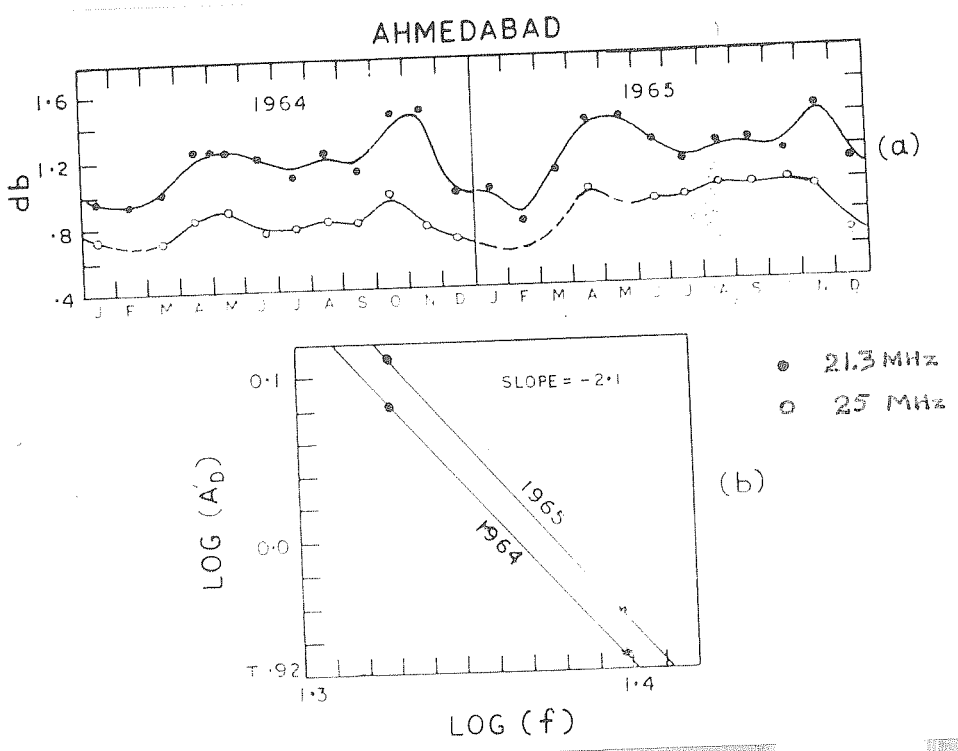


Fig.3.9(a) Variation of noon $A_D'$ at 21.3 MHz and 25 MHz during 1964-65,
(b) Logarithm of yearly average values of $A_D'$ plotted against logarithm of frequency corresponding to Fig.3.9(a).

## 3.7 F region component of the total cosmic radio noise absorption

The method of finding the absorption $A_D'$ in lower ionosphere is explained above. This absorption may be assumed to take place in D and E regions which have $\cos^m\chi$ dependence. The difference between the total absorption and $A_D'$ gives an asymmetrical component which can be attributed to the F region. When all the lower layers disappear following sunset, the total absorption measured will be F region attenuation. Bhonsle (1960) found that the F region attenuation showed good correlation with $f_oF_2$ both during daytime and nighttime. He also found that the F attenuation increased rapidly with $f_oF_2$ above 8 MHz. From the present analysis it is shown that while there is strong correlation between F region attenuation and $f_oF_2$ during daytime, there is in general poor correlation between them during nighttime at certain hours. This can be seen in Fig.3.6(a) and 3.10(a), where we have shown the individual values of total absorption for 12 and 20 hrs in May 1965. While the former shows good correlation with $f_oF_2$, the latter shows hardly any. Similar behaviour is seen for all months during the low sunspot years. However the mass plot of monthly mean absorption data against the corresponding $f_oF_2$ for night hours of 1963, 1964 and 1965 shown in Fig.3.10(b) shows a tendency for the absorption to increase with $f_oF_2$ almost linearly.

On the basis of the relationship between individual absorption values and $f_oF_2$, it is convenient roughly to classify F region attenuation in low sunspot years as follows :

57(a)

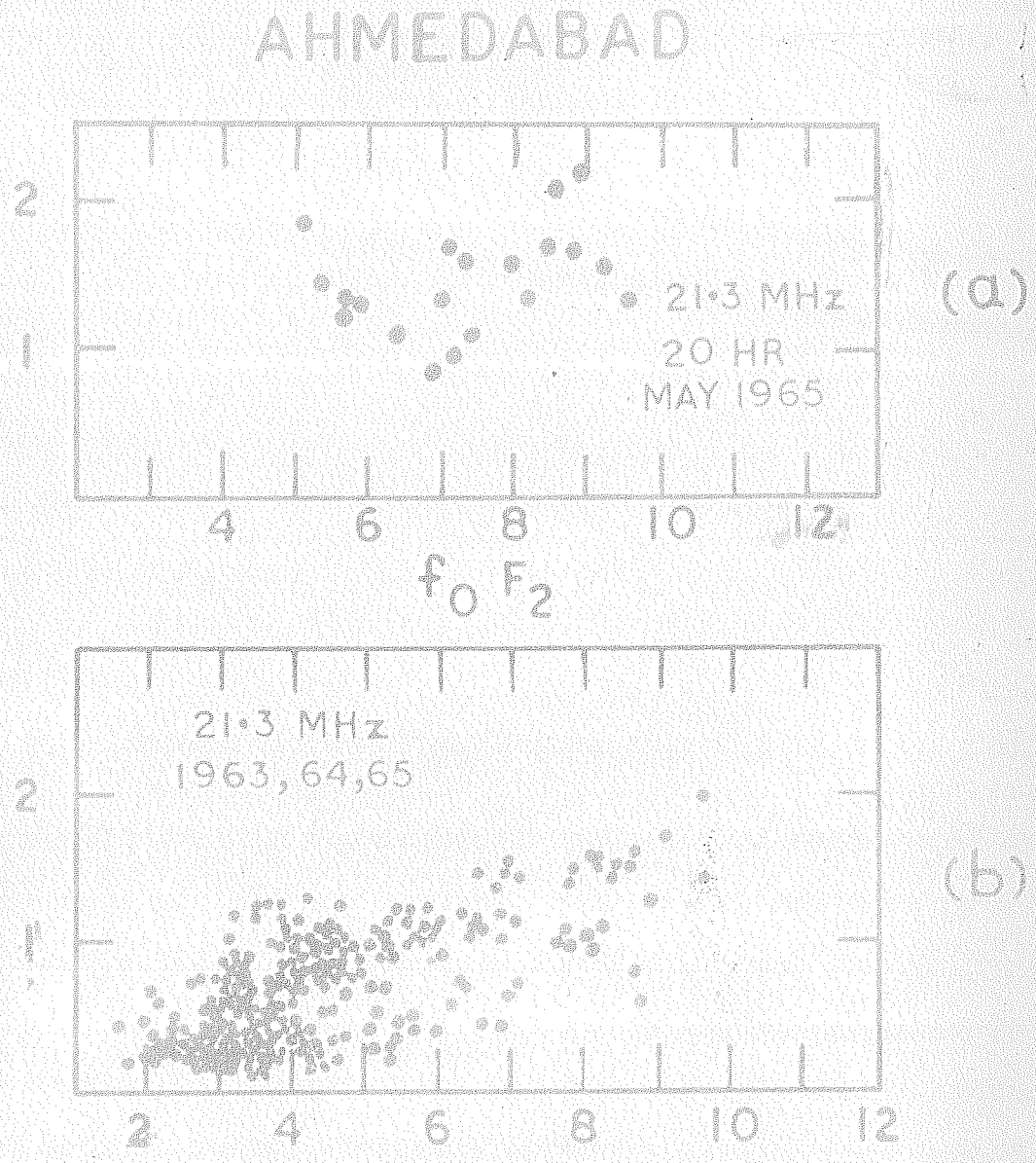


(a) TOTAL ATTENUATION Vs $f_0F_2$ FOR 20 HR MAY 1965

(b) MONTHLY MEAN TOTAL ATTENUATION Vs MONTHLY MEAN $f_0F_2$ DURING 1963, 64, 65 (NIGHT HOURS)

FIG. 3.10

(1) Attenuation which is closely correlated with $f_oF_2$ and (2) that which is not so well correlated with $f_oF_2$. The first case in general applies to daytime and the second to nighttime phenomena.

3.8 F region attenuation which depends on $f_oF_2$ $(A-A_1')$

This is obtained by removing the $f_oF_2$ independent component from the total attenuation. The residual absorption varies with $f_oF_2$ as

$$A_{f_o} = K(f_o)^n$$

where n is around 4.2 for $f_oF_2/f$ less than 0.6 as shown above.

The monthly mean diurnal variation of absorption which is dependent on $f_oF_2$ for January, July, April and October are shown in Fig.3.10. The corresponding $f_oF_2$ values are also shown. The monthly mean diurnal variation shows a minimum generally after sunrise in contrast with the time of $f_oF_2$ minimum which occurs before sunrise. During the forenoon hours when $f_oF_2$ is below 6-7 MHz the correlation with $f_oF_2$ is not appreciable, but increases during afternoon hours when the values of $f_oF_2$ are usually high. The diurnal maximum of absorption occurs around 14-15 hours LMT. There are some exceptions when it occurred at a much later or earlier hour. In such cases $f_oF_2$ also showed a similar behaviour. An interesting feature is that the attenuation of CR noise continues to be high at night, particularly in the equinoctial months, even though $f_oF_2$ decreased after sunset.

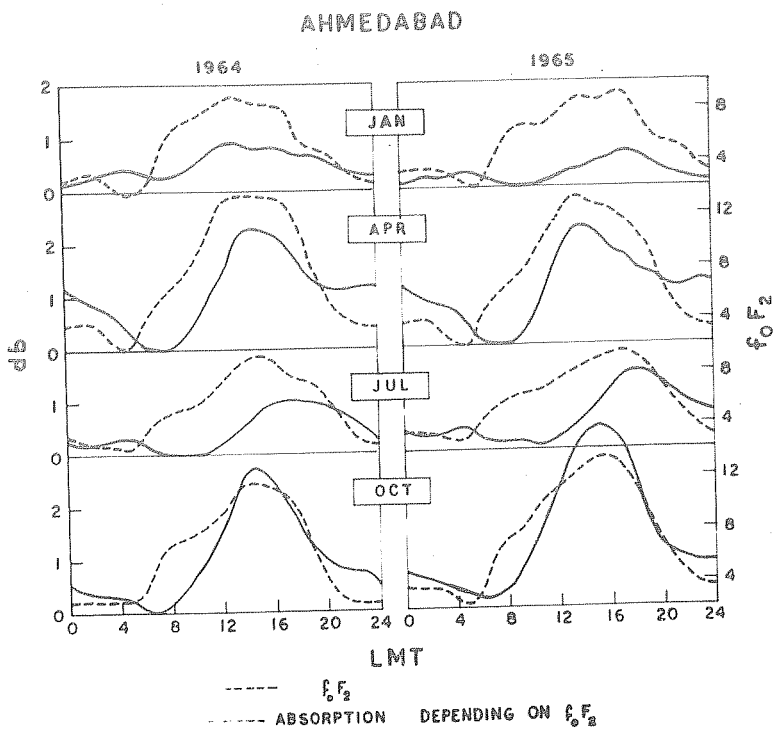


Fig.3.11 The monthly mean diurnal variation of the $f_0F_2$ dependent attenuation of 21.3 MHz CR noise (solid line) and the corresponding $f_0F_2$ (broken line) for January, April, July and October during 1964-65.

The diurnal maximum of F region attenuation showed a peak in equinoxes and a minimum in summer and winter. The minimum value in summer and winter is about the same. This behaviour differs from that during high sunspot years when the summer value was found to be lower than the winter value. The monthly mean noon values of this attenuation and of $f_0F_2$ are plotted for all months of 1964 and 1965 in Fig.3.12(a) and of 1957-59 in Fig.3.12(b).

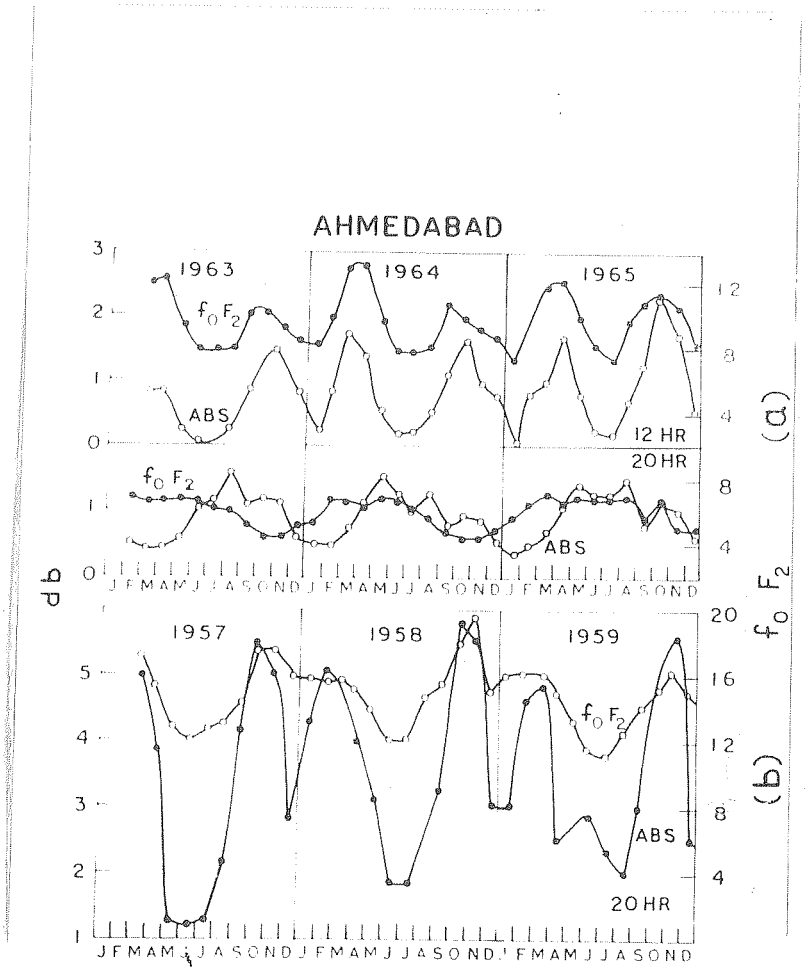


Fig.3.12(a) Variation of monthly mean values of the $f_0F_2$ dependent absorption at 21.3 MHz for 12 and 20 hrs and corresponding $f_0F_2$ during 1963-65.

(b) Variation of monthly mean values of the $f_0F_2$ dependent absorption for 20 hrs at 25 MHz and the corresponding $f_0F_2$ during 1957-59.

## 3.9 F region attenuation not correlated with $f_oF_2$

Mitra and Shain (1953) found that the F region absorption during night was much higher than that during day for the same $f_oF_2$. This became apparent immediately after sunset. They attributed it to F scatter. Similar observations were reported by Bhonsle and Ramanathan (1958) for Ahmedabad. When both day and night F attenuation showed dependence on $f_oF_2$, the night attenuation was markedly higher than the day value for a given $f_oF_2$. The present study during low sunspot years while confirming this, shows that the difference between night and day absorption increased considerably and that $f_oF_2$ did not control the night time attenuation. This can be seen in Fig.3.12(a) and (b) where the F-attenuation and $f_oF_2$ at 20 hr are plotted from 1963 to 1965 and from 1957 to 1959 respectively. While the latter shows good correspondence with $f_oF_2$, the former does not.

An increase in the nighttime over daytime F-attenuation can also be ascribed to a decrease of F region temperature after sunset. But the observed difference is much more than can be accounted for by this reasoning. A quantitative study of this has been made in Chapter IV where it is shown that the absence of any correlation of the attenuation with $f_oF_2$ calls for a different mechanism. Another prominent peak in the F attenuation was observed after sunset in equinoctial and winter months in high sunspot years over Ahmedabad. Part of this was considered possible by Ramanathan and Bhonsle (1959) due to spread F.

However since the $f_0F_2$ values were also high at that time, the relative contribution due to spread-F could not be separated. Such increases in $f_0F_2$ in the night were not observed during 1963-65, but the frequency of occurrence of spread activity showed an increase in low sunspot years (Kotadia, 1959). From Fig.3.12(a) it can be seen that the F attenuation at 20 hr shows maximum in summer (generally, period April to August shows more attenuation than the rest of the year). From a preliminary analysis it is found that the frequency of spread-F occurrence over Ahmedabad in the summer of 1964 was more than 60 % while in the equinoctial months, March and October, it was less than 10 %. Thus while the noon values show good correlation with $f_0F_2$, the 20 hr attenuation is very much affected by the occurrence of spread F activity. Shirke (1962) examined CR noise records at instances when there was F-scatter, and reported that the CR noise absorption can increase as well as decrease due to F-scatter, the effect very much depending on the sidereal time.

## 3.10 Discussion

If we compare the nighttime attenuation at 21.3 and 25 Mlz in Fig.3.1 and 3.2, we find that the attenuation at 25 Mlz is sometimes more than that at 21.3 Mlz which is against the frequency law. The daytime absorption varies as $1/f^2$ as expected. If the nighttime attenuation is due to the scattering of galactic radio noise by irregular horizontal gradient of ionisation in the F region, the observed difference in nighttime absorption at the two frequencies can be explained. Anastassiades (1962) working

on 27.6 and 56 MHz riometers in Athens noticed that while the 27.6 MHz absorption could be explained on the basis of $f_0F_2$, that at 56 MHz was independent of $f_0F_2$, especially during night hours. The nighttime absorption at 56 MHz was often more than that at 27.6 MHz. He also found correlation between the frequency of occurrence of spread-F and 56 MHz attenuation. These arguments tend to support the idea that the nighttime attenuation of cosmic radio noise observed at Ahmedabad during the low sunspot period is mainly due to scattering by ionospheric irregularities.

3.11 Summary

We summarise our main findings below :

(1) The total attenuation of galactic radio noise at 21.3 and 25 MHz over Ahmedabad during low sunspot years is maximum in equinoxes and is minimum in summer and winter. The secondary premidnight peak observed in equinoctial and winter months of high sunspot years is not observed in low sunspot years.

(2) The total attenuation shows good correlation with $f_0F_2$ during day and can be expressed as $A - A'_D = K(f_0F_2)^n$ Use of this relation has led to a determination of the $f_0F_2$ independent component of absorption $A'_D$.

(3) The index n was found to be about 4.2 for $f_0F_2/f < 0.6$ at Ahmedabad. When $f_0F_2$ approaches the exploring frequency the deviative absorption increases rapidly.

(4) The $f_0F_2$ independent absorption is found to vary as $\cos^m \chi$ where the value of m is 1.35, 1.15 and 0.8 for summer, equinox and winter respectively. m has shown a slight increase in low sunspot years. If the increase in m is assumed to be correct, then it will mean that the absorption takes place at a higher level in low sunspot years than in high sunspot period.

(5) The nighttime attenuation is not correlated with $f_0F_2$ in low sunspot years, while there is good correlation in high sunspot years. Evidence is given to support the idea that scattering by ionospheric irregularities effectively attenuates galactic radio noise intensity.

## APPENDIX 3.1

The antenna array used for receiving cosmic radio noise intensity at Ahmedabad has got beam-width of $30^{\circ}$ in E-W and $40^{\circ}$ in N-S planes. The equivalent reflection frequency corresponding to the maximum angle of reception of the antenna is $f_0F_2 \sec\theta$, where $\theta$ is the semiangle of reception in any plane i.e. $15^{\circ}$ in E-W and $20^{\circ}$ in N-S plane. The ionospheric window effect sets in when the semiangle of the cone of ionospheric apperture is smaller than that of the antenna solid angle i.e. when $f_0F_2 > f\cos\theta$

The following table shows the variation of the semiangle of the cone of ionospheric apperture for different $f_0F_2$ values corresponding to the exploring frequencies 21.3 and 25 Mhz. It can be seen that the 'iris' effect is not important for $f_0F_2$ less than 0.9 of the exploring frequency.

Table

| $f_0F_2$ Mhz | Semiangle of the cone subtending ionospheric apperture at (in degrees) at | |
|---|---|---|
| | 25 Mhz | 21.3 Mhz |
| 5 | 78 | 77 |
| 10 | 66 | 62 |
| 15 | 53 | 45 |
| 17 | 47 | 37 |
| 18 | 44 | 32 |
| 19 | 40 | 27 |
| 20 | 37 | 20 |
| 21 | 33 | 9 |
| 22 | 28 | |
| 23 | 22 | |
| 24 | 16 | |

# CHAPTER IV

## SOLAR CYCLE VARIATIONS IN COSMIC RADIO NOISE ABSORPTION OBSERVED DURING 1958-64

### 4.1 Introduction

The main features of cosmic radio noise absorption at 21.3 and 25 MHz and its diurnal and seasonal variations in the low sunspot years 1963 to 1965 were described in Chapter III. In this chapter the continuous data of 25 MHz cosmic radio noise absorption obtained at Ahmedabad from 1958 to 1964 are analysed and the changes from solar maximum to solar minimum conditions studied. The results of the study on 25 MHz CR noise absorption, made during the IGY and IGC period were reported by Bhonsle, Ramanathan and Degaonkar (1958-61). We recall the important points which emerged from their study:

(1) The total absorption has a primary daytime maximum at about 15 hr LMT and a secondary nighttime maximum in winter and equinox at about 20 hr.

(2) There was generally more absorption in winter and equinox than in summer, and

(3) For the same $f_0F_2$ the nighttime absorption was in general more than the daytime absorption. Part of this was attributed to attenuation by F scatter (Ramanathan and Bhonsle, 1959, Shirke, 1962).

In a paper by Ramanathan et al (1961), the collision frequency of electrons with positive ions was calculated, and using true height profiles of electron density, the attenuation below $F_2$ peak was computed. It was shown that the ionosphere above $F_2$ peak also caused a significant absorption of radio waves and that there were large changes in the electron density during and after a magnetic storm.

Further study of these problems is made here. Particular attention is given to the changes in radio noise absorption above the $F_2$ peak through a solar cycle. The data of 21.3 MHz riometer are utilised to deduce the topside absorption during 1964-65. This was done because the data on 25 MHz was not satisfactory during this period.

## 4.2 Total attenuation of CR noise and its changes from 1958-64

The monthly mean diurnal variation of total attenuation for January, April, July and October is shown from 1958 to 1964 in Fig.4.1. The corresponding $f_0F_2$ variations are also plotted in the same figure. There is generally a minimum absorption before sunrise, which increases afterwards to reach maximum around 15 hr IMT in all seasons and in all years. The following features may be noted :

(1) In equinoctial and winter months in high sunspot years, there is a pronounced secondary maximum after sunset. The secondary maximum decreased with decrease of solar activity. The reduction in the magnitude of the evening peak began in 1960.

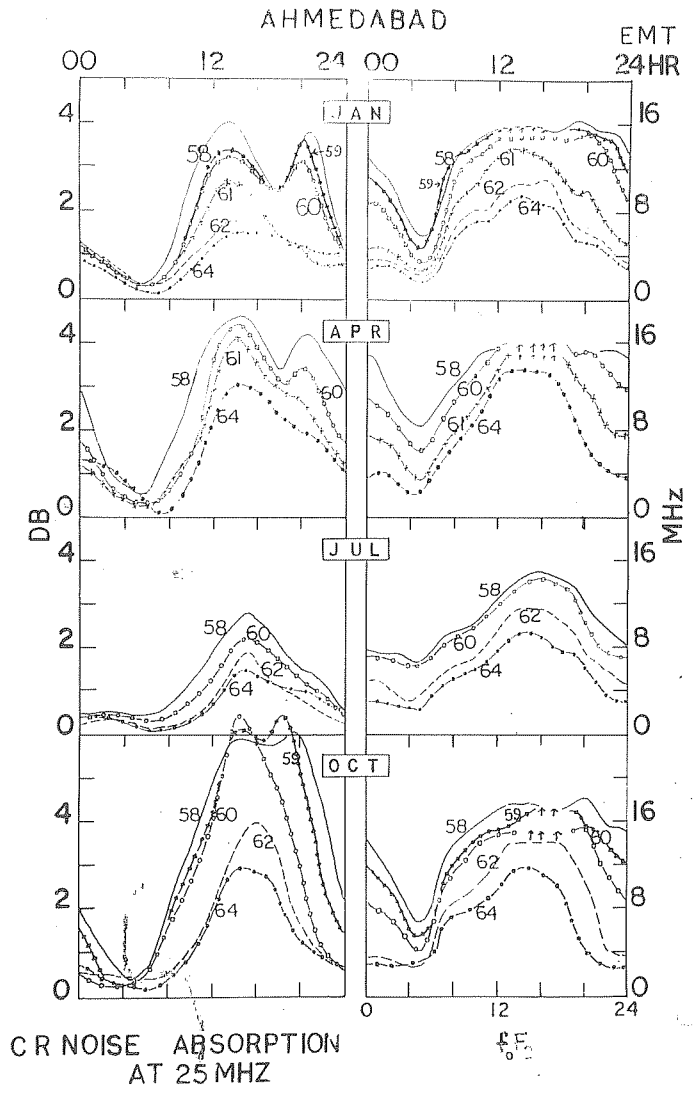


Fig.4.1 Monthly mean diurnal variation of total absorption and $f_0F_2$ for January, April, July and October from 1958 to 1964.

(2) A large difference in the total attenuation between summer and winter is characteristic of high sunspot years only. The $f_0F_2$ values also show a similar behaviour. In low sunspot years the equinoctial months show maximum absorption.

Fig.4.2 shows the variation of monthly mean diurnal maximum of the total CR noise absorption at 25 MHz from 1958 to 1964 and the corresponding $f_0F_2$ variation. As can be judged from this figure the average total absorption in 1958 and 1964 were 4.4 and 2.2 db respectively, indicating a decrease of 50 % from high to low sunspot years.

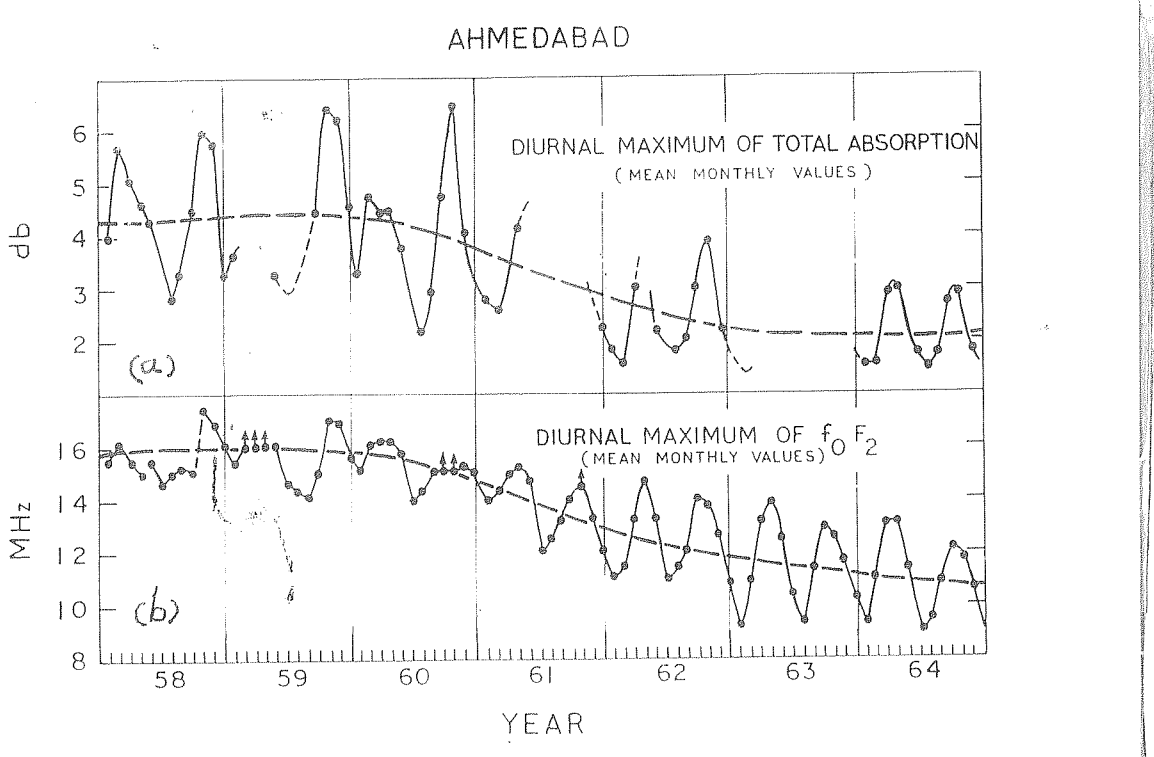


Fig.4.2 Monthly mean values of (a) diurnal maximum of total attenuation of 25 MHz galactic radio noise and (b) diurnal maximum of $f_0F_2$.

## 4.3 $A_D'$ and its variations with sunspot number

The method of seperating the absorption due to the lower layers (mainly D layer) from the total absorption was described in detail in the previous chapter. It was shown there that the total absorption A is given by

$$A - A_D' = K(f_0F_2)^n \qquad (1)$$

The average value of n obtained was 4.2 which is close enough to the expected value 4.0 for the F region when the electron temperature in the thermosphere is constant (see Appendix 4.1). $A_D'$ was calculated from eqn(1) for noon hours for each month from 1950 to 1964. These values are plotted in Fig.4.3(a)&(b).The monthly mean sunspot number is also shown for comparison. In Fig.4.3(c), $A_D'$ is plotted against sunspot number R and it can be seen that they are linearly correlated. $A_D'$ has decreased by a factor of approximately 2/3 from sunspot maximum to minimum, its average value being 1.2 and 0.8 for 1958 and 1964 respectively. The linear relation between $A_D'$ and R may be represented analytically as

$$A_D' = a(1 + bR) \qquad (2)$$

The constants a and b can be obtained from the intercept and the slope of the line. For 25 MHz, the values of a and b are 0.7 and 0.004 respectively. The numerical value of b based on the analysis of vertical incidence sounding at Slough was found to be 0.004 (Davies, 1965). Shirke (1961) obtained $b = 0.002$ from pulse reflection observations at 2.5 and 2.6 MHz at Ahmedabad,

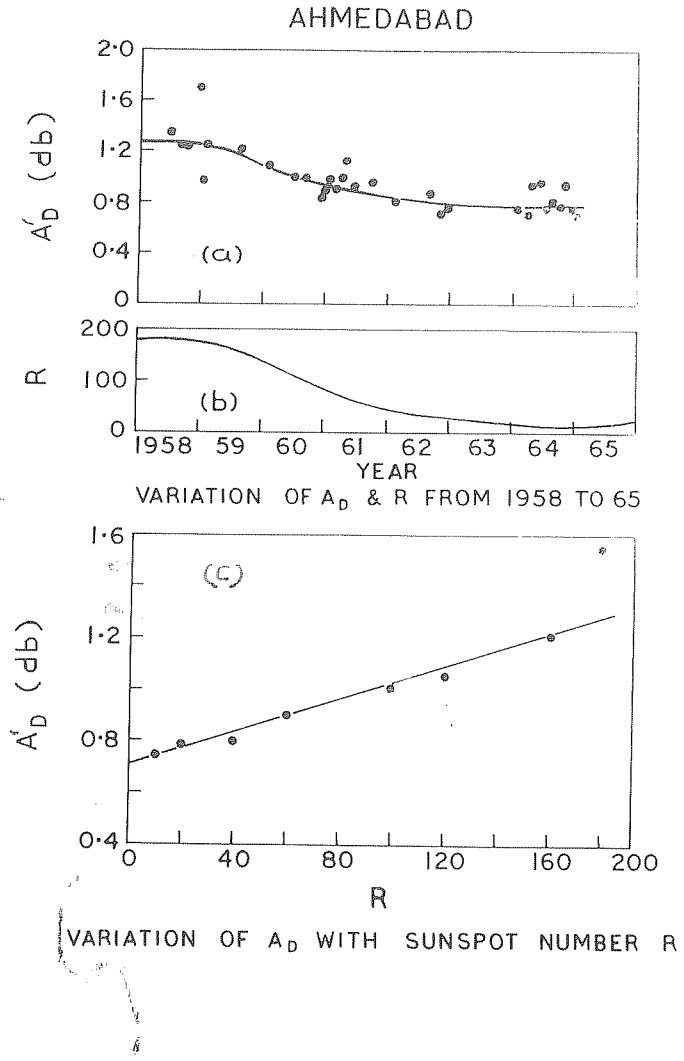


Fig.4.3(a) Variation of $A'_D$ the component of absorption independent of $f_0F_2$ for midday from 1958-64,

(b) The corresponding sunspot number variation, and

(c) Plot of sunspot number against $A'_D$.

and 0.0018 respectively. The value of $A_f$ derived from the total cosmic radio noise absorption will now be compared with the D region absorption computed from expected electron densities and collision frequencies.

## 4.4 Calculation of D region absorption using electron density profiles

The absorption of a radio wave passing through the ionosphere in the vertical direction has been shown by Chapman and Little (1959) to be

$$D = A/f^2$$

where D is absorption in db, A is defined as

$$A = 1.17 \times 10^{-14} \int N_e \nu \, dh \qquad (3)$$

$N_e$ = number density of electrons per $cm^3$

$\nu$ = effective collision frequency of electrons with other particles namely

where $\nu_{em}$ is the frequency of collision between electrons and neutral molecules and $\nu_{ei}$ is that between electrons and positive ions. The collision frequency of electrons with neutral molecules given by Nicolet (1959) is

$$\nu_{em} = 5.4 \times 10^{-10} N_m T^{1/2} \qquad (4)$$

where $N_m$ = number density of neutral particles

and T = the temperature in degrees Kelvin.

The height distribution of $N_m$ and T were taken from the CIRA model atmosphere (1961). The electron density distribution for high sunspot years was taken from Nicolet and Aikin (1961) given for a disturbed zenith sun and their quiet sun profile was assumed for low sunspot years. The integration of equation (3) was made by quadrature, by calculating the absorption values at intervals of 5 km from 55 to 130 km. The absorption at 25 Mhz or 21.3 Mhz due to electron-neutral particle collisions is small above 130 km. Table 4.1 gives the product of the average collision frequency $\nu_{em}$ and electron density N from 55 to 130 km for a high sunspot year. It can be seen that the value of $N\nu_{em}$ above 120 km is negligibly small compared to those below this level. Maximum value occurs at about 82 km. The computed absorption for the zenith sun is 0.7 db for low sunspot years and 1.0 db for high sunspot year at 25 Mhz. The corresponding mean $A_D'$ values are 0.75 and 1.2 db respectively. The difference between the calculated values and $A_D'$ is not negligible.

4.5 The component of absorption which depends on $f_0F_2$

As mentioned earlier, the component of absorption which depends on $f_0F_2$ can be written as follows :

$$A_{f_0} = A - A_D' = K(f_0F_2)^n \qquad (5)$$

It can be seen from Appendix 4.1 that

$$K \propto H/(f^2 T_e^{3/2})$$

where H = scale height of ions at the $F_2$ peak,

f = exploring frequency, and

$T_e$ = electron temperature in $^0K$.

From equation (5) it is clear that for any exploring frequency the ratio $(f_0F_2)^4/(A-A'_D)$, plotted for different years gives an idea of the variations of $T_e^{3/2}/H$ with solar activity. Such a plot is shown in Fig.4.4. If the variation of scale height H with sunspot number at these hours is known, one can calculate the variation of $T_e$ from high to low sunspot years. The monthly mean value of 2800 MHz solar radio flux (in units of $10^{-22}$ watts per $m^2$ $(c/s)^{-1}$) and the corresponding noon thermosphere temperatures taken from Harris and Priester (1964) are shown in Fig.4.4 for comparison. It can be seen that all the curves show similar trends of variation. The ratio of $(f_0F_2)^4/(A-A'_D)$ for 1958 to 1964 at 12 hr and 20 hr LMT is found to be 2.0 and 12.0 respectively. This means that the nighttime absorption did not decrease as much as the daytime absorption in years of low solar activity. It will be shown later that the high nighttime absorption in low sunspot years 1964-65 cannot be explained by electron-ion collision processes alone. (See Fig.4.8).

## 4.6 Note on the calculation of absorption from 130 km to $F_2$ peak

When the D region absorption calculated on the basis of electron-neutral particle collisions is removed from the total attenuation, the residual part must be due to absorption

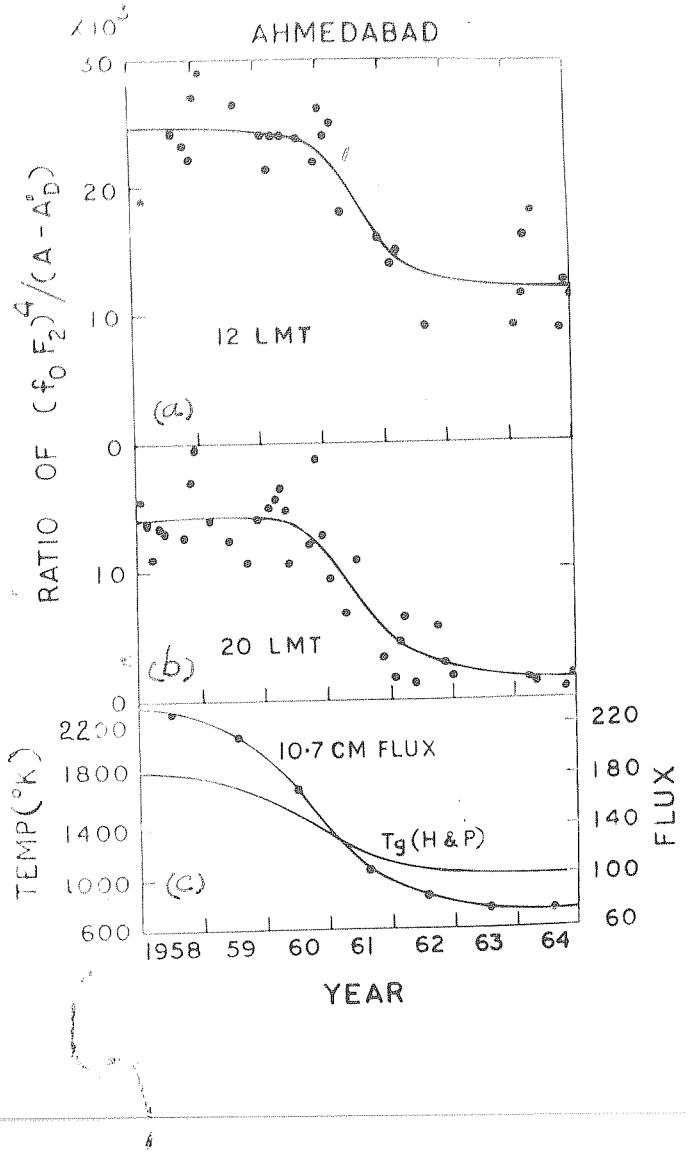


Fig.4.4 Monthly mean ratio $(f_0F_2)^4/(A-A_D^*)$ at 25 MHz from 1958-64 at (a) 12 hr LMT, (b) 20 hr LMT, (c) Solar radiation flux at 10.7 cm in units of $10^{-22}$ $m^{-2}(c/s)^{-1}$ and noon exospheric temperatures given by Harris & Priester (1964).

above 130 km, i.e. mainly in the F region either below or above $F_2$ peak. In this region, the total observed absorption is the sum of the nondeviative and deviative absorptions, the latter becoming more important as $f_oF_2$ approaches the operating frequency. The absorption due to deviative effect which is sometimes as much as 20-25 % of the total absorption was removed from the observed absorption. The deviative absorption for 25 MHz was calculated as explained in Appendix 4.2. Table 4.2 shows the monthly mean of observed total attenuation A of cosmic radio noise at each hour and the corresponding deviative component of attenuation P expressed as percentage of A for January, April, July and October during 1957-58 when the $f_oF_2$ values were generally high.

Thus we can get nondeviative component of CR noise attenuation in the F region by removing the D region absorption and the deviative absorption from the total observed attenuation. The mean monthly diurnal variation of this component is plotted for 1957-58 and 1964-65 in Fig.4.5 and 4.6, with the corresponding values of $M_m^2$ derived from monthly median $f_oF_2$ at Ahmedabad. It can be seen clearly that the two quantities show exactly similar variation.

The nondeviative absorption of radio waves in this height range and above is mostly due to collisions between electrons and positive ions. The collision frequency between electrons and positive ions has been shown by Nicolet (1959) as

$$\nu_{ei} = \left[34 + 4.18 \log\left(\frac{T_e^3}{N_e}\right)\right] N_i T_e^{-3/2} \qquad (6)$$

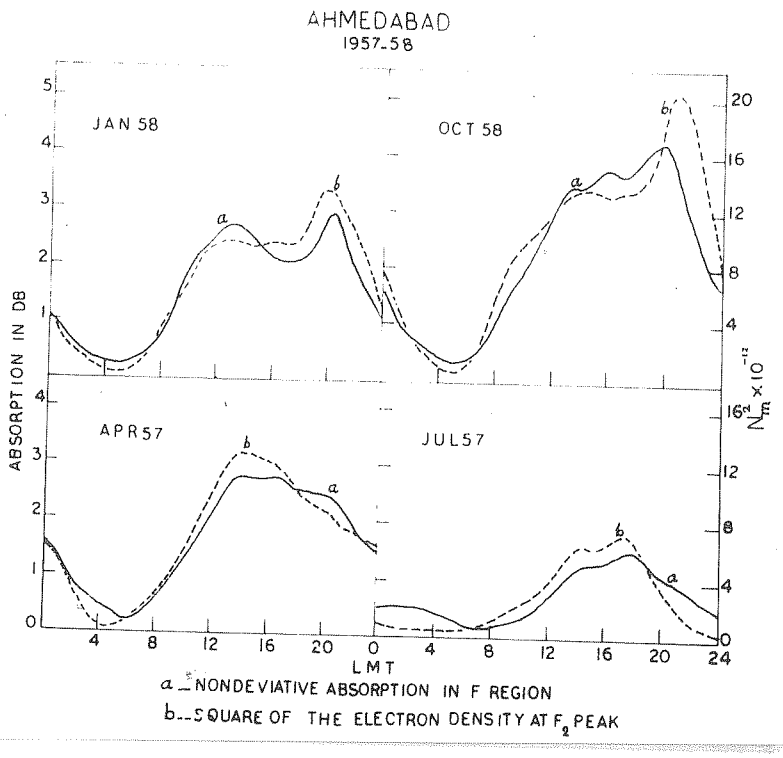


Fig.4.5 Nondeviative absorption of CR noise at 25 MHz attributable to altitude above 120 km (curve a) and square of electron density at the $F_2$ peak (curve b) for January, April, July and October 1957-58.

where $N_i$ = positive ion number density per cc (if we assume that ions are singly charged, we may put $N_i = N_e$) and $T_e$ = temperature of electrons in $^0K$. The absorption in the F region is therefore proportional to $\int N_e^2 \, dh$ (see Appendix 4.1). This would mean that the main absorbing region occurs near the $F_2$ peak. Using the electron-ion collision frequency given by equation (6) and electron density profile as obtained from the monthly median ionogram, the absorption

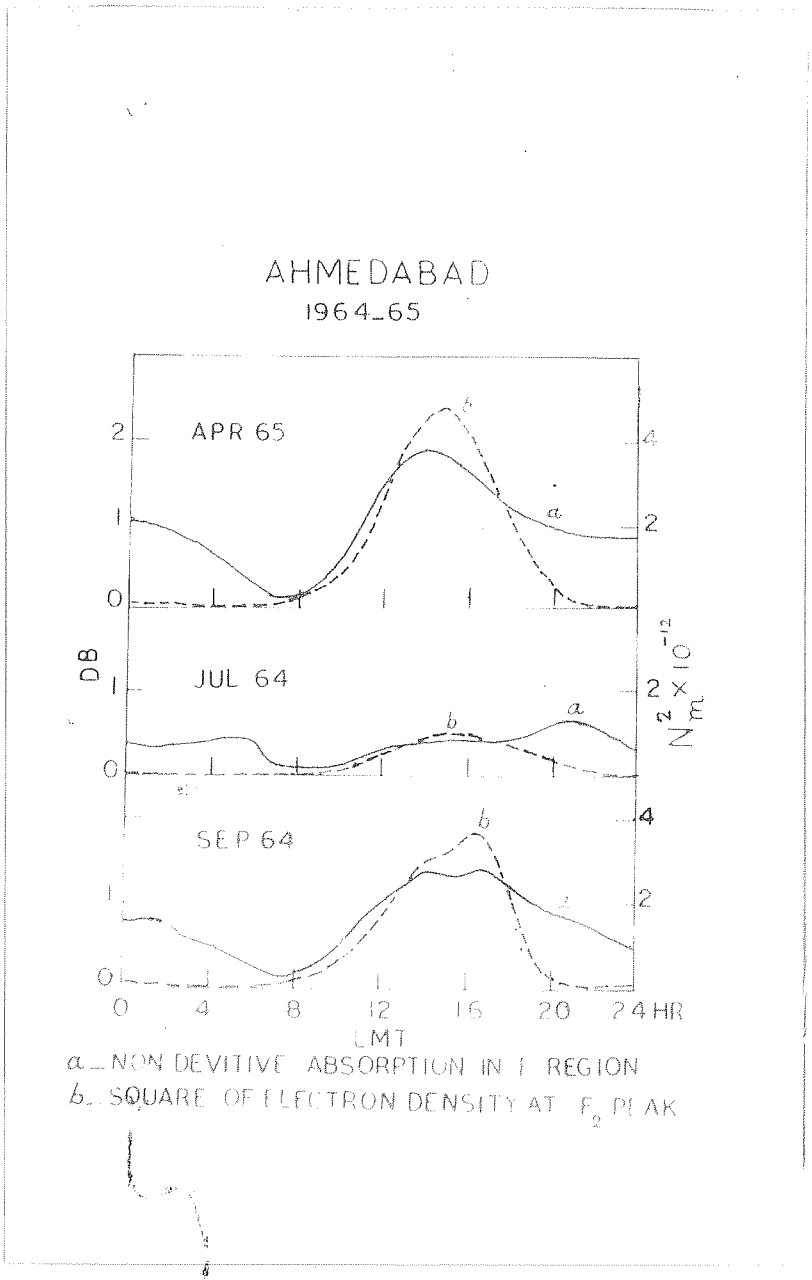


Fig.4.6 Curve (a), nondeviative absorption at 21.3 MHz attributable to altitude above 120 km and curve (b), square of the electron density at $F_2$ peak for April, July and September 1964-65.

was calculated at intervals of 10 km from 120 km to $F_2$ peak. Following King (1960) the monthly median electron density-true

height profiles upto the level of maximum electron density were derived from the median h'(f) curves for each hour obtained by superposing all the h'(f) records at that hour in each month. The data for the period 1957-58 was taken from the earlier analysis made by Shirke (1963) following King's method (1960), and the analysis was extended further by the present author to contain the low sunspot years 1964-65. The summation of absorption at these height intervals gave the total absorption in the region below $F_2$ peak. The diurnal variation of temperature for this calculation was assumed to be that given by Harris and Priester (1964).

## 4.7 Absorption above $F_2$ peak

The residual absorption (after removing the contribution due to absorption below $F_2$ peak) is assumed to have taken place above $F_2$ peak.

Fig.4.7(a) shows the monthly mean diurnal variation of total observed attenuation at 25 MHz for the period 1957-58 and the calculated D region absorption which varies as $\cos^{0.75}\chi$ ($\chi$ is the solar zenith angle). For the zenith angles at different hours in a particular month the values at the corresponding hours on the 15th day of each month were used. n was taken to be 0.75 as was shown by Appleton and Piggott (1954) for high latitudes and also shown by Shirke (1959) to hold good for Ahmedabad during IGY period also. Fig.4.7(b) shows the total nondeviative F region attenuation, the residual absorption above $F_2$ peak and the

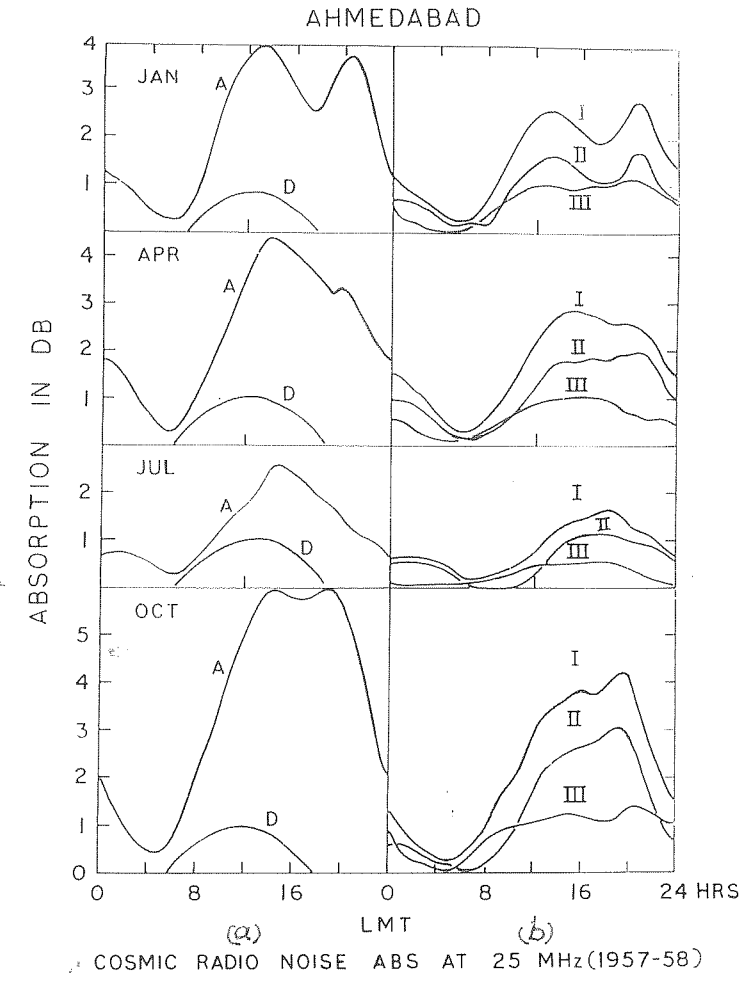


Fig.4.7 (a) The monthly mean diurnal variation of the total CR noise absorption at 25 MHz (Curve A) and the $(\cos^{0.75}\chi$ variation of the calculated D region absorption (Curve D) for January, April, July and October 1957-58.

(b) Monthly mean diurnal variation of the total nondeviative absorption at 25 MHz in the F region (Curve I), the residual absorption above $F_2$ peak (Curve II), and the calculated bottom side absorption (Curve III).

calculated bottom side absorption. These are numbered I, II and III respectively. The corresponding quantities for 21.3 MHz for 1964-65 are shown in Fig.4.8(a) and (b).

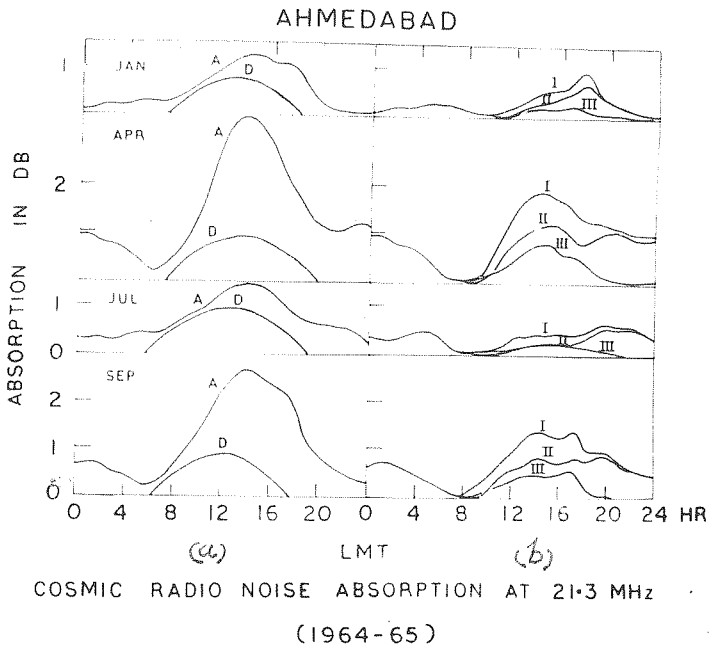


Fig.4.8 (a) Monthly mean total attenuation A and computed D region absorption of galactic radio noise at 21.3 MHz during 1964-65.

(b) Curves I, II and III represent the same quantities as in Fig.4.7(b) (total, topside and bottom-side absorption).

As can be seen in Fig.4.7 and Fig.4.8, the topside absorption is generally higher than the bottomside absorption. This is to be expected because the ratio of the topside to bottomside electron content is known to be in the neighbourhood

of 2 to 3 (see, for example, Evans and Taylor, 1961). If the temperature at the $N_m$ level is assumed to be nearly isothermal, then the ratio of topside to bottomside absorption is also expected to be greater than one. When calculation is made to find the absorption in the topside, using some reasonable extrapolation (such as Chapman $\alpha$ type) of electron densities above $F_2$ peak upto 1000 km, it is found that the ratio is always greater than one. However, a departure from this behaviour is seen between sunrise and noon hours in Fig.4.7 and 4.8. The bottomside absorption being much greater than the topside F region absorption suggests that this may be due to the lack of thermal equilibrium between electrons and neutral particles in the region below $F_2$ peak in the morning hours. Since the absorption in the F region varies as $T_e^{-3/2}$, higher electron temperatures than the neutral gas temperatures at these hours in the bottomside could account for less absorption in the bottomside, so that the ratio of topside to bottomside absorption would rise to the values observed for other hours. The morning phenomenon therefore indicates the existence of a significant temperature difference between the electron and the neutral gas in the morning hours. The difference is maximum immediately after sunrise and gradually disappears towards noon. Satellite results also point out the existence of high electron temperature in the F region following ground sunrise (Bourdeau and Donley, 1964).

Electron temperatures needed to explain the observed F region is discussed in the next chapter.

## 4.8 Discussion

Fig.4.8(b) shows that the nighttime absorption in the F region, calculated on the basis of electron-ion collision is only a small part of the total observed attenuation during 1964-65. This is true in all months of low sunspot years. The possibility that the excess absorption be due to the phenomena of F scatter whose frequency of occurrence increases considerably over Ahmedabad during low sunspot years was mentioned in Chapter III.

The ratio of absorption of topside to bottomside of the $F_2$ peak is calculated for January, April, July and October during 1957-58 at 25 MHz and at 21.3 MHz during 1964-65. This ratio is plotted against local time in Fig.4.9. As indicated in the last section this ratio is significantly small during morning hours. It is emphasised that the small difference in the ratio of top to bottomside absorption between high and low sunspot years is not due to the difference in the exploring frequencies used. The smaller value of this ratio in low sunspot years as compared to high sunspot years indicates that the temperature difference between electron and neutral gas is more in low sunspot years. An analysis to compute electron temperatures is described in Chapter V. The abnormally high ratio that is seen in Fig.4.9 around 04 hr LMT and also throughout night in the low sunspot years 1964-65 is due to very low absorption that could be computed from N(h) profiles in the bottomside F region.

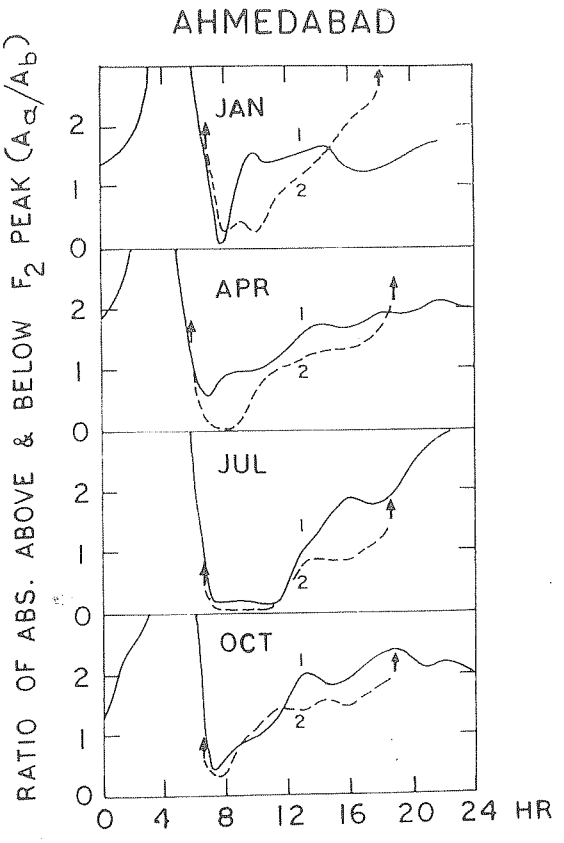


MONTHLY MEAN DIURNAL VARIATION OF THE RATIO OF ABSORPTION ABOVE & BELOW $F_2$ PEAK

1 HIGH SUN SPOT YEARS 1957 58
2 LOW " " " 1964-65

Fig.4.9 The diurnal variation of the ratio of topside absorption above $F_2$ peak to bottomside absorption below $F_2$ peak at 25 MHz during 1957-58 and at 21.3 MHz during 1964-65.

4.9 Summary

The following is the summary of the present study of 25 MHz CR noise through a solar cycle :-

(1) Galactic radio noise absorption at 25 MHz decreased with decrease of solar activity from 1958 to 1964.

(2) Electron-positive ion collisions are mainly responsible for short wave absorption in the F region in latitudes of high $f_0F_2$.

(3) Collisions between electrons and neutral molecules are important only in the D and E regions and the contribution due to these to the total noon value of galactic noise absorption is on the average less than 30 % in low sunspot years.

(4) The evening peak in total absorption occurred in equinoctial and winter months in high sunspot years only.

(5) The nighttime absorption in low sunspot years is considerably higher than can be explained by electron-ion collision processes alone.

(6) There is evidence for high electron temperatures exceeding neutral gas temperatures in the morning hours.

## Table 4.1

$N_e \nu_{em}$ and $N_e \nu_{ei}$ from altitudes 60 km to 900 km. $N\nu_{ei}$ values are for 14 hr in July 1957.

| ALT. Km. | $10^{-8} \times N_e \nu_{em}$ | $10^{-8} \times N_e \nu_{ei}$ | ALT. Km. | $10^{-8} \times N_e \nu_{em}$ | $10^{-8} \times N_e \nu_{ei}$ | ALT. Km. | $10^{-8} \times N_e \nu_{ei}$ |
|---|---|---|---|---|---|---|---|
| 60 | 36.00 | - | 180 | 0.92 | 1.80 | 400 | 43.50 |
| 70 | 61.00 | - | 200 | 0.64 | 1.53 | 450 | 29.50 |
| 80 | 115.00 | - | 220 | 0.43 | 1.95 | 500 | 20.00 |
| 90 | 73.00 | - | 240 | 0.30 | 2.45 | 550 | 15.00 |
| 100 | 71.00 | 0.99 | 260 | 0.26 | 2.99 | 600 | 11.00 |
| 110 | 44.00 | 1.70 | 280 | 0.21 | 5.18 | 650 | 8.00 |
| 120 | 16.00 | 3.58 | 300 | 0.18 | 8.31 | 700 | 6.10 |
| 130 | 4.77 | 2.30 | 320 | - | 14.50 | 750 | 4.70 |
| 140 | 2.72 | 1.46 | 340 | - | 21.01 | 800 | 3.60 |
| 150 | 1.86 | 1.40 | 360 | - | 28.85 | 850 | 2.80 |
| 160 | 1.41 | 1.30 | 380 | - | 39.14 | 900 | 2.30 |

## Table 4.2

The monthly mean of observed total attenuation A of cosmic noise at each hour and the corresponding deviative component of attenuation P as a percentage of A.

| Time 75° EMT | APR. 1957 | | JUL. 1957 | | JAN. 1958 | | OCT. 1958 | |
|---|---|---|---|---|---|---|---|---|
| | A | P | A | P | A | P | A | P |
| 00 | 1.80 | 15 | 0.65 | 4 | 1.30 | 13 | 1.60 | 16 |
| 01 | 1.70 | 15 | 0.65 | 4 | 1.10 | 10 | 1.05 | 10 |
| 02 | 1.35 | 10 | 0.70 | 4 | 0.90 | 8 | 0.85 | 10 |
| 03 | 0.90 | 6 | 0.65 | - | 0.60 | 3 | 0.50 | - |
| 04 | 0.65 | 4 | 0.55 | - | 0.45 | 4 | 0.30 | - |
| 05 | 0.35 | 3 | 0.45 | 3 | 0.25 | 2 | 0.25 | - |
| 06 | 0.25 | 6 | 0.30 | 3 | 0.25 | 7 | 0.25 | - |
| 07 | 0.70 | 8 | 0.35 | 6 | 0.45 | 7 | 0.85 | 10 |
| 08 | 1.30 | 10 | 0.70 | 8 | 0.95 | 13 | 1.50 | 15 |
| 09 | 1.70 | 11 | 1.00 | 7 | 1.85 | 12 | 2.00 | 15 |
| 10 | 2.20 | 14 | 1.15 | 9 | 2.75 | 16 | 2.60 | 18 |
| 11 | 2.82 | 15 | 1.40 | 11 | 3.25 | 17 | 3.50 | 19 |
| 12 | 3.65 | 15 | 1.40 | 11 | 3.70 | 17 | 4.35 | 20 |
| 13 | 4.00 | 19 | 2.10 | 13 | 3.85 | 14 | 5.25 | 21 |
| 14 | 4.45 | 21 | 2.70 | 13 | 3.80 | 19 | 5.55 | 22 |
| 15 | 4.25 | 21 | 2.65 | 12 | 3.45 | 17 | 5.75 | 22 |
| 16 | 4.10 | 21 | 2.40 | 12 | 2.90 | 18 | 5.75 | 20 |
| 17 | 3.90 | 19 | 2.30 | 16 | 2.55 | 17 | 5.25 | 22 |
| 18 | 3.50 | 20 | 2.10 | 14 | 2.80 | 16 | 5.30 | 20 |
| 19 | 3.20 | 18 | 1.80 | 14 | 2.75 | 24 | 5.90 | 21 |
| 20 | 3.25 | 19 | 1.40 | 9 | 3.60 | 23 | 5.00 | 27 |
| 21 | 2.90 | 16 | 1.30 | 11 | 3.65 | 21 | 4.60 | 26 |
| 22 | 2.65 | 17 | 1.10 | 7 | 2.75 | 21 | 3.70 | 29 |
| 23 | 1.95 | 17 | 0.85 | 0 | 1.80 | 17 | 2.40 | 21 |

A = Total attenuation in db

P = Percentage deviative component.

## Appendix 4.1

We have seen that the effective collision frequency in the $F_2$ layer is mainly $\nu_{ei}$ where

$$\nu_{ei} = \left[34 + 4{\cdot}18 \log\left(\frac{T^3}{N_e}\right)\right] N_e T_e^{-3/2}$$

The quantity within the bracket which we shall denote by B is approximately constant varying only by about 8 % when $N_e$ changes by an order of magnitude. Thus for the F region, equation (3) of the text may be written as

$$A = 1{\cdot}17 \times 10^{-14} \frac{B}{T_e^{3/2}} \int N_e^2 \, dh \qquad (1)$$

If we assume parabolic electron density distribution in the neighbourhood of $h_{max}$, then we get from the Chapman Theory

$$N_e = N_m \left(1 - z^2/4H_1^2\right) \text{ for } z < 0 \qquad (2)$$

and

$$N_e = N_m \exp\left(-z/H_2\right) \text{ for } z > 0 \qquad (3)$$

where $z = h - h_{max}$

$H_1, H_2$ = ion scale height just below and above $h_{max}$ respectively

$h_{max}$ = height of maximum electron density

$h$ = height above the ground.

Substituting eq.(2) and (3) in eq.(1), we get

$$A = 1{\cdot}17 \times 10^{-14} \frac{B N_m^2}{T_e^{3/2}} \int_{z=-2H_1}^{z=0} \left(1 - z^2/4H_1^2\right) dz \int_{z=0}^{z=\infty} \exp\left(2z/H_2\right) dz \qquad (4)$$

On integrating (4) the absorption in db becomes

$$D = A/f^2 = 1.17 \times 10^{-14} \frac{B N_m^2}{f^2 T_e^{3/2}} \left[\frac{16}{15} H_1 + \frac{H_2}{2}\right] \qquad (5)$$

Now $N_m = 1.24 \times 10^4 (f_0 F_2)^2$

and taking $H_1$ and $H_2$ to be the average scale height H near the $F_2$ peak, we get from eq.(5)

$$D = 2.2 \times 10^{-6} BH(f_0 F_2)^4 / (f^2 T_e^{3/2})$$

We thus see that K in eq.(1) of the text is proportional to H/

## Appendix 4.2

The total absorption in the vertical, when $\mu$ changes with height, can be written as

$$\int K ds = 1.17 \times 10^{-14} \frac{}{f^2} \int \frac{N_e^2}{\mu} ds \qquad (1)$$

where ds is a height element in the vertical and $\mu$ is the refractive index. When $\mu = 1$, the total calculated absorption corresponds to nondeviative absorption only. When $f_0 F_2$ is high and approaches the operating frequency, $\mu$ departs significantly from unity and in simple ray theory it is equal to (see Ratcliffe, 1962)

$$\mu = \sqrt{1 - f_0^2/f^2}$$

Where $f_0$ is the critical frequency of the $F_2$ layer and f the CR noise operating frequency.

Since most of the F region absorption takes place in the neighbourhood of $h_{max}$, we can calculate $\mu$ from eq.(2) straightaway and treat it as constant near $h_{max}$ and thus can be taken out of the integral in eq.(1). Therefore we get near $h_{max}$

$$\mu \int k\,ds = 1.17 \times 10^{-14} \frac{}{f^2} \int N_e\,ds$$

Now from the observed total CR noise attenuation, the F region component of absorption was separated as explained in the text. This absorption which comprises both deviative and nondeviative components is in effect $\int k\,ds$. Multiplying it by $\mu$, we get reduced absorption which is equal to nondeviative absorption. We can thus estimate approximately the percentage deviative component knowing the value of $f_0F_2$. This component is upto 30 % of the total absorption at Ahmedabad.

# CHAPTER V

## COMPUTATION OF ABSORPTION OF COSMIC RADIO NOISE IN THE F REGION UPTO 1000 KM :- ELECTRON TEMPERATURE FROM COSMIC RADIO NOISE ABSORPTION

### 5.1 Introduction

In the previous chapter we described the method of calculating the absorption up to $h_{max}$ using N(h) profiles and the effective electron collision frequencies. A similar method is adopted here to calculate the absorption in the topside of F region from $h_{max}$ to 1000 km using certain electron density distribution models. On the basis of rocket and satellite experiments, it is found that in the region immediately near the $F_2$ peak, the electron distribution is of the Chapman $\alpha$ type, while well above the peak (where diffusive equilibrium of electrons and ions exists) an exponential distribution holds ((Yonezawa (1955), Jackson and Bauer (1961), Bungey (1962), Seddon (1963)). Bauer (1962) discussed the problem of electron density distribution above the $F_2$ peak under diffusive equilibrium of a ternary mixture of $O^+$, $H^+$ and $He^+$ in an isothermal ionosphere and derived a formula which would fit in with the observed distribution.

### 5.2 Absorption upto 1000 km

In the present analysis, we have first calculated the topside electron density model on the following basis :-

(i) From $h_{max}$ to $(h_{max} + H/2)$, Chapman distribution, $N = N_o \exp(1-z-e^{-z})$, where $z = (h-h_{max})/H$ and

(ii) From $(h_{max} + H/2)$ to 1000 km, Bauer's distribution.

Near $h_{max}$, H was taken to be the scale height of atomic oxygen.

In the topside ionosphere, the distribution depends on the temperature and relative concentrations of ions, $O^+$, $He^+$ and $H^+$ assumed. Table 5.1 gives the ratio $n(H^+)/n(O^+)$ and $n(He^+)/n(O^+)$ used in the analysis with the values of temperatures and scale height H at $h_{max}$.

Table 5.1

Altitude = 400 km

| Temperature | H | $n(H^+)/n(O^+)$ | $n(He^+)/n(O^+)$ |
|---|---|---|---|
| $T_g$, $^oK$ | Km | | |
| 1000 | 53 | $6 \times 10^{-3}$ | $2 \times 10^{-2}$ |
| 1500 | 80 | $1.3 \times 10^{-4}$ | $2 \times 10^{-2}$ |

The average value of $h_{max}$ in high sunspot years was in the range 350-400 km and in the low sunspot years around 300 km. The values shown in the table were taken to be 400 km, roughly the level of $(h_{max} + H/2)$. These values agree with those of Hanson (1963). The same ratio of $n(H^+)/n(O^+)$ as at 1000 $^oK$ was assumed between 750 $^oK$ and 1200 $^oK$ to hold good for all

thermospheric temperatures and that at 1500 $^{o}K$ for temperatures between 1200 $^{o}K$ and 2000 $^{o}K$. Electron density profiles up to 1000 Km were worked out according to this model for all the 24 hours using monthly median $N_m$ and $h_{max}$ values at Ahmedabad. Complete profiles were obtained for January, April, July and September-October 1957-58 and 1964-65. The diurnal variation of temperature as in HP model was used for the calculations. Two examples of electron density profiles obtained by this method are shown in Fig.5.1 (broken line), one of which corresponds to $T_g$ equal to 1000 $^{o}K$ and the other 1650 $^{o}K$. These are typical of noon conditions in low and high sunspot years. The topside absorption was then calculated for each hour from $h_{max}$ to 1000 km by the method already explained. To this was added the bottomside absorption to get the total absorption in the region 120 km to 1000 km. Fig.5.2 shows the monthly mean diurnal variation of observed nondeviative absorption for 25 MHz in the F region deduced from cosmic noise absorption (curve 1) and the calculated absorption in 120-1000 km region (curve 2) for 25 MHz during 1957-58. Fig.5.3 shows similar plot for 21.3 MHz during 1964-65. It will be seen that though the two curves show similar behaviour, there is no complete agreement between the calculated and observed absorptions. The departures are more noticable during morning and forenoon hours in all the months. It is known from rocket and satellite results that the assumption of thermal equilibrium between electron and neutral atmosphere in the F region is not correct (Boudeau and Donely (1964), Brace and Spencer (1964 )). The difference is therefore probably due to the assumption that $T_e = T_g$ used in the calculation.

Electron density profiles from 120 to 900 km for 14 hr April during 1957 and 1964.

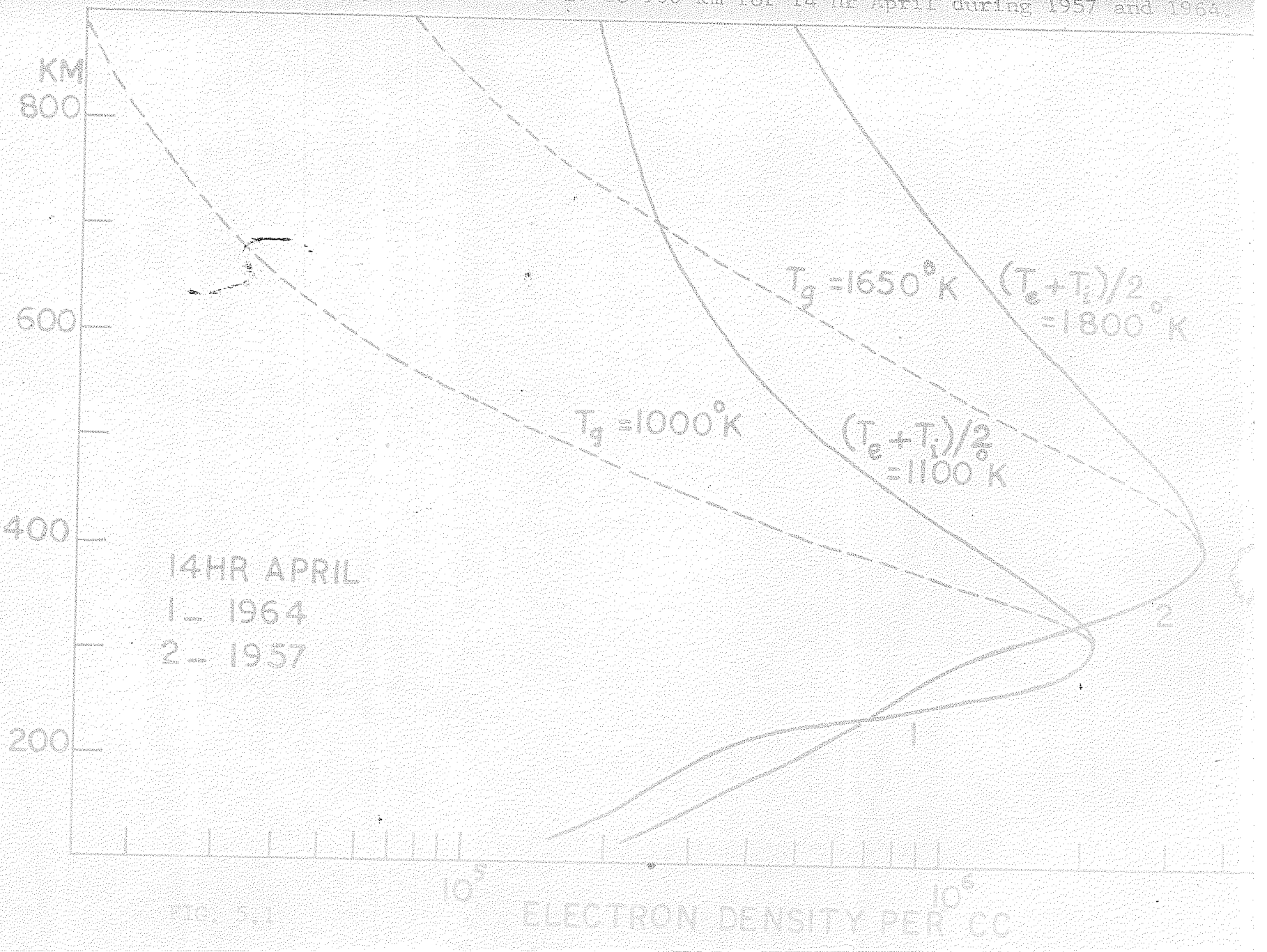


FIG 5.1

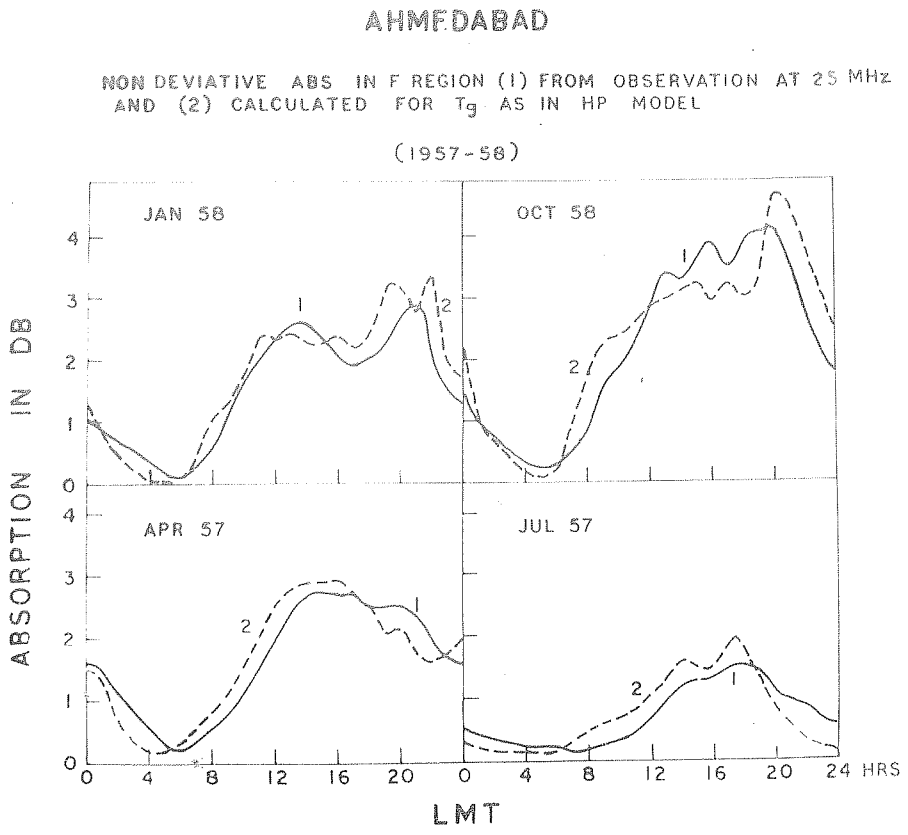


Fig.5.2 Nonderiative absorption of CR noise at 25 MHz attributable to altitudes above 120 km (curve 1), and that calculated for the same frequency from 120 to 1000 km using $T_g$ as in HP model (curve 2) for January, April, July and October 1957-58.

It may be thought that the disagreement between the observed and calculated absorptions may be due to absorption beyond 1000 km. This point was examined by calculating the absorption using the $H^+$ concentration data obtained by Taylor et al (1965) between 1000 and 20000 km. In extreme cases of electron density and temperature the calculated absorption was

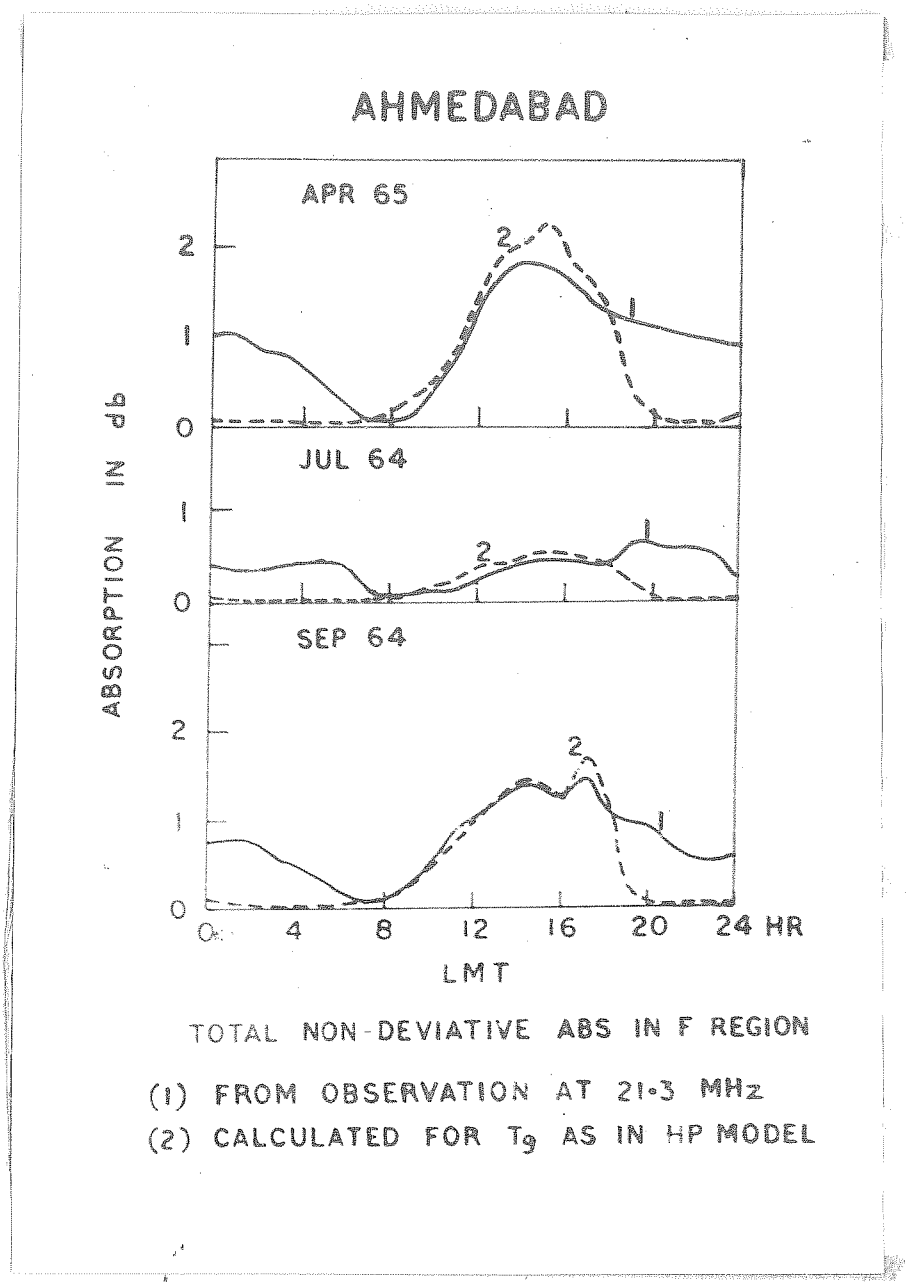


Fig.5.3 Nondeviative absorption of CR noise at 21.3 MHz attributable to altitudes above 120 km (curve 1), and that calculated for the same frequency from 120 km to 1000 km using $T_g$ as in HP model (curve 2) for April, July and September 1964-65.

less than 0.002 db which is well within the limits of error of the measurements and hence we concluded that it could be ignored.

## 5.3 Calculation of electron temperature $T_e$

The difference between the calculated and observed absorptions becomes less if we change the temperature assumed for the electrons in calculating the absorption. Thus the electron temperatures necessary to make the observed and calculated results to agree can be evaluated. This was done by recalculating the absorption in the region 120-1000 km by varying the temperature till the difference between the observed and calculated values became either zero or very small. These calculations were performed on IBM computor and the solution was obtained by iteration. Two examples of electron density profiles obtained in the final iteration are shown in Fig.5.1 (solid line) corresponding to plasma temperatures $(T_e+T_i)/2$ equal to 1150 $^oK$ and 1800 $^oK$ (assuming $T_i = T_g$).

We would like to make a remark here that the electron temperature shows maximum deviation from the neutral gas temperature around 180 km below which most of the solar EUV is absorbed (Hanson and Johnson, 1961). This however does not alter substantially the value of absorption if we use such an electron temperature profile. This is because the product $N\nu$ which determines the cosmic noise absorption is minimum at these altitudes (see Table 4.1 in Chapter IV) and the temperature change in this region has very little effect on the calculated absorption as compared to that near the $F_2$ peak.

It will be seen that the absorption values during night in low sunspot years have not been calculated by this method

since the absorptions are exceptionally large at those times and cannot be explained by change of $T_e$ only. During low sunspot years a different mechanism is needed to explain the observations as mentioned earlier. The same reasoning would apply to the absorption condition before sunrise in high sunspot years.

## 5.4 Results and discussion

Monthly mean hourly values of electron temperatures ($T_e$) obtained for January, April, July and October in 1957-58 and for April, July and September in 1964-65 are shown in Fig.5.4 and 5.5 respectively.* Maximum number of SCNA was observed in July 1957. January and October were less disturbed and therefore may be taken to represent less disturbed ionospheric conditions in the high sunspot year. The temperature $T_e$ derived in the present analysis is the electron temperature near the $F_2$ peak since it is temperatures and electron densities near this level that most affect the absorption. The general features of $T_e$ at $F_2$ peak will therefore be discussed. The $h_{max}$ level during 1957-58 was between 350-400 km and that during 1964-65 around 300 km.

### (i) Diurnal variation of $T_e$

The monthly mean hourly values of $T_e$ shows the following well defined diurnal features :

---

* Absorption data during winter 1964-65 were not satisfactory and hence have not been included in these calculations.

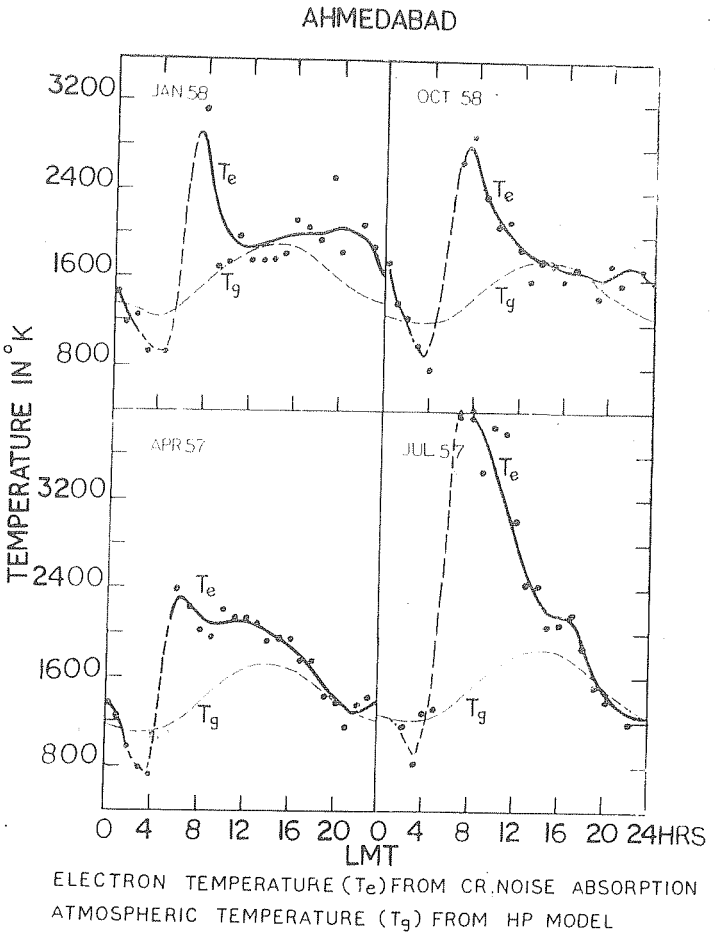


Fig.5.4 Monthly mean diurnal variation of $T_e$ deduced from CR noise absorption and $T_g$ (broken line) for the same period, during January, April, July and October 1957-58.

(1) A rapid increase after sunrise reaching a maximum at 07-08 hr LMT.

(2) A gradual fall towards an afternoon plateau. The value of the plateau depends on the season, solar activity and geomagnetic disturbance.

(3) A general decrease after sunset to reach a minimum just before sunrise. A nighttime secondary peak at 20-22 hr LMT is observed in January and October 1958 at the same time as that of $N_{max}$ (see Fig.4.5).

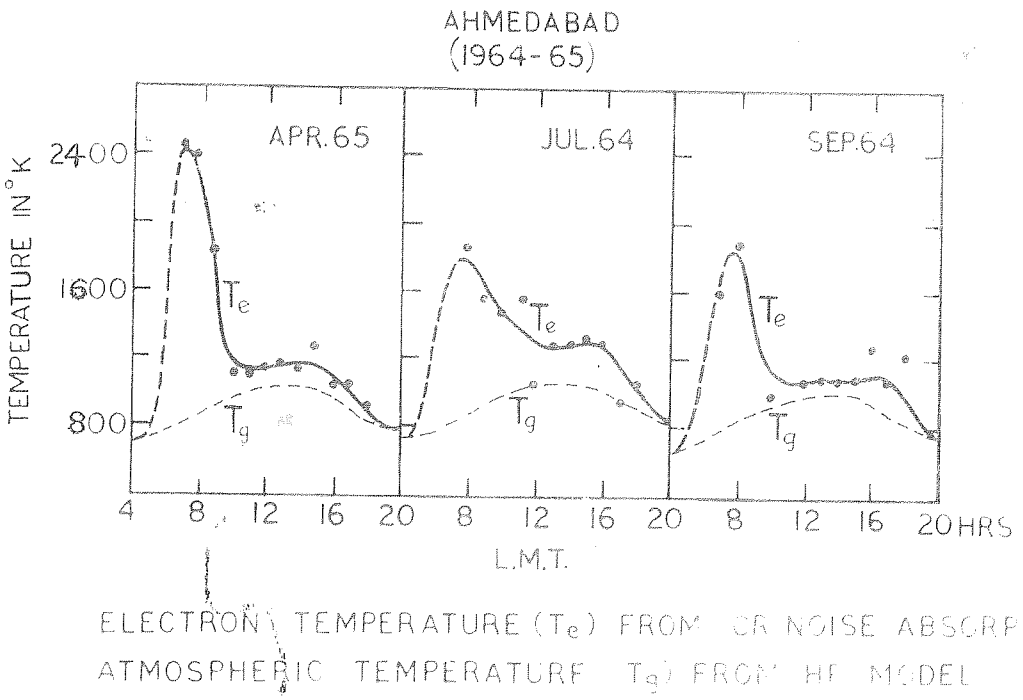


Fig.5.5 Monthly mean diurnal variation of $T_e$ deduced from CR noise absorption and the corresponding $T_g$ for April, July and September 1964-65.

Thermosphere temperature ($T_g$) given by the NP model corresponding to the period of our observations is shown in the same figure. It is seen that the departure of electron temperature from neutral gas temperature is a regular feature during forenoon hours in all seasons in both high and low sunspot years. This departure, ($T_e$-$T_g$), is maximum during the hours immediately following the sunrise. Midday values also show appreciable departure from $T_g$ except in January and October 1958.

It is useful to compare the present results with those obtained from satellite measurements. The occurrence of a diurnal maximum of electron temperature in the morning is in good agreement with the results of Explorer VIII obtained by Bourdeau and Donley (1964) at 1000 km between 50 and 70 $^{o}$S latitude in 1960. The time of occurrence of maximum according to Bourdeau and Donley (1964) was during the sunrise period, namely 06-07 hr LMT. This time difference can be expected since as noted by Bourdeau (1964) there might be enough absorption of EUV above 300 km to shift the $T_e$ maximum to later hours. Brace and Spencer (1964 b) have also reported from Explorer 17 measurement that $T_e$ was maximum between 09 and 10 hr between 250-400 km.

It is interesting to see how the values of ($T_e$-$T_g$) obtained from the present analysis compare with the theoretical calculations of Hanson and Johnson (1961) and Dalgarno et al (1962) made on the basis that EUV is the only source of ionization in the F region. The equilibrium electron temperature which exists in the F region is by collisions with positive ions and is given by the equation

$$Q/n_e^2 = 5.5\times10^{-7}\times(T_e-T_i)/T_e^{3/2} \quad \ldots (1)$$

On the basis of local heating by photo ionisation Dalgarno et al (1963) showed that the value of $Q/n_e^2$ in the F region is of the order of $10^{-9}$. The solution of eq.(1) for different values of $T_e$ and $n_e$ showed that $(T_e-T_i)$ is very sensitive to the value adopted for $T_i$ and $n_e$ when $Q/n_e^2$ exceeds $10^{-9}$. At the level of maximum electron density where Q may be taken to be proportional to the number density of atomic oxygen n(O), the magnitude of $Q/n_e^2$ calculated for Ahmedabad is of the order $10^{-8}$ immediately after sunrise. n(O) values for these calculation were taken from the MP model. $(T_e-T_i)$ was calculated for April and July in both high and low sunspot years and is shown in Fig.5.6 along with that obtained from the CR noise absorption analysis. The values for 1964-65 appear to show better correspondence with the theoretically inferred values than those for 1957-58. The large departure in high sunspot years may be due to the high magnetic activity during those months. However it must be emphasised that such a comparison is of qualitative significance only until more direct measurements are made.

(11) Seasonal variation of daytime $T_e$

As can be seen in Fig.5.4 and 5.5 the daytime $T_e$ is higher in July than in other months for high and low sunspot years. The difference is much more in high sunspot years than in low sunspot years. The seasonal variation of electron-ion temperatures has been reported by many workers. Schmelovsky

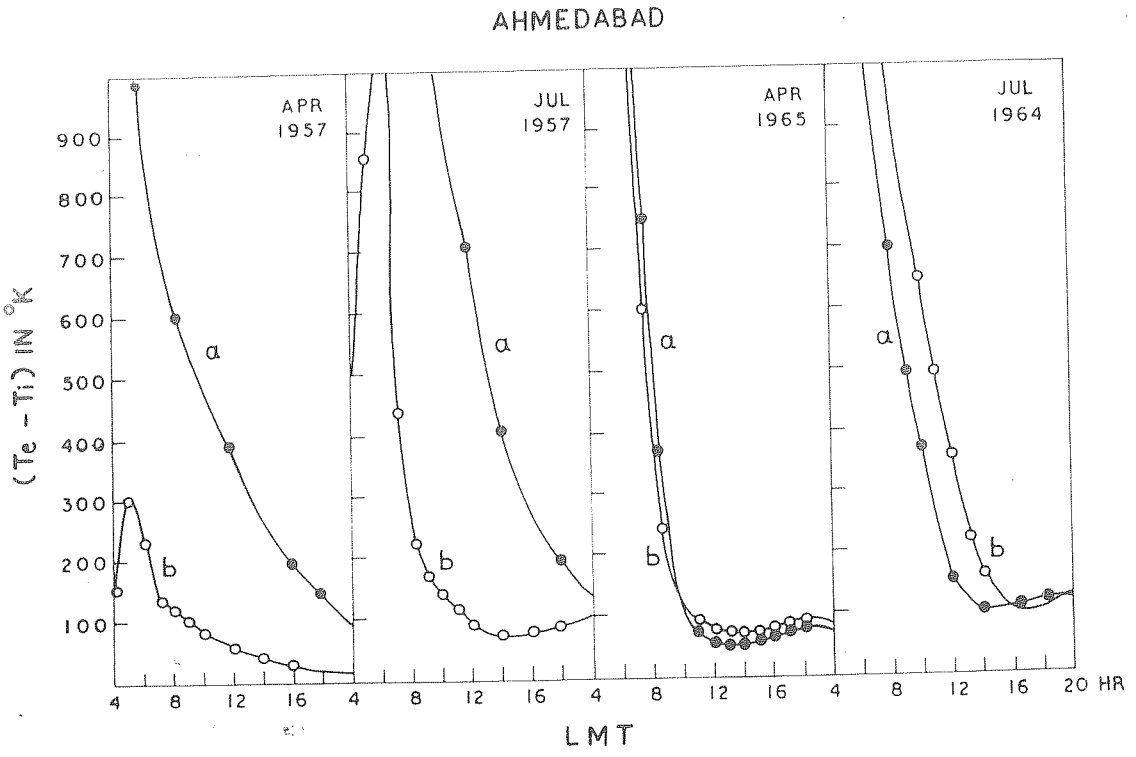


Fig.5.6 $(T_e - T_i)$ assuming $T_i = T_g$, deduced from CR noise data, curve (a), and that calculated according to Dalgarno's method.

(1964) obtained large plasma temperatures in summer (2865 °K) than in winter 1550 °K) from rocket and satellite data and from Faraday fading of radio signals. Larger values of the equivalent slab thickness of the topside ionosphere (which is a measure of the scale height and hence temperature) in summer than in winter are reported by Roger (1964). However the larger difference between July and other months observed in high sunspot years seems to be due to the highly disturbed ionospheric conditions in July 1957.

The seasonal variation of $f_0F_2$ is characterised by lower values in summer than in winter or equinox over Ahmedabad. Accordingly, one should expect higher values of $Q/n_e^2$ during summer than in other seasons, if Q remains constant throughout. Thus $(T_e-T_i)$ would be more during summer. The difference between $T_e$ and $T_i$ will be larger if, as stated earlier, the quantity $Q/n_e^2$ exceeds $10^{-9}$ or if the electron density decreased considerably. The noon value of $(T_e-T_i)$ inferred from the formula shows seasonal variation as can be seen in Fig.5.6, in agreement with the value of $(T_e-T_i)$ obtained from the analysis and is larger in July than in April both during high and low sunspot years. It is also seen that the value of $(T_e-T_i)$ obtained for July 1957 is much higher than that for quiet ionospheric conditions on the basis of the variation of the ratio $Q/n_e^2$.

# CHAPTER VI

## TOTAL ELECTRON CONTENT IN THE IONOSPHERE FROM COSMIC RADIO NOISE ABSORPTION

### 6.1 Introduction

The electron densities from 120-1000 km which accounted for the observed amount of CR noise absorption were used to calculate the total electron content above and below the $F_2$ peak. In addition, the ratio $n_a/n_b$ of the electron content above to that below the $F_2$ peak and $n_a/N_m$, the ratio of the topside content to the maximum electron density and their variation with season and solar activity were studied and compared with those from Faraday feding analysis of S66 satellite signals made at Ahmedabad during the same period. We shall discuss the results of each of these in the following pages.

### 6.2 Total electron content in a vertical column and its variations

Fig.6.1 shows the monthly mean diurnal variation of total electron content for January, April, July and October for 1957-58. The total electron content above the $F_2$ peak ($n_a$) and below it ($n_b$) are also shown in the same figure. It may be noted that the minima in these curves usually occur just before sunrise. This is followed by a rapid rise of electron content both below and above the ionization peak. The diurnal peak occurs around

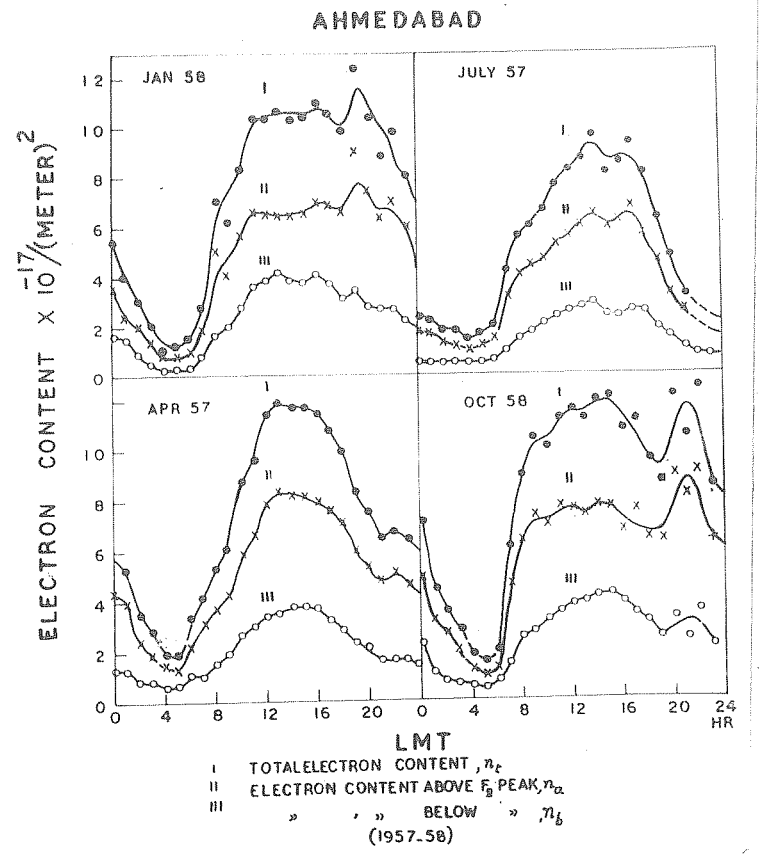


Fig.6.1 Monthly mean diurnal variation of total electron content $n_t$ (curve I), electron content above $F_2$ peak $n_a$ (curve II) and that below $F_2$ peak $n_b$ (curve III) for January, April, July and October 1957-58.

14 hr LMT, after which the values either decrease gradually towards a morning minimum or do this after passing a secondary maximum around 22 hr.

Considering first the seasonal aspect, both in October and January of 1958 the morning increase in the total content following ground sunrise is very sharp. The ionization appears to remain at a steady level till sunset, after which it develops a secondary maximum whose amplitude is comparable with the daytime maximum. These characteristics were more pronounced in the topside content than in the bottomside content and the secondary nighttime peak in the topside was as prominent as the daytime peak. The decrease of ionization after 22 hr LMT was also sharp. April and July 1957 showed a much more gradual increase in ionization after sunrise and a gradual decrease after sunset and the diurnal curves were more symmetrical about 14 hrs LMT. Quantitatively speaking the electron content increased at a rate of $2.0 \times 10^{13}$ electrons per $cm^2$ per hour in January and October and at $1.4$ and $1.0 \times 10^{13}$ in April and July respectively. The rate of ionization content in the night was also approximately of the same order. The seasonal variation of the total electron content during high sunspot years obtained from our analysis is in agreement with the results obtained for the same period from satellite measurements. Yeh and Swenson (1961), using 20 and 40 Mhz signals from Sputnik III calculated the total electron content for the period 1958-59 and found that the maximum diurnal amplitude occurred in April and October and the minimum in July with an intermediate value in January.

Monthly mean values of the electron contents, $n_a$, $n_b$ and $n_c$ for April, July and September during the low sunspot years 1964-65 are shown in Fig.6.2. The nighttime values were calculated

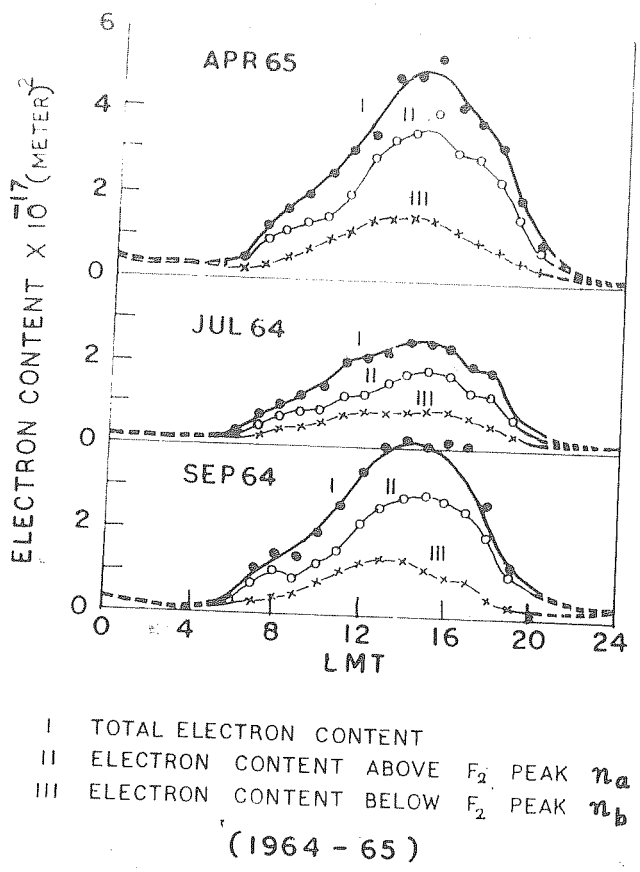


Fig.6.2 Monthly mean diurnal variation of $n_t$, $n_a$ and $n_b$, curves I, II and III respectively, for April, July and September 1964-65.

using $T_g$ values given in HP model and are shown by broken lines. The maxima are seen to occur around 14-15 hr LMT. No secondary maximum in electron content is observed in the low sunspot years.

It is interesting to compare these results with those obtained from Faraday fading records of 5 satellite signals recorded at Ahmedabad for the same period. This is shown in Fig.6.3(a) for the summer months of 1965. The diurnal maximum which occurs around 14 hr IMT has got an average value of $3 \times 10^{13}$ electrons per $cm^2$. This compares reasonably well with the average value for July 1964 obtained from the present analysis, which is around $3.5 \times 10^{13}$ electrons per $cm^2$.

## 6.3 Solar cycle variation in $n_t$

The maximum electron content is seen to occur in equinoxes both in high and low sunspot years. The values of diurnal maximum are 12.0, 11.0 and $9.0 \times 10^{13}$ $el/cm^2$ respectively in equinoxes, winter, and summer during high sunspot years and 4.5 and $2.5 \times 10^{13}$ for equinox and summer respectively in low sunspot years. The yearly average values of the total content showed a decrease by a factor of 3 from high to low sunspot years. From the measurement of total electron content using differential Doppler measurements of radio transmission from satellite Transit 4A made over Washington and Ottawa, Bhonsle et al (1965) found a linear relation between $n_t$ and the mean sunspot number R of the form $n_t = a(1+bR) \times 10^{13}$ $el/cm^2$ when R was greater than 40. The values of the coefficient b changes with season, being higher in winter and equinoctial months than in summer. If we assume that a similar relationship between R and $n_t$ exists from high to low solar activity at Ahmedabad, the value of b comes out to be 0.04 as an average for all seasons.

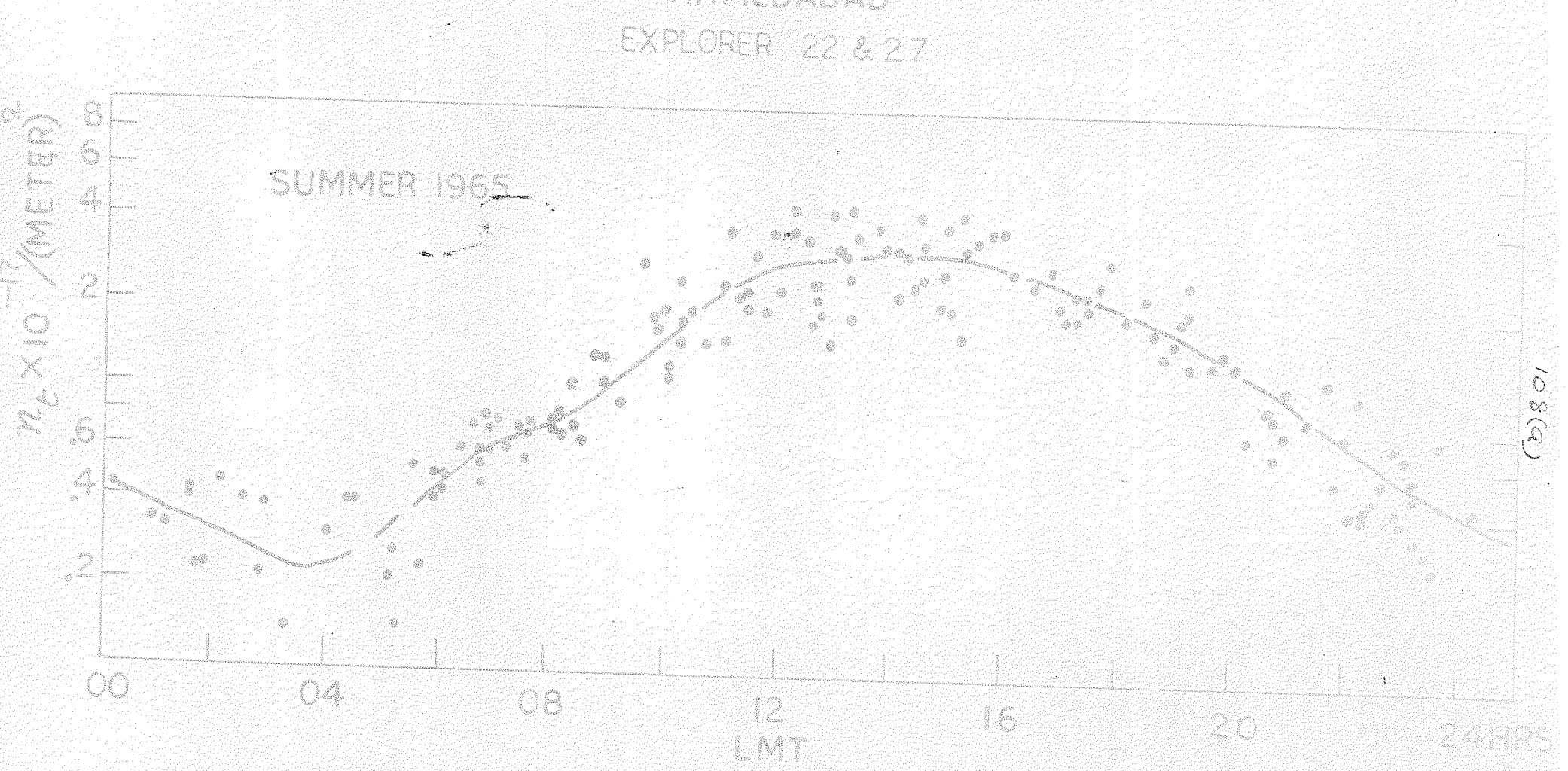


FIG. 6.3

Diurnal variation of total electron content obtained by Mr. S. Ramakrishnan from measurement of Faraday fading of signals from Explorer 22 and 27 during Summer 1965.

This is in good agreement with the values obtained by Bhonsle et al (1965) for equinox and winter months, namely 0.045. No remarkable seasonal variation in b was observed over Ahmedabad though Bhonsle obtained a variation from 0.02 to 0.047.

6.4 Variation of the ratio $n_a/n_b$ during day and night

The monthly mean diurnal variation of this quantity is shown in Fig.6.4(a) for 1957-58. The values are in general lower during daytime than during nighttime. A minimum appears around noon and then gradually increases towards night. Similar variation in this ratio is seen in the results of topside sounder Alouette published by King et al (1963). The values during the sunrise period being ambiguous are not shown in the figure, but it can be seen that there is a trend for this ratio to be high during these hours. As regards the seasonal variation of $n_a/n_b$, January shows minimum and July shows maximum with midday values 1.7 and 2.3 respectively. Such a seasonal variation in daytime $n_a/n_b$ obtained from the present analysis is consistent with that of Evans and Taylor (1961, 1964) obtained from Faraday rotation measurements of moon echo signals during 1960-61 for middle latitudes. The ratio obtained by these authors is however higher than the present values (2.5 and 5 for winter and summer respectively).

The so-called seasonal anomaly which is more pronounced in high sunspot years and in middle latitudes is the occurrence of larger critical frequencies in winter than in summer. It is

interesting to note that the anomaly is also seen at Ahmedabad below $h_{max}$ but since the ratio of the top to bottomside ionosphere electron content is less in winter than in summer, the anomaly is not well marked in the topside. Similar features are seen in

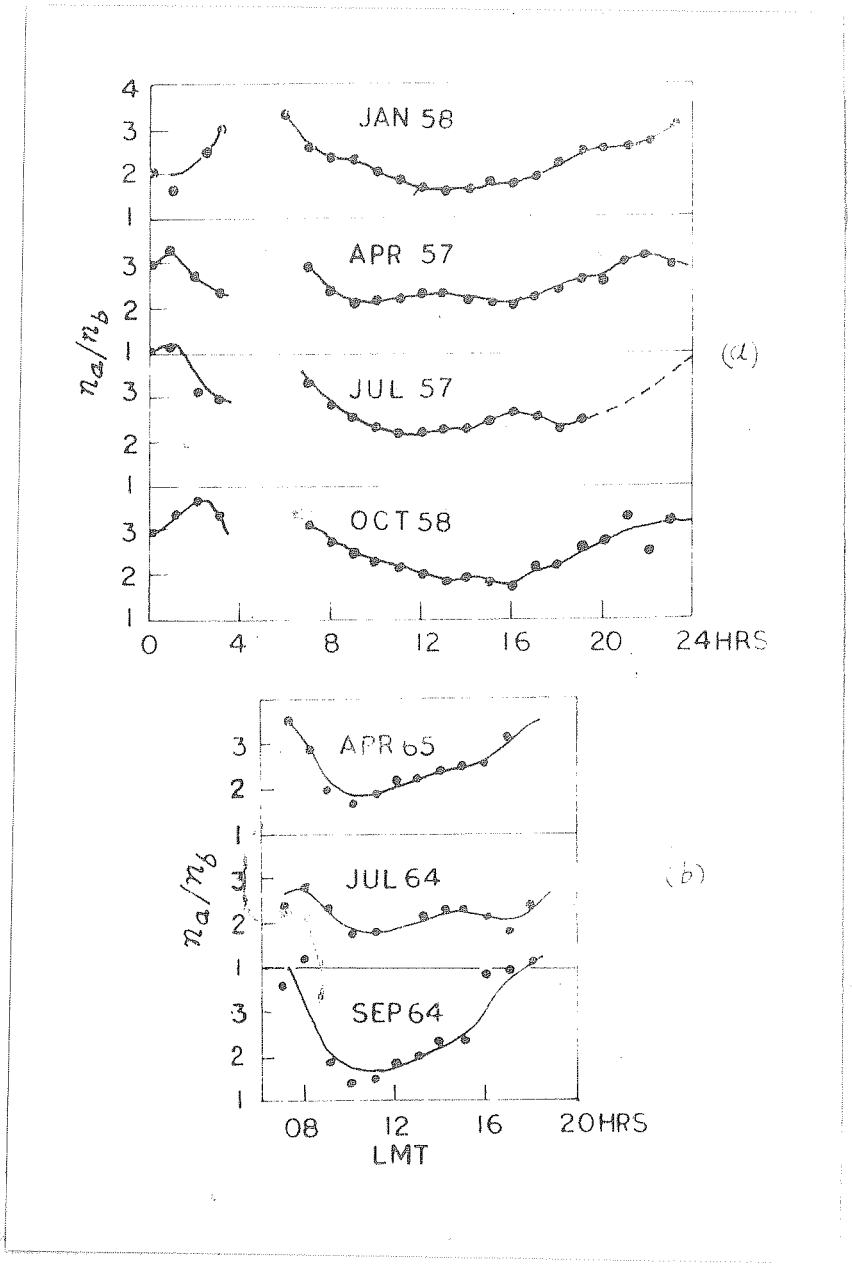


Fig.6.4(a) Monthly mean diurnal variation of $n_a/n_b$ for January, April, July and October 1957-58,
(b) for April, July and September 1964-65.

satellite results also. Ross (1960) measured the total electron content by dispersive Doppler method and studied its seasonal variation during 1958-59 and noticed that the seasonal anomaly in the total electron content is only half that seen in the ionization maximum at the $F_2$ peak. The monthly mean diurnal variation of the ratio $n_e/n_p$ for April, July and September for the low sunspot years 1964-65 are shown in Fig.6.4(b). The diurnal characteristics are similar to those for high sunspot years. In general, the average value of $n_e/n_p$ over Ahmedabad has not changed significantly from high to low sunspot years. The values of $n_t/n_p$ derived by S.Ramakrishnan (private communication) from 866 satellite measurements at Ahmedabad during 1964-65 are shown in Fig.6.5. It can be seen that there is general agreement between the diurnal variation of this ratio deduced from the present analysis and that obtained from the satellite observations.

## 6.5 The ratio of total electron content above the $F_2$ peak to the maximum ionization ($n_e/N_m$)

Fig.6.6(a) shows the diurnal variation of topside electron content expressed in terms of electron density at the $F_2$ peak for the period 1957-58. As can be seen from this figure there is a diurnal variation in this quantity with maximum around noon (except January when the diurnal variation is not clear). Minimum noon $n_e/N_m$ is observed in winter and maximum in summer. These observations are in agreement with the satellite results of Ross (1960) which were obtained during 1957-58. From satellite

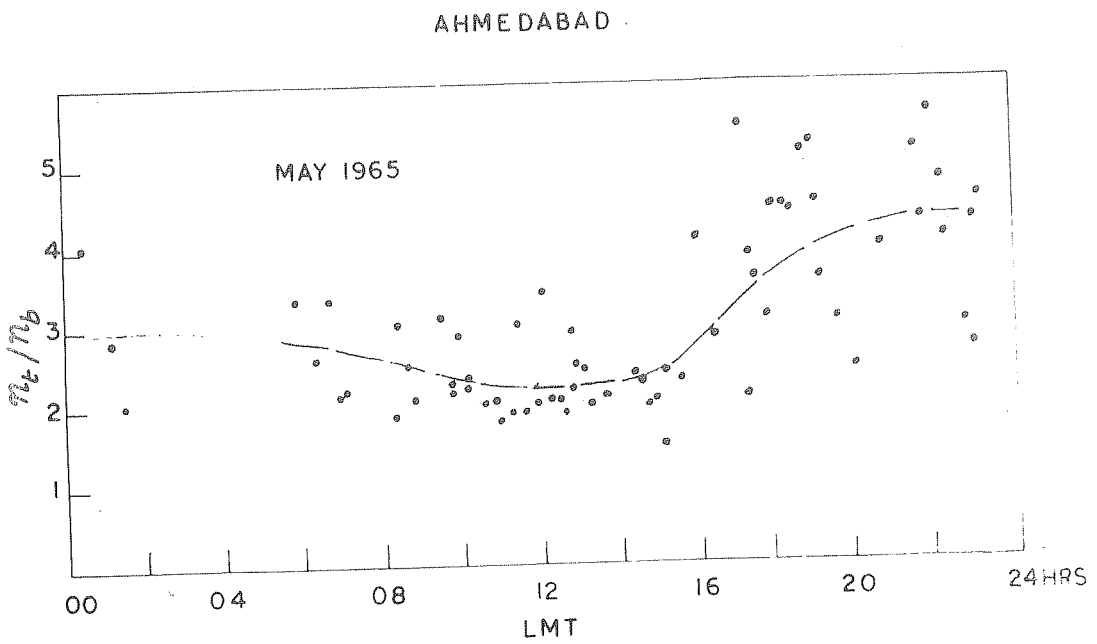


Fig.6.5 $n_a/n_b$ from Faraday fading measurements from Explorer 22 and 27 during summer 1965 (Mr.S.Ramakrishnan).

Doppler measurements made during 1961-62, Hibberd and Ross (1966) also observed that the ratio $n_e/N_m$ was greater during daytime and in summer. The monthly mean diurnal variation of $n_e/N_m$ for April, July and September during the low sunspot years 1964-65 are shown in Fig.6.6(b). For reasons mentioned earlier the nighttime values have not been evaluated. According to Fig.6.6(b), July shows maximum in low sunspot years also. The daytime average of this ratio for 1957-58 was 260 km while in 1964-65, it was 175 km.

PHYSICAL RESEARCH LABORATORY
AHMEDABAD

The parameter $n_a/N_m$ is also called the slab thickness of the topside ionosphere and its variations gives an approximate idea of the scale height changes in the topside. Thus the decrease in this ratio from high to low sunspot years indicates a significant decrease of the ion-electron scale height in the topside ionosphere.

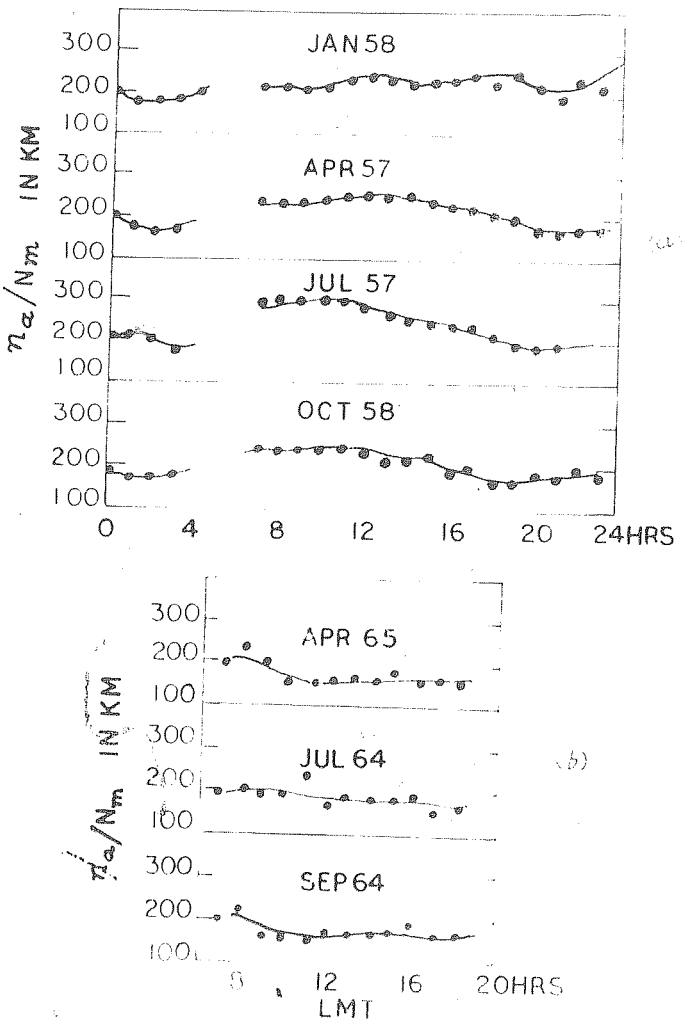


Fig.6.6(a) Monthly mean diurnal variation of $n_a/N_m$ for January, April, July and October 1957-58,
(b) For April, July and September 1964-65.

The scale height is also a measure of the temperature of the ionospheric plasma and hence the ratio is expected to show higher value during daytime than nighttime similar to the diurnal thermospheric temperature variations. This is found to be so as can be seen in Fig.6.6(a). All these curves show a maximum around noon (except in January). However such a diurnal variation is not seen in the curves for low sunspot years shown in Fig.6.6(b). The ratio appears to be steady all day.

## 6.6 Discussion

We saw in Fig.4.5 that the electron density maximum at the $F_2$ peak showed a prominent secondary peak after sunset around 22 hr in equinoctial and winter months of high sunspot years. From Fig.4.1 also, we see that the total absorption shows a similar nighttime peak. An increase in $N_m$ associated with increased absorption after sunset can occur as a result of subsidence of ionization in a vertical column due to decrease of temperature following sunset. But the fact that this phenomenon is observed only in equinoctial and winter months of high sunspot years cannot be accounted for by temperature decrease. Ramanathan and Bhonsle (1959) attributed part of the secondary absorption peak to the occurrence of F scatter, but we find that the total absorption calculated up to 1000 km using appropriate temperatures agrees tolerably well with the observed attenuation and hence the contribution by F-scatter may be small. It is interesting to note that the total electron content in a vertical column also shows a secondary peak around 22 hr in winter and equinox during 1957-58.

In conclusion we may add that our present results are in conformity both as regards electron temperature and total electron content in the F region with those obtained by direct and indirect experiments in middle latitudes.

# CHAPTER VII

## IONOSPHERIC DISTURBANCES AND COSMIC RADIO NOISE ABSORPTION

### 7.1 Introduction

The changes observed in cosmic radio noise attenuation due to solar flares and geomagnetic storms are studied in this chapter. Three types of changes can be recognised from the record of cosmic radio noise intensity : (1) Short period absorption events during which the intensity of cosmic radio noise drops off suddenly within 1 to 10 minutes and recovers at a slower rate within 10 to 30 minutes. These absorption events are known as SCNA's (Sudden Cosmic radio Noise Absorption) which are due to enhanced ionization in the D region by X-rays of wavelength less than 10 Å emitted during a solar flare, (2) A general depression or rise in the noise level from the normal level which lasts for several days and are associated with geomagnetic disturbances and (3) A sharp increase of intensity which may exceed the peak value of the galactic noise. These are usually due to radio bursts from the sun and sometimes also from Jupiter.

### 7.2 Solar flare effects on cosmic radio noise absorption

A solar flare is a sudden brightening of a part of the Sun's surface accompanied by enhanced emission of wave and particle radiations. Large flares consist of a complex pattern of "white-hot" filaments which reach their maximum intensity five or ten minutes after their first appearance and then decay within an hour or two.

Small flares are associated with minor bright patches, usually without any filamentary structure. Flares are classified on a visual scale of importance from Class 1 (smallest) to Class 3 (largest), class $3^+$ is reserved for flares of exceptional brightness area and intensity.

The enhanced light emitted by a flare is made up chiefly of individual spectral lines. The emission lines of hydrogen and the H and K lines of singly ionized calcium are prominent. The Lyman $\alpha$ line (1216 Å) of hydrogen and the hellium line at 584 Å are also enhanced. Rocket observations of the spectra of flares show that X-rays also are emitted and with the increase in the intensity of the flare, increasing amount of X-rays of the shortest wavelength are emitted (Friedman, 1964).

Jansky (1937) was the first to show that cosmic radio noise undergoes absorption during an SID. Shain and Mitra (1954) compared their results on the absorption of 18.3 MHz cosmic radio noise in Australia with the observation of SPA's on 16 KHz observed by Bracewell and Straker (1949) in England and showed that an increase of 1 db in the absorption of 18.3 MHz radiation was probably associated with an SPA of size about 200 degrees at 16 KHz. Ramanathan et al (1956) reported two flares on 23rd February 1956 and 10th March 1956, the former became famous due to its exceptional intensity and caused spectacular cosmic ray increases near the geomagnetic equator (Sarabhai et al, 1956).

Bhonsle (1960) analysed SCNA's recorded on 25 MHz at

Ahmedabad during the period 1956-60. A large number of SCNA's were recorded during this period. From an examination of over 80 events, he broadly classified the SCNA's observed at Ahmedabad into four groups, depending on the nature of the absorption curve. (1) Type A was characterised by a sudden increase in absorption, (2) Type B was accompanied by burst of solar radio noise, (3) Type C was associated with multiple or extended solar flares and (4) Type D when the SCNA was observable when the sun was low near horizon. It was found that most of the SCNA's were preceded by a solar radio burst (Type B). The most frequent value of maximum absorption produced during an SCNA was between one and two decibels and the number of SCNA's decreased with increase in their size. The time of growth was of the order of 5 minutes which was in good agreement with those observed by earlier workers. The duration and strength observed at Ahmedabad was markedly larger than those observed at 18.3 MHz by Shain and Mitra (1954). It was also noticed that the duration of an SCNA tended to increase with size.

With the decline of sunspot activity since 1960 the number of SCNA's recorded decreased considerably. However a few of those recorded since 1965 will be described below.

7.3 <u>SCNA's recorded on 25 MHz, 21.3 MHz and 16.5 MHz at Ahmedabad and Thumba during 1964-66</u>

Some of the SCNA events recorded at the three frequencies at Ahmedabad and Thumba during 1965-66 are analysed. In Table 1

we have listed all the SCNA's recorded at 21.3 MHz riometer at Ahmedabad during 1965-66. Fig.7.1 shows some actual records which generally show simple features, namely a sharp or gradual fall in intensity of the cosmic radio noise lasting 1 to 5 minutes and a much more gradual recovery extending 10 to 30 minutes.

Table 7.1

SCNA's recorded on 21.3 MHz at Ahmedabad during 1965-66

| Date | Time of beginning UT | Time of maximum absorption UT | Maximum absorption dB |
|---|---|---|---|
| 2-10-65 | 0415 | 0418 | 1.62 |
| 7-11-65 | 0712 | 0718 | 0.60 |
| 29-12-65 | 0641 | 0643 | 0.90 |
| 28-2- 66 | 0353 | 0358 | 0.46 |
| 19-3 -66 | 0339 | 0347 | 1.34 |
| 20-3 -66 | 0955 | 1000 | 3.09 |
| 24-3 -66 | 0235 | 0240 | 1.07 |
| 25-3 -66 | 0515 | 0518 | 0.97 |
| 28-3 -66 | 0438 | 0445 | 0.78 |
| 29-3 -66 | 0327 | 0331 | 1.94 |

However some exceptions to this general behaviour can be seen in the flare record of 2 October, 1965 where the drop and the recovery are equally sharp. Incidentally, it should be noted that

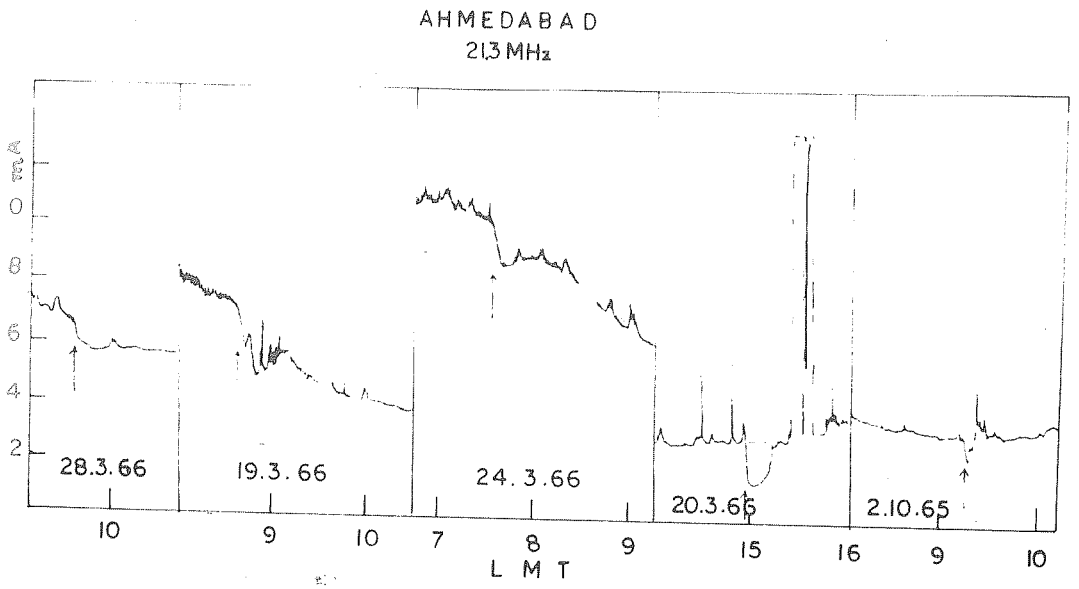


Fig.7.1 Records of SCNA's on 21.3 MHz observed at Ahmedabad during 1965-66.

the SCNA records in Fig.7.1 are arranged in the order of decreasing time of growth. It should be noted that the fine structure of SCNA on 19 March 1966 is due to the interference from a neighbouring pulse transmitter. Unlike during high sunspot years 1956-60, none of the SCNA's in low sunspot years was preceded by a solar radio noise burst. The tendency for the durntion of the event to increase with the size of the flare is also not seen. Fig.7.2 shows two SCNA's observed on two frequencies simultaneously at 25 MHz and at 21.3 MHz at Ahmedabad and at

21.3 MHz and 16.5 MHz at Thumba. The increase in the strength of the SCNA with smaller exploring frequency can be clearly seen.

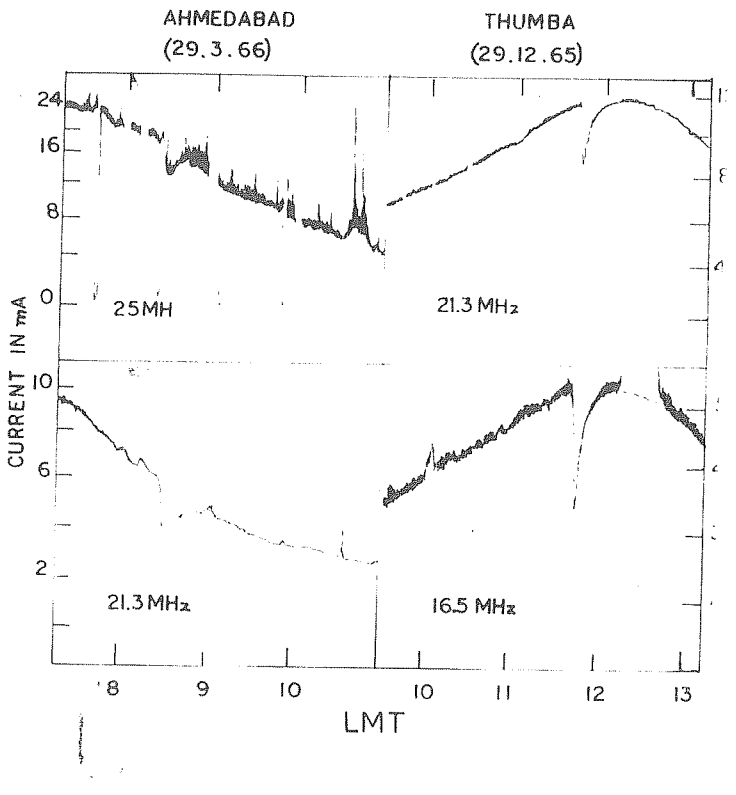


Fig.7.2 SCNA's records simultaneously on 25 MHz and 21.3 MHz at Ahmedabad and on 21.3 MHz and 16.5 MHz at Thumba.

## 7.4 Dependence of the strength of SCNA on solar zenith angle

Simultaneous measurement of an SCNA at a given frequency and at a number of stations at different solar zenith angles can be used to verify the dependence of D region absorption on the zenith angle of the incoming ionizing radiation during a solar flare. Early calculations made by Appleton (1937) for a simple Chapman layer showed that the absorption varied with the solar zenith angle according to $\cos^{n}\chi$ where n = 3/2. Most of the results obtained later (Appleton and Piggott, 1954) by pulse reflection method showed that the value of n was much less than 3/2. We saw in Chapter III that the value of n can be larger at the cosmic radio noise recording frequencies since at those frequencies the assumption, $f \gg \nu$ made in the original derivation of n, is generally satisfied.

Two SCNA events recorded on 2 October 1965 and 27 December 1965 at 21.3 MHz at Ahmedabad and Thumba are listed in Table 7.2 with the corresponding zenith angles appropriate to the time of observations.

Table 7.2

SCNA's observed simultaneously on 21.3 MHz at Ahmedabad and at Thumba

| Date | Time of SCNA maximum UT | AHMEDABAD | | THUMBA | |
|---|---|---|---|---|---|
| | | Maximum absorption db | Solar zenith angle | Maximum absorption db | Solar zenith angle |
| 2-10-65 | 0418 | 1.62 | $47^{\circ}36'$ | 2.08 | $37^{\circ}10'$ |
| 29-12-65 | 0643 | 0.90 | $46^{\circ}46'$ | 1.30 | $31^{\circ}14'$ |

Fig.7.3 shows a plot of log A vs. log ($\cos\chi$). The slope of these lines gives m = 1.6 which is very close to the theoretically predicted value 1.5. More accurate values however can be obtained if observations are made at a number of stations. From the observations of a solar flare on April 15, 1963 at 5 stations (Accra, Addis Ababa, Bed Ford, Athens and New Delhi), Horowitch and Goldman (1963) also found that m was about 1.5.

## 7.5 Frequency dependence of D region absorption, obtained from SCNA

Multifrequency observation of a solar flare is useful to find the dependence of D region absorption on the exploring frequency. This dependence is of the form $A \propto f^{-n}$, where A is absorption and f the exploring frequency. In the case of nondeviative absorption in the quasilongitudinal mode, when $f \gg \nu$ the value of n can be shown to be equal to 2.0. A plot of log f vs log $\Delta A$, where $\Delta A$ is the maximum absorption of cosmic radio noise during an SCNA is shown in Fig.7.4 for a few SCNA events recorded at Ahmedabad on 21.3 MHz and 25 MHz. It can be seen that in majority of the cases the points lie on a straight line whose slope is around 2.2. This indicates that during these SCNA's the maximum ionization of the D region took place at an altitude where the collision frequency $\nu$ was very much less than the exploring frequency. A similar plot of frequency vs absorption at 21.3 and 16.5 MHz at Thumba is shown in Fig.7.5 which yielded n = 1.6. Similar low values of n have

FIG. 7.3

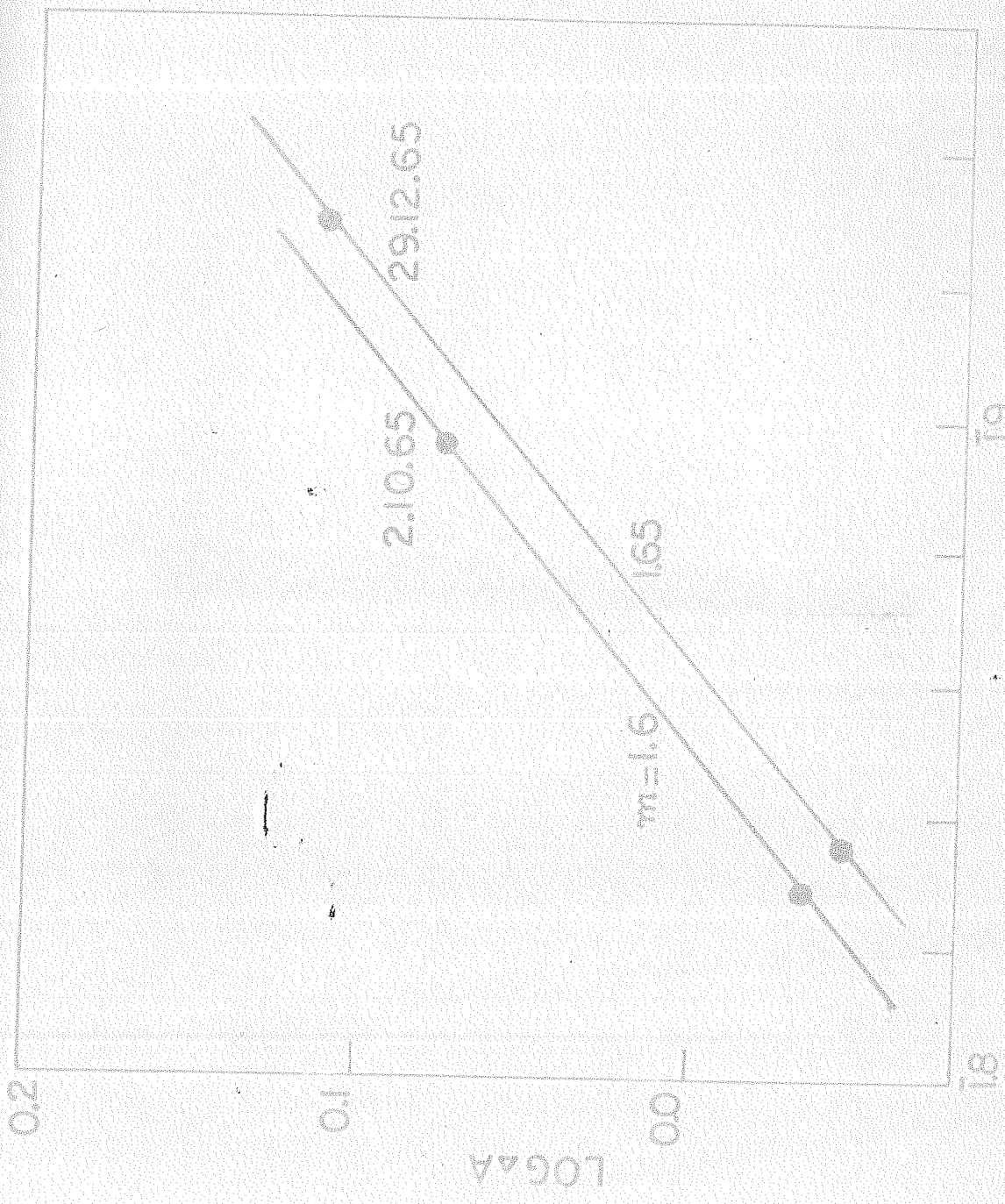

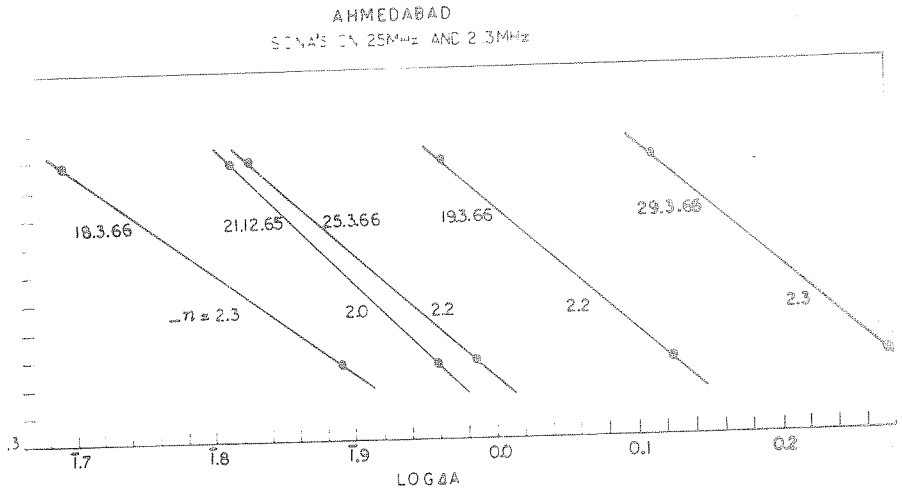


Fig.7.4 Plot of log( $\Delta A$) vs log (f) for Ahmedabad.

been reported by some workers at low latitude stations. Skinner and Wright (1956) obtained n = 1 for Ibadan using pulse reflection method and explained the low values of n as due to the collision frequency in the absorbing region being comparable to the exploring frequency. Ramamurthy and Ramachandra Rao (1964) obtained n = 1.5 for Waltair, a low latitude station. There is probably a latitudinal change in this index.

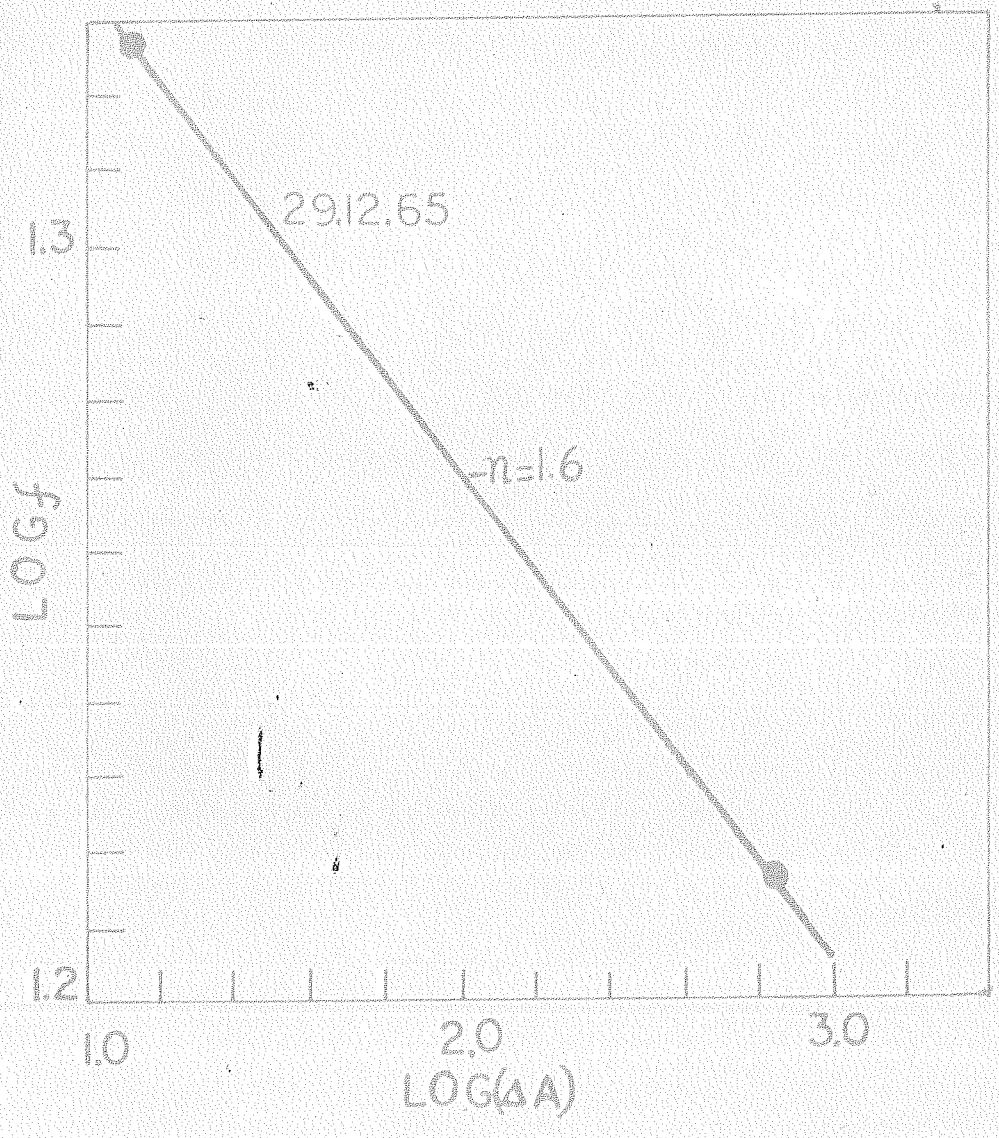


FIG. 7.5

Plot of log(f) vs log(ΔA) for SCNA's recorded on 16.5 MHz and 21.3 MHz at Thumba.

## 7.6 Conclusions

(1) The SCNA's observed during 1965-66 are less intense than those observed during 1957-58.

(2) Simultaneous observation of SCNA's at Ahmedabad and Thumba on 21.3 MHz has made it possible to determine the dependence of D region absorption on solar zenith angle. The value of the index obtained is very close to the theoretically predicted value.

(3) Multifrequency observation of SCNA's at 25 MHz and 21.3 MHz at Ahmedabad has shown that the absorption in the D region over Ahmedabad varies as $f^{-2.2}$. The index compares well with that obtained from the magnetoionic theory when absorption takes place at altitudes where the collision frequency of electrons with neutral particles is negligible compared with the cosmic radio noise frequency.

(4) At the equatorial station Thumba, the D region absorption is found to vary as $f^{-1.6}$. The number of occasions for this study have however been small.

## 7.7 A study of the effect of magnetic storms on cosmic radio noise absorption

It is known that magnetic storms are caused by the arrival at the earth of clouds of charged particles from the sun. Some of the magnetic storms are preceded by solar flares

by some 20-30 hours. Every magnetic storm cannot however be shown to be associated with a flare; many of the weaker ones have a marked tendency to recur at intervals of 27 days, the solar rotation period, from the so-called M regions of the sun. Worldwide storms frequently begin with a sudden commencement which is simultaneous within a few seconds all over the world. A magnetic storm is characterised usually by a sudden increase in H, the horizontal component of the magnetic field above the normal value. The increase lasts for two-three hours and is followed by a decrease below the normal level known as the main phase. After the main phase a slow recovery takes place which continues for several days.

## 7.8 The F region of the ionosphere during a magnetic storm

Berkner, Seaton and Wells (1939) were the first to study the effect of magnetic storms in the ionosphere. They observed a large decrease in the electron density during a severe sc storm on April 16, 1938 at Kensington and Huancayo. Later Berkner and Seaton (1940) reported changes in electron density and height of the $F_2$ region following the sc. These results indicated that changes in F region started almost simultaneously with the storm. Appleton, Ingram and Naismith (1937) showed that the changes in $\Delta f_0F_2$ associated with a magnetic storm varied with season and local time. Maeda and Sato (1959) summarised the characteristics of the daily variations of $\Delta f_0F_2$. At higher latitudes $\Delta f_0F_2$ was negative and occurs usually around noon throughout the years. The duration of the depression depends

on season. At low latitudes $\Delta f_0F_2$ is positive with few exceptions. In middle latitudes both types of changes occur. Increase in $f_0F_2$ usually occurs from noon towards night in winter. Depression generally occurs around noon hours in summer.

Kotadia and Ramanathan (1959) studied the behaviour of $F_2$ region over Ahmedabad under magnetically disturbed conditions during 1953-57 and found that the disturbance variation of $f_0F_2$ showed morning rise and day-time depression. Kotadia (1959) also examined the relation between spread F and magnetic activity and conclusively showed that the occurrence of spread F was less frequent in magnetically disturbed periods.

## 7.9 Cosmic radio noise absorption during magnetic storms

We have seen that the total absorption of cosmic radio noise is made up of two components namely, one which does not depend upon $f_0F_2$ and the other which varies as $f_0F_2^4/T_e^{3/2}$. It was shown that the absorption in the night can also be caused partly by the phenomenon of F-scatter. During a magnetic storm both $f_0F_2$ and spread F activity are known to undergo significant changes. Bhonsle and Ramanathan (1960) studied the effect of magnetic storms on the absorption of 25 Mhz cosmic radio noise absorption at Ahmedabad during 1957-58. They analysed a number of sudden commencement type magnetic storms. A decrease in the total absorption on the first two days after the sudden commencement of the storm was noticed. The day following the end of the storm showed a large increase over the normal level of absorption. The degree of departure of the total attenuation

from the normal expected value depended on the local time. Maximum deviation in total attenuation was observed around 20-21 hr LMT. Minimum change was observed around 04 hr LMT. Degaonkar and Bhonsle (1962) found that isodense levels of electron density spread out on the day following the storm, with decrease in CR noise absorption.

## 7.10 Magnetic storms and cosmic radio noise attenuation at 21.3 MHz during 1964-65

A list of magnetic storms during 1964-65 for which analysis was made, is shown in Table 7.3.

Table 7.3

List of magnetic storms analysed during 1964-65

| Date | Storm time UT of beginning hour | minute | UT of ending date | hour | Intensity |
|---|---|---|---|---|---|
| 10-6 -64 | 03 | 02 | 11 | 22 | moderate |
| 3-8 -64 | 01 | 31 | 5 | 19 | moderate |
| 22-11-64 | 16 | 06 | 23 | 16 | moderate |
| 20-2 -65 | 12 | 30 | 21 | 21 | slight |
| 22-2 -65 | 14 | 30 | 24 | 01 | moderate |
| 3-6 -65 | 13 | 20 | 05 | 06 | moderate |
| 14-6 -65 | 08 | 00 | 15 | 01 | slight |
| 15-6 -65 | 11 | 00 | 18 | 22 | moderate |
| 27-7 -65 | 06 | 15 | 29 | 22 | moderate |

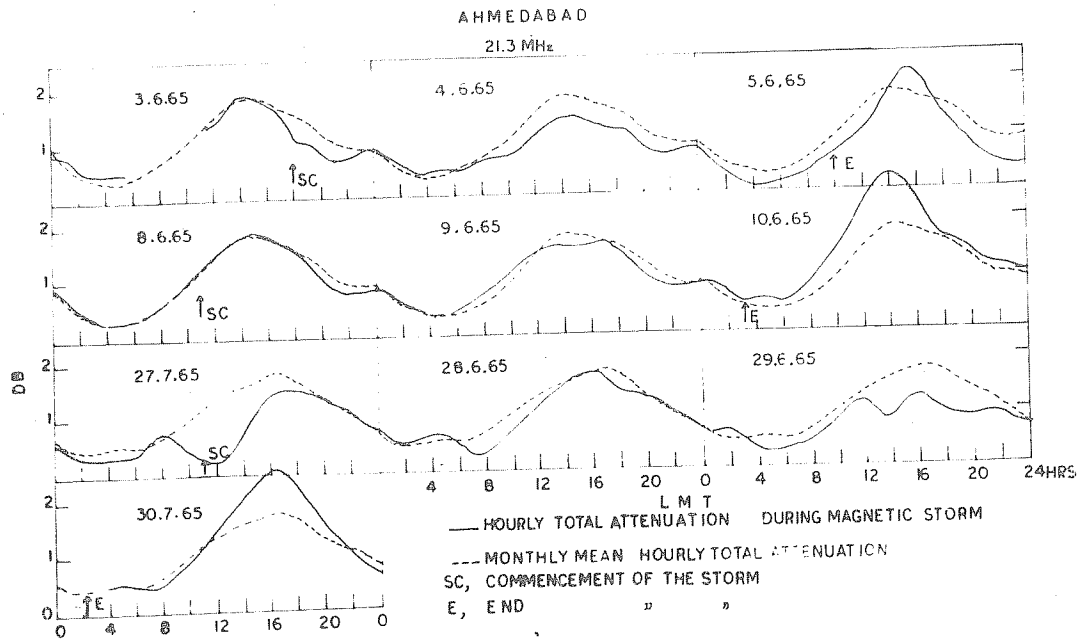


Fig.7.6 Hourly values of total attenuation during three magnetic storms superposed on the monthly mean values.

We have plotted in Fig.7.6 hourly values of attenuation of cosmic radio noise at 21.3 MHz at Ahmedabad during three magnetically disturbed periods in 1965 along with the monthly mean attenuation. We note that a decrease in the total attenuation is seen following the commencement of the storm and lasts till the end of the storm. On the day following the end of the storm, the attenuation generally shoots up above the monthly mean level. The effect of a magnetic storm on the total attenuation of cosmic radio noise can be judged from its

deviation from the monthly mean values. The average diurnal variation in attenuation $\Delta A$ on the two days preceding the end of the storm is shown in Fig.7.7(a). It is clear that the effect of a magnetic storm is to reduce the cosmic radio noise attenuation. The maximum deviation is found at about 18 hr LMT. The change in absorption $\Delta A$ in the morning and night hours is not appreciable. In Fig.7.7(b), the diurnal variation of $\Delta A$ obtained by Bhonsle and Ramanathan (1960) during 1957-58 is shown for comparison. It can be seen that the maximum deviation during 1957-58 occurred at a later hour (20-21 hr LMT).

The cosmic radio noise intensity rises above the monthly average value after the end of the storm. We have plotted in Fig.7.8(a) the average hourly departures $\Delta A$ in attenuation associated with the three magnetic storms shown in Fig.7.6, two days preceding and two days after the end of the storm. Zero hour is taken as that day on which the storm ended. On the first day after the end of the storm an overall increase in attenuation can be seen, the maximum amplitude of deviation occurs around 15 hr LMT. The post-storm increase in total cosmic radio noise attenuation is much more pronounced than the decrease during the storm. Fig.7.8(b) shows a similar curve obtained by Bhonsle and Ramanathan during the IGY. A comparison of the two curves shows that the maximum effect of a magnetic storm on cosmic radio noise attenuation occurs at a slightly different hour during 1964-65 and 1957-58. It is to be noticed that the maximum increase and decrease was around the same local time i.e. 20-21 hr

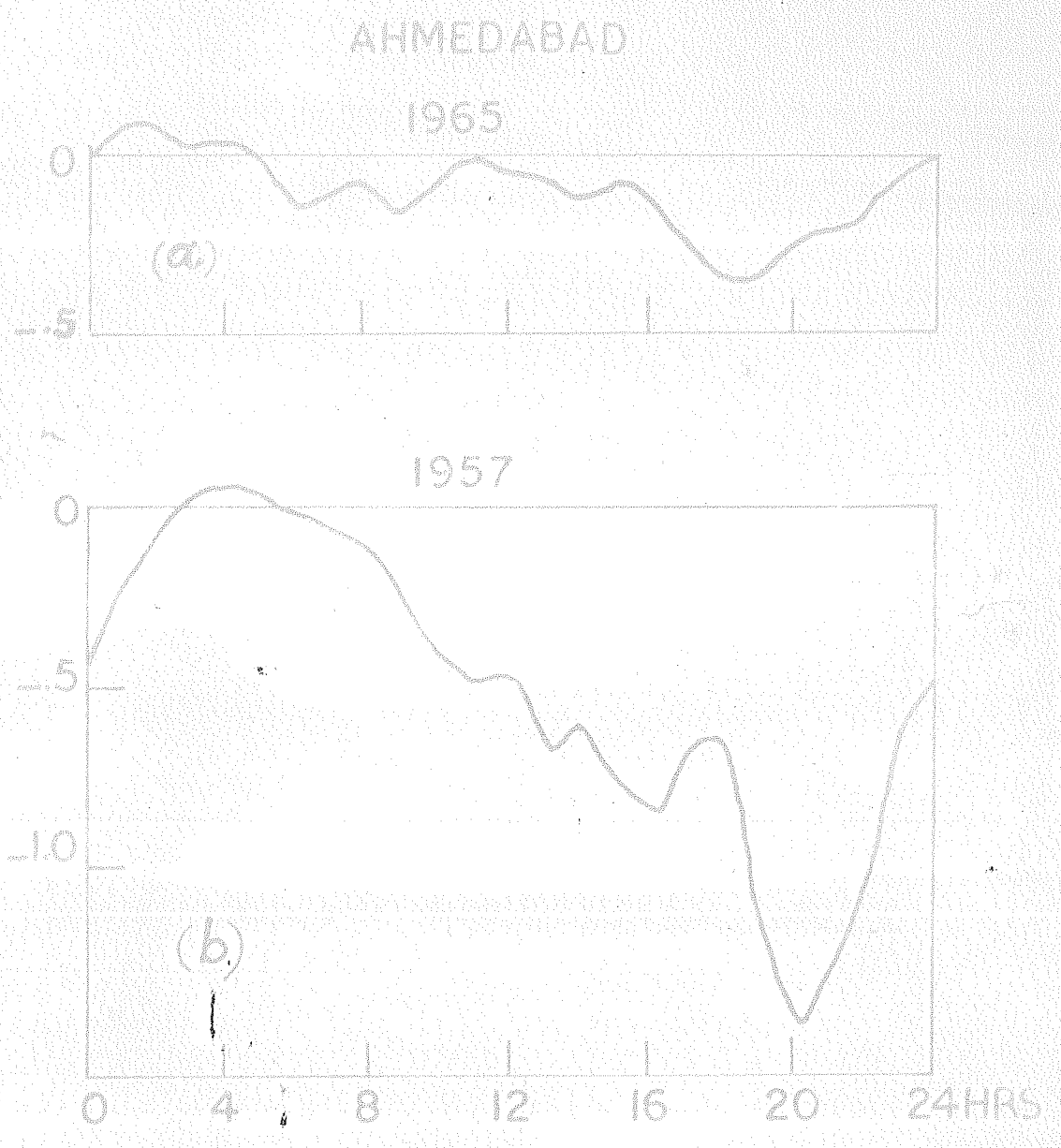


THE AVERAGE DIURNAL CHANGE IN ΔA ON TWO DAYS PRECEEDING THE END OF THE STORM

FIG. 7.7

LMT during 1957-58 while maximum depression was around 17-18 hr and increase around 15 hr LMT during 1964-65.

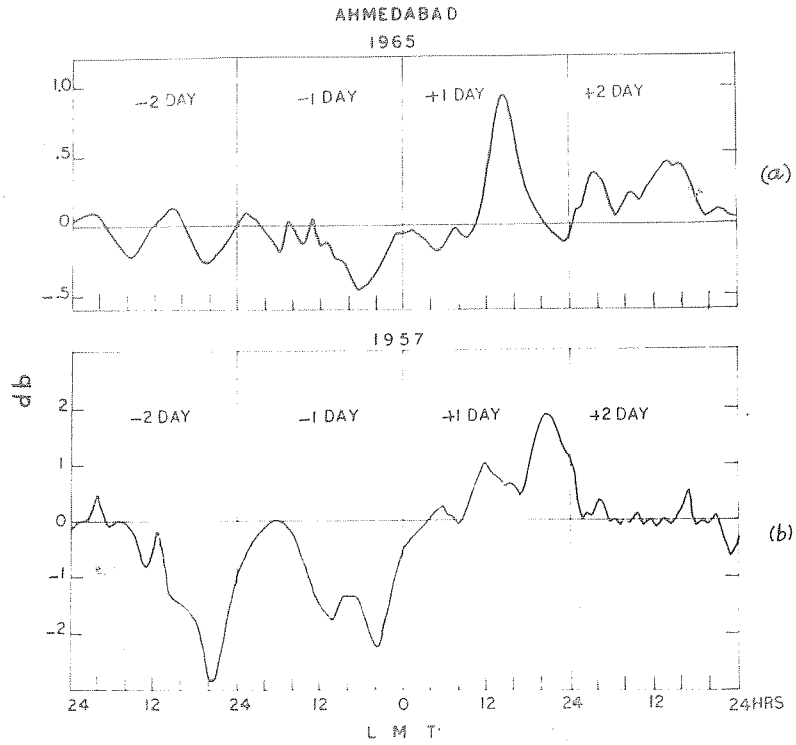


Fig.7.8(a) The hourly departure $\Delta A$ plotted for two days before, and two days after the storm as average for three storms shown in Fig.7.6.

(b) $\Delta A$ plotted as in Fig.7.8(a) for storms during 1957-58.

The storm effect observed during 1957-58 was attributed by Bhonsle and Ramanathan partly to change in F-scatter during

magnetically disturbed nights. In the present analysis the changes in attenuation due to magnetic storms take place mostly during daytime and the effect is mostly due to changes in the ratio $f_0 F_2^4 / T_e^{3/2}$.

In some of the magnetic storms during 1964-65, we found that the post-storm rise in cosmic radio noise attenuation occurs two or three days after the end of the storm. The hourly attenuation values during two such storms are plotted in Fig.7.9.

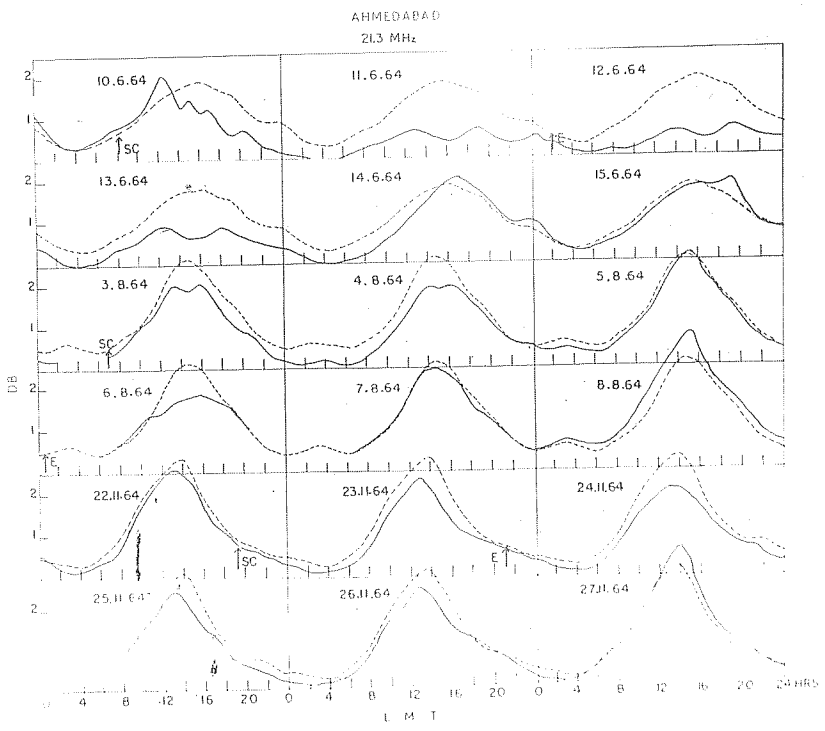


Fig.7.9 Hourly values of attenuation of 21.3 MHz CR noise during magnetic storm which produces decreases of attenuation for longer duration.

As can be seen in this figure, low attenuation continues after the commencement of the storm for 4 to 5 days, whereas in Fig.7.6 the depression lasted only for 2 to 3 days. There are two instances when a second storm occurred before the effect of a previous one subsided and are shown in Fig.7.10. On 20 February, 1966, there occurred a storm of moderate intensity which ended on 22 February. Immediately on the same day another storm of larger intensity was observed. The usual depression in attenuation

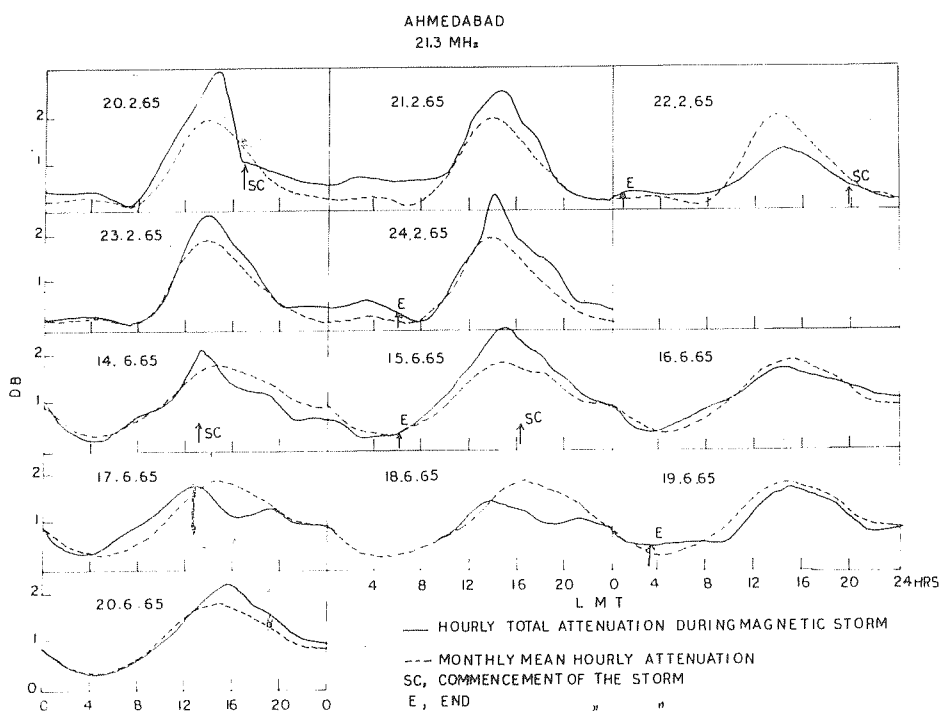


Fig.7.10 Hourly values of attenuation when a second storm occurs before the effect of a previous one subsides.

which was expected to occur on 23-2-66 as a result of the second storm is completely absent in this case. On the other hand the attenuation was found to be above the usual value at the end of the storm. Similar features are seen in the case of the two storms which occurred on 14 and 15 June 1965 and are shown in the same figure.

7.11 Conclusions

(1) The effect of magnetic storms on the attenuation of cosmic radio noise was less marked in 1964-65 than in 1957-58.

(2) The changes in absorption produced by magnetic disturbances show local time dependence. The maximum decrease during the main phase of the storm was observed to occur at 17-18 hr LMT. The maximum increase was found to take place after the end of the storm at 14-15 hr LMT.

(3) The changes in absorption during storm time noticed during 1964-65 was mainly due to changes in the ratio $f_o F_2^4 / T_e^{3/2}$.

(4) A decrease in attenuation could not be seen when a second sudden commencement took place before the effect of a previous storm had ended.

# CHAPTER VIII

## SUMMARY AND CONCLUSION

The present study deals with the attenuation of cosmic radio noise in the atmosphere over Ahmedabad and over Thumba at 25 Mlz, 21.3 Mlz and 16.5 Mlz. Particular attention is given to the absorption in the F region, both on the bottomside and topside of the $F_2$ peak. A summary is given below.

In Chapter I we have given the theory of radio wave absorption in the ionosphere and a brief summary of the results of ionospheric absorption measurements. Cosmic radio noise method of measuring ionospheric absorption was started in 1953 and since then, it has been used at different latitudes. It is pointed out that cosmic noise absorption measurements is particularly useful for studying F region absorption in low latitudes. Diurnal and seasonal variations of F region absorption observed at Ahmedabad are discussed in the subsequent chapters. Data of 25 Mlz cosmic noise recorded at Ahmedabad since 1956 has made it possible to study changes in absorption during more than half a solar cycle.

In Chapter II, the experimental set-up of riometers at 21.3 Mlz at Ahmedabad and 21.3 Mlz and 16.5 Mlz at Thumba have been described. At 16.5 Mlz, interference from broadcast stations was found to be severe and certain modifications had to be made to reduce the interference. Sample records of cosmic radio noise

at 45, 25, 21.3 and 16.5 MHz are shown. The unattenuated intensity normalised to the minimum of cosmic radio noise at 45 MHz was found to be significantly higher than the corresponding values at 21.3 MHz in the direction of the galactic equator.

A study of the extrapolated standard unattenuated curve at 25 MHz from 1958 to 1964 did not show any detectable longterm change in its shape. Synchrotron radiation of significant intensity was recorded at 25 MHz following the high altitude nuclear explosion over Johnston Island on 9th July 1962. This appeared as a short term increase in the noise level superposed on the quiet day curve and persisted for about two months.

Chapter III deals with the results of the analysis of 21.3 MHz and 25 MHz cosmic radio noise attenuation during the low sunspot years 1963-65 over Ahmedabad. It is shown that the total day time attenuation A is the sum of two components, (1) a component $A_D'$ which arises due to absorption in the lower ionosphere mainly in the D region and (2) a component which varies as some power of $f_0F_2$ according to the relation $A-A_D' = K(f_0F_2)^n$. The value of n depends on the ratio of $f_0F_2/f$, where f is the exploring frequency. For $f_0F_2/f < 0.6$, the average value of n remained at nearly constant value 4.2 and increased rapidly afterwards. This increase in n has been shown to be due to the retardation of the radio waves near the ionization peak when the group refractive index is considerably greater than unity at high $f_0F_2$ values.

A reasonably accurate method of separating $A_D'$ from the plot of A vs $f_0F_2$ is described. $A_D'$ at 21.3 MHz and 25 MHz were determined using this method during 1964-65. This showed a variation with frequency of the form $A_D' \propto 1/f^{2.1}$ over Ahmedabad.

It was shown that the daytime attenuation showed good dependence on $f_0F_2$ but the night time attenuation was not well correlated with $f_0F_2$. A large extra component which could not be accounted for by collision process alone was present in the night attenuation during low sunspot years. The possibility that this might be due to scattering of the incoming radiations by ionospheric irregularities during night was examined but no firm conclusion could be drawn.

In Chapter IV we have studied the changes in the attenuation of 25 MHz cosmic radio noise for 1958 through 1964 and shown that the total attenuation decreased significantly from high to low sunspot years, by as much as 50 percent. The secondary peak in absorption which occurred in equinoxes and winter of high sunspot years was found to be absent in the low sunspot years. The maximum daytime attenuation took place in equinoxes during both high and low sunspot years. The night attenuation decreased much less with decrease in solar activity, than the day attenuation. The attenuation for a given $f_0F_2$ was found to be more during 1964 than during 1958. The noon ratio of $f_0F_2^4$ to F region attenuation showed marked decrease towards low sunspot years. This indicated a corresponding decrease in the electron temperature near the $F_2$ peak.

Nondeviative absorption of cosmic radio noise due to electron-ion collision in the F region was calculated using N(h) profiles and neutral gas temperature upto $F_2$ peak. This was found to be a significant part of the observed total attenuation. The F region absorption due to electron-ion collision was on an average more than 70 percent of the total during high sunspot years and less than 50 percent during low sunspot years. The values of the ratio of topside to bottomside absorption during forenoon hours were found to be much less than what one would expect on the basis of electron density models for the topside which assumed electron temperatures to be equal to neutral gas temperatures. This led us to an evaluation of electron temperature which was found to be much higher than neutral gas temperatures.

The diurnal variations of electron temperature derived by this method showed reasonable agreement with those obtained from satellite measurements. It was found that during the hours following sunrise, the electron temperatures were maximum. The large electron temperatures in the morning hours are possible because of the low electron density at that time. Under less disturbed ionospheric conditions in high sunspot years, the midday electron temperature was nearly the same as neutral gas temperature, but during disturbed periods, large differences were noticed between the two. Since the electron density at the $F_2$ peak decreased considerably from high to low sunspot years, the ratio $T_e/T_i$ increased in low sunspot years.

The diurnal, seasonal and sunspot variations of the total electron content are studied in Chapter VI. The total electron content showed a secondary nighttime peak around 21 hr in equinoctial and winter months of high sunspot years. Daytime maxima in both cases occurred around 15 hr LMT. The amplitude of the diurnal peak during low sunspot years is only one third of that in high sunspot years.

In Chapter VII we have studied some of the changes in cosmic radio noise attenuation during solar flares and magnetic storms. Multifrequency observation of cosmic radio noise absorption during solar flares was used to find the frequency dependence of nondeviative absorption in the D region. The comparison of a few results obtained at Thumba and at Ahmedabad with those obtained at other low latitude stations indicate a latitudinal variation of the frequency index. Simultaneous observation of solar flare events at Thumba and Ahmedabad at the same CR noise frequency was used to find the dependence of D region absorption on the zenith angle of the sun.

During a magnetic storm, cosmic radio noise attenuation decreases significantly. The decrease lasts for two to four days. After the end of the storm the attenuation is above normal. The changes in attenuation have local time dependence, the maximum effect being around 15-17 hr LMT. The time of maximum effect was found to be different from that found in high sunspot years. The changes in attenuation observed in low sunspot years followed closely the changes in the ratio $f_0F_2^4/T_e^{3/2}$.

The following are main conclusions from the present study :-

(1) The total cosmic radio noise attenuation, A, during daytime, is the sum of (a) a component which is independent of $f_0F_2$, $A_D'$ and (b) another component which varies with $f_0F_2$ according to the relations $A - A_D' = K(f_0F_2)^n$. The value of n is close to 4.0 when the ratio $f_0F_2/f$ is less than 0.6.

(2) The amplitude of the diurnal peak in the total attenuation is maximum in equinoctial months and minimum in winter and summer months during both low and high sunspot years.

(3) For a given $f_0F_2$ the attenuation is found to be more during low sunspot years than during high sunspot years.

(4) A large extra attenuation which cannot be accounted for by electronic collision with ions is present during the night in low sunspot years.

(5) Total cosmic radio noise attenuation on 25 MHz during daytime decreased significantly, by as much as 50 percent, with decrease in solar activity since 1958. The secondary nighttime peak which was present in equinoctial and winter months of high sunspot years completely disappeared in low sunspot years. The average nighttime attenuations did not decrease as much as the daytime absorption with decrease of solar activity.

(6) Electron ion collisions in the F region can explain more than 70 percent of the total daytime absorption during high sunspot years and about 50 percent during low sunspot years.

(7) Electron temperature near the $F_2$ peak is maximum around 08 hr LMT.

(8) Under comparatively quiet ionospheric conditions, the noon electron temperature is nearly the same as neutral gas temperature in high sunspot years, but there is a significant difference between the two in low sunspot years.

(9) Midday electron temperature shows a decrease by a factor of 0.6 from high to low sunspot years.

(10) The total electron content decreased from high to low sunspot years by a factor of 0.3.

(11) During solar flares the enhanced absorption in the D region of the ionosphere varies with exploring frequency as $1/f^n$, where n is 2.2 over Ahmedabad and 1.6 over Thumba. The enhanced absorption varies with solar zenith angle $\chi$ as $\cos^{1.6}\chi$.

(12) The changes in absorption due to magnetic storm are dependent on local-time, the maximum effect is observed around 21 hr LMT during high sunspot years and 17 hr LMT during low sunspot years. These changes follow closely the changes in the ratio $f_0F_2^4/T_e^{3/2}$.

# R E F E R E N C E S


| | | | |
|---|---|---|---|
| 1. | Agy, V. and Davies, K. | 1962 | J.Atmos.Terr.Phys., 26, Radiowave absorption in the ionosphere, p.202. |
| 2. | Anastassiades, M. | 1962 | Space Research, III ed. Priester, p.265. |
| 3. | Appleton, E.V. | 1937 | Proc.Roy.Soc., 162A, 451. |
| 4. | Appleton, E.V., Ingram, L.J. and Naismith, R. | 1937 | Phil.Trans.Roy.Soc. (London), 236, 191. |
| 5. | Appleton, E.V. and Piggott, W.R. | 1954 | J.Atmos.Terr.Phys., 5, 144. |
| 6. | Bauer, S.J. | 1962 | J.Atmos.Sci., 19, 276. |
| 7. | Berkner, L.V., Seaton, S.L. and Wells, H.W. | 1939 | Terr.Mag., 44, 283. |
| 8. | Berkner, L.V. and Seaton, S.L. | 1940 | Terr.Mag., 45, 393. |
| 9. | Bhonsle, R.V. and Ramanathan, K.R. | 1958 | J.Sci.Indust.Res., 17A, 40. |
| 10. | Bhonsle, R.V. | 1960 | Proc.Ind.Acad.Sci., 51, 189. |
| 11. | Bhonsle, R.V. and Ramanathan, K.R. | 1960 | Planet Space Sci., 2, 99. |
| 12. | Bhonsle, R.V., da Rosa, A.V. and Garriot, O.K. | 1965 | J.Res.Nat.Bur.Standard, 69D, 637. |
| 13. | Blum, Denisse and Steinberge | 1954 | C.R.Acad.Sci., Paris, 238, 1695. |
| 14. | Bolton and Stanley | 1948 | Aust.J.Sci.Res., A1, 58. |
| 15. | Bourdeau, R.E. and Donely, N.L. | 1964 | Proc.Roy.Soc., A281, 487. |

16. Bourdeau, R.E. 1964 Space Research, ed.King Hele, Muller and Reghini, p.77.

17. Bowles, K.L., Ochs, E.R. and Green, J.L. 1962 J.Res.Nat.Bur.Sten., 66, 395.

18. Bowles, K.L. 1963 Science, 139, 389.

19. Brace, L.H. and Spencer, N.W. 1964 J.Geophys.Res., 69, 4686.

20. Bracewell, R.N. and Strnker, J.W. 1949 Mon.Not.Roy.Astron.Soc., 109, 28.

21. Carl Seddon, J. 1963 NASA Technical Report, TND-1670.

22. Chapman, S. and Little, C.G. 1957 J.Atmos.Terr.Phys., 10, 20.

23. CIRA 1961 Committee on Space Research COSPAR International Ref.Atm.

24. Cowling, T.G. 1945 Proc.Roy.Soc., A183, 453.

25. Degaonkar, S.S. and Bhonsle, R.V. 1962 Proc.International Conference on cosmic rays and earth storm, Kyoto, Sept.1961, p.286.

26. Dalgarno, A., McElroy, M.B. and Moffet, R.J. 1962 Technical Report 62-11-N Geophys.Corp.America.

27. Dalgarno, A. 1963 Technical Report No.63-11-N Geophys.Corp.America.

28. Davies, K. 1965 Ionospheric Radio Propagation NBS Monograph, 80, p.147.

29. Dungey, J.W. 1956 J.Atmos.Terr.Phys., 9, 90.

30. Dyce, R.B. and Horowitch 1963 J.Geophys.Res., 68, 713.

31. Ellis, G.R.A. 1963 Aust.Jour.Phys., 16, 411.

| | | | |
|---|---|---|---|
| 32. | Ellis, G.R.A. and Hamilton, P.A. | 1964 | Nature, Oct.17, 272. |
| 33. | Evans, J.V. and Taylor, G.N. | 1961 | Proc.Roy.Soc., A263, 189. |
| 34. | Evans, J.V. and Taylor, G.N. | 1964 | Proc.Roy.Soc., 279, 407. |
| 35. | Hanson, W.B. and Johnson, F.S. | 1961 | Memoires Soc.R.Sc.Liege Cinquieme Serie tome IV, Fasc.Extrait 391. |
| 36. | Hanson, W.B. | 1963 | "Electron density distribution in Ionosphere", Nato-Science Committee, ed.Thrane, E. p.361. |
| 37. | Harris, I. and Priester, W. | 1964 | The upper atmosphere in the range 120 to 800 km. |
| 38. | Hey, J.S., Parson, S.J. and Phillips, J.W. | 1948 | Proc.Roy.Soc., A192, 425. |
| 39. | Hibberd, F.H. and Ross, W.J. | 1966 | J.Geophys.Res., 71, 2243. |
| 40. | Horowitch, S. and Goldman, S.C. | 1963 | Nature, Sept.21, 1147. |
| 41. | Jansky, K.G. | 1932 | Proc.IRE, 20, 1920. |
| 42. | Jansky, K.G. | 1937 | Proc.IRE, 25, 1517. |
| 43. | Jackson, J.E. and Bauer, S.J. | 1961 | J.Geophys.Res., 66, 3055. |
| 44. | King, G.A.M. | 1960 | J.Geophys.Res., 65, 1623. |
| 45. | King, J.W., Smith, P.A., Eccles, D. and Helm, H. | 1963 | Rad.Res.Station Report Slough, IM. 94. |
| 46. | Kotadia, K.M. | 1959 | Proc.Ind.Acad.Sci., 50, 259. |

| | | | |
|---|---|---|---|
| 47. | Kotadia, K.M. and Ramanathan, K.R. | 1959 | Annals of IGY. |
| 48. | Lusignan, B. | 1962 | J.Atmos.Terr.Phys., 23, Radiowave absorption in the ionosphere, 126. |
| 49. | Little, C.G. and Leinbach, H. | 1958 | Proc.IRE, 46, 334. |
| 50. | Little, C.G. and Leinbach, H. | 1959 | Proc.IRE, 47, 315. |
| 51. | Maeda, K.I. and Sato, T. | 1959 | Proc.IRE, A47, 232. |
| 52. | Mitra, A.P. and Shain, C.A. | 1953 | J.Atmos.Terr.Phys., 4, 204. |
| 53. | Mitra, A.P. and Sarada, K.A. | 1962 | J.Atmos.Terr.Phys., 23, Radiowave absorption in the ionosphere, 348. |
| 54. | Nicolet, M. | 1959 | Phys.Fluids, 2, 95. |
| 55. | Nicolet, M. and Aikin, A.C. | 1960 | J.Geophys.Res., 65, 1409. |
| 56. | Oches, G.R., Farley, D.T.JR, Bowles, K.L. and Bandopadhyay, P. | 1963 | J.Geophys.Res., 68, 201. |
| 57. | Pineo, V.C. and Hynek, D.P. | 1962 | J.Geophys.Res., 67, 5119. |
| 58. | Parthasarathy, R., Ierford, G.M. and Little, C.G. | 1963 | J.Geophys.Res., 68, 3581. |
| 59. | Pawsey, J.L. and Hill, E.R. | 1961 | Report on progress in Physics, 26, 69. |
| 60. | Rober, G. | 1940 | Proc.IRE, 28, 68. |
| 61. | Ramamurthy, V.V. & Ramachandra Rao,B.R. | 1964 | J.Atmos.Terr.Phys., 26, 849. |

| | | | |
|---|---|---|---|
| 62. | Ramanathan, K.R., Bhonsle, R.V. and Degaonkar, S.S. | 1961 | J.Geophys.Res., 66, 2763. |
| 63. | Ramanathan, K.R. & Bhonsle, R.V. | 1959 | J.Geophys.Res., 69, 1635. |
| 64. | Ramanathan, K.R. et al | 1956 | Proc.Ind.Acad.Sci., 43A, 306. |
| 65. | Ratcliffe, J.A. | 1962 | The magneto ionic theory and its application to the ionosphere, Cambridge University Press, p.32. |
| 66. | Roger, R.S. | 1964 | J.Atmos.Terr.Phys., 26, 475. |
| 67. | Rose, W.J. | 1960 | J.Geophys.Res., 65, 2001. |
| 68. | Sarabhai, V. et al | 1956 | Ibid. 43A, 309. |
| 69. | Schmelovesky | 1964 | Space Research, IV ed. Muller, 508. |
| 70. | Shain, C.A. and Mitra A.P. | 1954 | J.Atmos.Terr.Phys., 5, 316. |
| 71. | Shain, C.A. | 1951 | Aust.J.Sci.Res., 4, 256. |
| 72. | Shirke, J.S. | 1959 | J.Ind.Tel.Comm.Eng., 5, 115. |
| 73. | Shirke, J.S. | 1962 | Proc.Ind.Acad.Sci., 56, 165. |
| 74. | Shirke, J.S. | 1961 | Proc.IGY Symp.1, 142. |
| 75. | Shirke, J.S. | 1963 | J.Atmos.Terr.Phys., 25, 429. |
| 76. | Skinner, J.J. and Wright, R.W. | 1956 | J.Atmos.Terr.Phys., 9, 103. |
| 77. | Stanley, C.J. and Slee, O.B. | 1950 | Aust.J.Sci.Res., 3A, 234. |
| 78. | Steiger, W.R. and Warwick, J.W. | 1961 | J.Geophys.Res., 66, 57. |
| 79. | Taylor, G.N. | 1964 | Proc.Roy.Soc.(London), 279, 407. |

2717.


80. Taylor, JR.H.A., Brinton, A.C. and Smith, C.R. 1965 J.Geophys.Res., 70, 6769.

81. Warwick, J.W. and Airin, H.J. 1957 J.Atmos.Terr.Phys., 11, 187.

82. Wright, J.W. 1960 J.Geophys.Res., 65, 185.

83. Onegawa, T. 1955 J.Rad.Res.Lab., Japan, 2, 125.

84. Yeh, K.C. and Swenson, JR.G.W. 1961 J.Geophys.Res., 66, 1061.

* Friedman, H. 1964 Res. geophys 1 MIT press P197